

**COMBATING  $\beta$ -CATENIN DRIVEN HEPATOCELLULAR CARCINOMA**

by

**Evan R. Delgado**

B.S. in Biochemistry and Molecular Biology, State University of New York at Albany, 2009

Submitted to the Graduate Faculty of  
School of Medicine in partial fulfillment  
of the requirements for the degree of  
Doctor of Philosophy

University of Pittsburgh

2014

UNIVERSITY OF PITTSBURGH

SCHOOL OF MEDICINE

This dissertation was presented

by

Evan R. Delgado

It was defended on

January 30, 2014

and approved by

Dr. George Michalopoulos, MD. PhD. Maud L. Menten Professor, Department of Pathology

Dr. Aaron Barchowsky, PhD., Professor, Department of Environmental and Occupational Health

Dr. Michael Tsang, PhD., Associate Professor, Department of Developmental Biology

Dr. Shanmugam Nagarajan, PhD., Associate Professor, Department of Pathology

Dissertation Advisor: Dr. Satdarshan P. S. Monga, MD., Professor, Department of Pathology

Copyright © by Evan R. Delgado

2014

## COMBATING BETA-CATENIN DRIVEN HEPATOCELLULAR CARCINOMA

Evan R. Delgado, B.S.

University of Pittsburgh, 2014

Hepatocellular Carcinoma (HCC) is the most common primary liver tumor and is a major cause of cancer related death worldwide with few avenues of treatment that benefit patients. There are many causes of HCC making the cancer difficult to treat as a homogenous disease. Many molecular pathways are deregulated during the onset of hepatocarcinogenesis, and one commonly activated signaling cascade in HCC is the Wnt/ $\beta$ -catenin pathway.  $\beta$ -Catenin plays multiple roles in cellular processes from maintenance of cellular adhesions to regulating regenerative signals required for the liver to grow. In cancer,  $\beta$ -catenin signaling is aberrantly regulated and has now been shown to play roles in tumor cell proliferation, survival and metabolism contributing to disease progression. Knowing the prevalence and importance of  $\beta$ -catenin in HCC, it is critical to develop targeted, personalized therapeutics which may impact multiple aspects of tumor biology. Here, we have identified several different avenues that target active Wnt signaling. We demonstrate the importance of computational biology to identify novel small molecules (SMs) to target  $\beta$ -catenin signaling. SM treatment results in decreased  $\beta$ -catenin signaling leading to decreases in downstream targets affecting HCC growth and survival. We also utilized antisense treatments which target  $\beta$ -catenin at the genetic level decreasing  $\beta$ -catenin protein expression and leading to subsequent cell death and decrease in tumor burden. Additionally, we identified angiogenesis as a notable event regulated by Wnt/ $\beta$ -catenin signaling

In fact, inhibiting Wnt signaling in HCC cells led to reduced production of pro-angiogenic secreted factors which in turn inhibited angiogenic characteristics in tumor associated endothelial cells. Our studies validate the significance of targeting  $\beta$ -catenin in HCC that should lead to notable effects on tumor growth and development. With the current studies providing the final proof-of-concept, we now believe that  $\beta$ -catenin directed therapies may in fact be plausible, and have potential clinical implications.

### **PUBLICATIONS**

- 1) **Evan Delgado**, Hiro Okabe, Jing Yang, Yixian Zhang, Lee M. Greenberger, Satdarshan P. S. Monga. Combatting  $\beta$ -catenin driven hepatocellular carcinoma by utilization of Locked Nucleic Acids. (*In progress*)
- 2) **Evan Delgado**, Jing Yang, Juhoon So, Stephanie Leimgruber, Michael Kahn, Tohru Ishitani, Donghun Shin, Gabriella Mustata, Satdarshan P. S. Monga. Identification and characterization of a novel small molecule inhibitor of beta-catenin signaling in hepatocellular carcinoma. American Journal of Pathology. (*submitted*).
- 3) **Evan Delgado**, Raman Bahal, Jing Yang, Jung Min Lee, Danith H Ly, Satdarshan P. S. Monga.  $\beta$ -catenin Knockdown by Cell Permeable Gamma Guanidine-Based Peptide Nucleic Acid Reveals its New Roles in Hepatocellular Cancer. Current Cancer Drug Targets. (Jul 1, 2013).

## TABLE OF CONTENTS

<b>PREFACE.....</b>	<b>15</b>
<b>1.0 INTRODUCTION.....</b>	<b>17</b>
<b>1.1 CANCER EPIDEMIOLOGY.....</b>	<b>18</b>
<b>1.1.1 Worldwide cancer burden .....</b>	<b>18</b>
<b>1.1.2 Cancer related deaths worldwide.....</b>	<b>19</b>
<b>1.1.3 Four most common cancers: Breast, Colorectal, Lung, and Liver .....</b>	<b>19</b>
<b>1.2 HEPATOCELLULAR CARCINOMA .....</b>	<b>21</b>
<b>1.2.1 Major Global Risk Factors for HCC .....</b>	<b>22</b>
<b>1.2.2 HCC in the United States .....</b>	<b>25</b>
<b>1.3 HEPATOCARCINOGENESIS .....</b>	<b>26</b>
<b>1.3.1 Stepwise process to hepatocellular oncogenesis .....</b>	<b>27</b>
<b>1.3.2 Biochemical Pathways known to be involved in HCC .....</b>	<b>30</b>
<b>1.4 WNT/<math>\beta</math>-CATENIN SIGNALING.....</b>	<b>34</b>
<b>1.4.1 Wnt/<math>\beta</math>-catenin signaling in HCC .....</b>	<b>35</b>
<b>1.5 CURRENT THERAPEUTIC STRATEGIES FOR HCC .....</b>	<b>37</b>
<b>1.5.1 Sorafenib and TACE in HCC.....</b>	<b>38</b>
<b>1.5.2 Current clinical trial developments .....</b>	<b>39</b>
<b>1.5.3 Preclinical Developments .....</b>	<b>43</b>

1.6	CURRENT CONTRIBUTIONS OF BETA-CATENIN TARGETED THERAPEUTICS IN HCC .....	46
2.0	IDENTIFICATION AND CHARACTERIZATION OF A NOVEL SMALL MOLECULE INHIBITOR OF BETA-CATENIN SIGNALING IN HEPATOCELLULAR CANCER CELLS .....	48
2.1	IDENTIFICATION OF SMALL MOLECULES TARGETING WNT/BETA-CATENIN SIGNALING .....	49
2.1.1	Structural similarity search reveals ICG-001 analogs .....	49
2.1.2	<i>In silico</i> toxicity prediction reveals promising small molecules .....	50
2.2	BIOLOGICAL VALIDATION OF LEAD SMALL MOLECULES.....	51
2.2.1	Identifying small molecules capable of inhibiting Wnt/ $\beta$ -catenin signaling <i>in vitro</i>	51
2.2.2	Toxicity studies reveal PMED-1 to be top candidate .....	52
2.3	INVESTIGATING TIME AND DOSE DEPENDENCY OF PMED-1 .....	52
2.3.1	Wnt/ $\beta$ -catenin activity assay studies PMED-1 efficacy .....	54
2.3.2	Inhibiting cell cycle progression and growth supports activity assay.....	54
2.4	HCC CELL LINE SPECIFICITY OF PMED-1 EXAMINED .....	56
2.4.1	Multiple HCC cell lines are susceptible to PMED-1 via TOPFlash assay	56
2.4.2	PMED-1 causes consistent inhibition of Wnt target gene expression in multiple HCC cell lines .....	57
2.5	ACTIVITY SPECIFICITY OF PMED-1 MIMICS ICG-001 .....	59
2.5.1	Co-immunoprecipitation of CBP/ $\beta$ -catenin shows PMED-1 activity .....	59
2.5.2	PMED-1 does not show off target kinase inhibition.....	60

2.6	POSSIBLE <i>IN VIVO</i> APPLICATION FOR PMED-1 .....	62
2.6.1	Addressing stability of PMED-1 <i>in vitro</i> .....	62
2.6.2	Inhibition of Wnt signaling in Zebrafish with PMED-1 .....	63
2.6.3	Characterizing duration of Wnt signaling inhibition <i>in vivo</i> .....	64
2.7	DISCUSSION OF APPLICABILITY OF PMED-1.....	66
3.0	$\beta$ -CATENIN KNOCKDOWN BY CELL PERMEABLE GAMMA GUANIDINE- BASED PEPTIDE NUCLEIC ACID REVEALS ITS NEW ROLES IN HEPATOCELLULAR CANCER .....	70
3.1	DEVELOPING AN ANTISENSE AGAINST BETA-CATENIN.....	71
3.1.1	Design and synthesis of Peptide Nucleic acids .....	71
3.1.2	Uptake of Peptide Nucleic Acids Leads to Inhibited Wnt/ $\beta$ -catenin Signaling in HCC cells .....	72
3.2	ANTISENSE TARGETING OF $\beta$ -CATENIN AGAINST HCC <i>IN VITRO</i> 75	
3.2.1	PNA results in reductions of $\beta$ -catenin downstream targets .....	76
3.2.2	Targeting $\beta$ -catenin via PNA effects HCC cell biology .....	76
3.3	SECONDARY ANTI-ANGIOGENIC EFFECTS DUE TO TARGETING BETA-CATENIN IN HCC VIA PNA.....	79
3.3.1	Inhibition of $\beta$ -catenin in HCC leads to inhibited expression of molecules involved in angiogenesis.....	80
3.3.2	Reduced expression of angiogenic factors due to $\beta$ -catenin directed PNA treatment leads to inhibition of angiogenesis in endothelial cells.....	82
3.4	DISCUSSION OF THE SIGNIFICANCE FOR DEVELOPMENT OF ANTISENSE FOR THERAPEUTICS .....	85

<b>4.0</b>	<b>ANTISENSE LOCKED NUCLEIC ACIDS TREAT BETA-CATENIN DRIVEN HEPATOCELLULAR CARCINOMA IN MICE .....</b>	<b>89</b>
<b>4.1</b>	<b>USE OF LNA LEADS TO REDUCED WNT/BETA-CATENIN SIGNALING .....</b>	<b>90</b>
<b>4.1.1</b>	<b>Optimization of LNA treatment <i>in vivo</i> in mouse liver .....</b>	<b>91</b>
<b>4.2</b>	<b>ESTABLISHING A WNT/<math>\beta</math>-CATENIN DRIVEN HCC MODEL <i>IN VIVO</i> .....</b>	<b>93</b>
<b>4.2.1</b>	<b>Characterizing biological impact of DEN with PB in mouse liver .....</b>	<b>93</b>
<b>4.2.2</b>	<b>Histological and protein confirmation of activated <math>\beta</math>-catenin in carcinogenesis model.....</b>	<b>95</b>
<b>4.3</b>	<b>USE OF LNA IN HCC MODEL LEADS TO REDUCED WNT/<math>\beta</math>-CATENIN SIGNALING AND TUMOR BURDEN .....</b>	<b>97</b>
<b>4.3.1</b>	<b>Baseline characterization of livers following LNA treatment under DEN + Phenobarbital model.....</b>	<b>97</b>
<b>4.4</b>	<b>DISCUSSING POSSIBLE THERAPUTIC IMPLICATIONS OF LNA ANTISENSE IN LIVER CANCER .....</b>	<b>100</b>
<b>5.0</b>	<b>CONCLUSIONS AND FUTURE PROSPECTS.....</b>	<b>103</b>
<b>5.1</b>	<b>TARGETING <math>\beta</math>-CATENIN IN HCC: A SAFE BET? .....</b>	<b>103</b>
<b>5.2</b>	<b>USING SMALL MOLECULES FOR HCC THERAPY .....</b>	<b>104</b>
<b>5.3</b>	<b>ANTISENSE THERAPY TARGETING <math>\beta</math>-CATENIN IN HCC .....</b>	<b>106</b>
<b>5.4</b>	<b><math>\beta</math>-CATENIN BIOMARKERS FOR PERSONALIZED MEDICINE.....</b>	<b>108</b>
<b>6.0</b>	<b>MATERIALS AND METHODS .....</b>	<b>111</b>
<b>6.1</b>	<b>DEVELOPMENT OF <math>\gamma</math>GPNA AND SMALL MOLECULES .....</b>	<b>111</b>
<b>6.1.1</b>	<b>Oligomer Synthesis .....</b>	<b>111</b>

6.1.2	Small Molecule Similarity Search .....	112
6.1.3	<i>In silico</i> ADME and toxicity screening of projected SMs .....	112
6.2	CELL CULTURE AND ASSAYS.....	113
6.2.1	Human HCC cell culture and establishing stable $\beta$ -catenin mutants.....	113
6.2.2	Preparation and Cell Culture Treatments .....	114
6.2.3	Kinase Assays.....	114
6.2.3.1	IMAP-based Plk2 TR-FRET Assay .....	115
6.2.3.2	IMAP-based PKD FP Assay.....	116
6.2.3.3	IMAP-based Plk1 TR-FRET Assay .....	116
6.2.3.4	IMAP-based CAK TR-FRET Assay .....	116
6.2.3.5	IMAP-based AKT FP assay .....	116
6.2.4	Transient Inhibition of $\beta$ -catenin via siRNA.....	116
6.2.5	$\beta$ -Catenin Luciferase Activity Assay.....	117
6.2.6	$\beta$ -Catenin Luciferase Activity Assay: Time Course .....	117
6.2.7	MTT Assay for Toxicity .....	118
6.2.8	Thymidine Incorporation Proliferation Assay.....	118
6.3	PROTEIN EXTRACTION AND WESTERN BLOTTING.....	119
6.3.1	Whole Cell Lysate Preparation: Cell Culture.....	119
6.3.2	Whole Cell Lysate Preparation: Whole Liver Tissue.....	119
6.3.3	Western Blot Analysis .....	120
6.3.4	Protein Complex Immunoprecipitation.....	120
6.4	RNA EXTRACTION AND QRT-PCR.....	121
6.5	IMAGING ANALYSIS .....	122

6.5.1	Live Cell Imaging.....	122
6.5.2	TUNEL Staining .....	122
6.5.3	Immunohistochemistry .....	123
6.5.4	Hematoxylin and Eosin Staining.....	123
6.5.5	Immunofluorescence .....	124
6.6	ENDOTHELIAL ASSAYS .....	124
6.6.1	<i>In vitro</i> Endothelial Spheroid Assay.....	124
6.6.2	<i>In vitro</i> Tubulogenesis Assay .....	125
6.7	ANIMAL MODEL UTILIZATION .....	126
6.7.1	Mouse Model Development.....	126
6.7.2	LNA Administration <i>In Vivo</i> .....	127
6.7.3	Zebrafish experiments.....	127
APPENDIX A .....		128
APPENDIX B .....		129
APPENDIX C .....		136
BIBLIOGRAPHY .....		137

## LIST OF TABLES

Table 1. Antibodies used for WB, IP, IF and IHC.....	128
Table 2. SM structures and ZINC IDs .....	129
Table 3. Categories of mice and LNA conditions.....	136

## LIST OF FIGURES

Figure 1. Pathological progression to HCC. ....	27
Figure 2. Schematic representation of Wnt/ $\beta$ -catenin signaling pathway. ....	35
Figure 3. Outline of molecules and respective targeted sites of action currently under investigation for therapeutic benefit in clinical and pre-clinical models. ....	45
Figure 4. Computational approach and structures of investigated small molecules. ....	50
Figure 5. Effect of PMED-1 and PMED-2 on HepG2 cell line and normal human hepatocytes .	53
Figure 6. PMED-1 targets $\beta$ -catenin signaling to affect cell proliferation in HepG2 cells .....	55
Figure 7. PMED-1 targets $\beta$ -catenin effectively in multiple HCC cell lines .....	58
Figure 8. PMED-1 specifically inhibits $\beta$ -catenin-CBP interactions and does not impact other common kinases. ....	61
Figure 9. Efficacy and duration of PMED-1's effect on $\beta$ -catenin activity in vivo and in vitro..	66
Figure 10. Structure and sequence of antisense oligonucleotides and controls that show an unaided cellular uptake .....	73
Figure 11. $\gamma$ GPNA designed against $\beta$ -catenin decreases its reporter activity in hepatoma cells with T1's impact being more pronounced .....	75
Figure 12. T1 PNA treatment affects expression of $\beta$ -catenin gene and Wnt target expression to impair HCC cell proliferation and survival .....	78
Figure 13. Modulation of $\beta$ -catenin regulates expression of angiogenic factors in HCC cells ....	81

Figure 14. Conditioned media from single T1 treatment of HepG2 cells collected after 72 hours diminished angiogenesis in SK-Hep1 cells.....	85
Figure 15. Nucleotide structures for LNA, DNA, and RNA .....	91
Figure 16. LNA administration significantly reduces $\beta$ -catenin and GS levels in normal mice ..	92
Figure 17. Successful recapitulation of DP model leads to HCC tumor burden .....	94
Figure 18. Histological analysis of $\beta$ -catenin driven HCC in DP murine model .....	96
Figure 19. Inhibiting $\beta$ -catenin expression via LNA treatment reduces tumor burden following DEN+PB carcinogenesis model.....	100

## **PREFACE**

I think the theme of my graduate work and life in general is support, without which my degree would have not even been possible. Of course it's the support and love from Kayla Rodabaugh that has ultimately aided in my ability to get to the point where I am today. The most important thing I would like to thank you for is just being there to listen to me. Without you being there to talk to about everything going on, even though much of it was difficult to understand, I would have no outlet. Thank you for being there for me allowing for me to get my mind out of the lab and take a much needed break from time to time. I started this process with you and now it is moving on to a next phase which I am deeply excited to continue with you. Thank you for understanding about all the late nights and weekends, about all the weekends I had to unfortunately cancel coming up to visit you in Mansfield because I had to do an injection or a drug treatment, and for all the unconditional love you give me.

I would also like to thank my family, of which without I would not have had the drive, motivation and opportunity to get to where I am today. Thank you for everything, and giving me the chances which led me to understanding where my passion is today. Without my parents Meryl, Craig, Jorge and Bunny, I may have not realized what I truly wanted to do. I also want to thank my brother, Andrew, for also playing a role in who I am today. You may not realize it, but you are the one who has pushed me the most in my life, so thank you for teasing and tormenting me as we grew up which taught me how to stand up for myself. I would also like to thank my

grandfather, Don, and my grandmother Estrella, who I strive to make proud every day of my career. You are the people who I try my best to make proud every time I do an experiment.

On a professional note, I truly want to thank my first academic research advisor Dr. Carla Theimer. Without you, Carla, I would have never realized my true passion. You really are one of the reasons why my passion for science is so strong because you were the one that showed me how much fun this really can be, while being able to do something you love. Your guidance and support laid the foundation for the scientist and researcher that I am today, and I hope that I have done your mentorship justice. I also want to thank everyone, no matter who it is, that had an impact on my life and helped shape me into a researcher with a drive to prove to you that I can do this and turn my life and career into something you could have never imagined.

Of course, I would also like to thank Paul. You are the one individual who I have literally said over a dozen times, I don't know where I would be without you. Without your guidance, mentorship and support I seriously would have not recognized my desire to solve puzzles and get to the deeper understanding of science. In your ways, you've pushed me harder and held me to higher standards more than anyone I've ever known. From all the conferences, posters, awards and manuscripts, I truly hope you realize you have done something right, not only with me, but with everyone whom you have mentored. I can only hope that once I become an established investigator I will be as successful as you, to which of course you would answer "You will be."

I ultimately want to dedicate this work to everyone who has been affected in some way, shape or form by cancer. It is my ultimate hope that at least some aspects of the work presented here, which is the culmination of several years of research aided by the guidance and support of many people, may fundamentally lead to new advances in cancer therapeutics.

## 1.0 INTRODUCTION

Among the leading causes of morbidity and mortality worldwide, cancer is one of the top 10 non-communicable diseases according to the World Health Organization (WHO). Cancer is the uncontrolled growth of a mass of cells which lead to debilitating inhibition of normal body functions. Cancer itself is characterized as poorly differentiated, and tends to resemble a state in development where cells and tissue are constantly in a proliferative status. Research has shown that depending on the geographical and economic environments the incidences and mortality rates of different types of cancer differs significantly (1, 2). Depending on the type of environment, oncogenesis can be dictated by a number of external factors such as cigarette smoke, ultraviolet light exposure, or even chronic viral infections. Current treatment methods consist of chemotherapy, hormone therapy, surgery and targeted therapies.

Targeted therapies are starting to become widely accepted as the most effective method of therapy for cancer. This belief stems from the presence of specific genetic mutations affecting proteins that normally regulate cell cycle progression or proliferation, such as p53,  $\beta$ -catenin, or c-myc, which lead to uncontrolled cell growth resulting in oncogenesis. The heterogeneous nature of each cancer makes it very difficult for developing a “magic bullet” which could treat every cancer. Even within one type of cancer, such as breast cancer, there can exist different mutations yielding a specific phenotype. It is entirely possible for one patient to present breast cancer positive for *BRCA1/2* mutations, but another patient without these mutations therefore a

therapy targeting *BRCA1/2* mutations would only benefit one of the two. Understanding the molecular mechanisms behind the heterogeneous development of the same type of cancer is critical in order to develop specific targeted therapies. Thus current research suggests that identifying and targeting multiple activated oncogenic pathways in specific cancers is the next step in revolutionizing cancer therapeutics.

## **1.1 CANCER EPIDEMIOLOGY**

### **1.1.1 Worldwide cancer burden**

In 2008 the global population reached 6.7 billion. Of these 6.7 billion people in the world, 12.7 million had cancer (1, 2). There are many causes for the incidence of cancer worldwide, which consist of the increased rates of smoking, alcoholism, as well as the Westernization of many cultural diets. Breast and lung cancers are the most frequently diagnosed cancers and causes of death in women and men worldwide (1, 2). The dichotomy is observed when comparing the incidence rates of different types of cancer between developed and developing nations. In Westernized countries the most frequently diagnosed cancers in both males and females are colorectal and lung cancers (1, 2). Cervical and lung cancers in females, and stomach and liver cancers in males are the most commonly diagnosed diseases in developing nations (1, 2). These statistics show that risk factors may vary depending on the environment. Underdeveloped countries tend to be more susceptible to cancers caused by infections such as stomach and liver cancers, whereas Westernized nations are more prone to cancers caused by

habits like smoking, inactivity and alcoholism, which have been associated with 2 to 5 times higher rate for prostate, colorectal, breast and lung cancers in developed countries (1, 2).

### **1.1.2 Cancer related deaths worldwide**

There were a total of 7.6 million cancer deaths in 2008 worldwide (1, 2). At 64%, the majority of cancer related deaths occurred in the developing world indicating a lack in medical resources needed to manage the disease burden in these areas (1, 2). Divergence in death rates associated with cancer in developing versus developed nations clearly highlights the differences in quality of oncology care (1, 2). Breast cancer is among the most frequently diagnosed cancer and leading cause of death in females worldwide accounting for 23% of total cancer cases and 14% of all deaths followed by lung cancer at 13% and then colorectal cancer at 9% (1, 2). In men, the leading cause of cancer related death is lung cancer at 23% followed by liver (11%) and stomach (11%) cancers (1, 2).

### **1.1.3 Four most common cancers: Breast, Colorectal, Lung, and Liver**

Breast cancer accounts for 23% of all new diagnoses and 14% of all cancer related deaths in 2008 (1, 2). The difference in incidence rates of breast cancer between developed and underdeveloped nations, 66.4 cases per 100,000 people compared to 27.3 cases per 100,000 respectively, are high largely due to differences in reproductive and hormonal factors stemming from such things as menstrual history, nulliparity, postmenopausal hormone therapy, oral contraceptives, and late age at first birth, as well as the availability of early detection services (3-5). In developed nations early detection methods are much more common (5). Early detection

more often than not increases the number of total number of diagnosed cases, but since they are detected early they can be easily treated. With the advent of lower use of postmenopausal hormone therapy and more widespread early detection methods such as mammography, incidence rates in the U.S., and other western nations, has sharply decreased at the beginning of the 2000's (5, 6).

Colorectal cancer is the 3<sup>rd</sup> most and 2<sup>nd</sup> most commonly diagnosed cancer in males and females respectively with 1.2 million new cases and a corresponding 600,000 estimated deaths (1, 2). The highest incidence rates tend to be in developed nations such as in Australia, New Zealand, Europe and North America (1, 2). Incidence rates have rapidly been increasing in areas of the world with historically low rates such as Eastern Asia and Europe due to the Westernization of diet and decreased activity (7, 8). The only country with significantly decreasing incidence rates in both males and females of colorectal cancer is the United States which is indicative of better and more accurate detection and removal of potential carcinogenic nodules (8, 9).

The most commonly diagnosed and leading cause of death globally in males is lung cancer (1, 2). It was the 4<sup>th</sup> commonly diagnosed cancer in females while being the second leading cause of death for women (1, 2). Lung cancer results in a total of 13% of all cancer cases globally (1, 2). The highest lung cancer incidence rates are in Westernized areas with high prevalence of smoking such as in Eastern and Southern Europe, North America, and East Asia with sub-Saharan Africa among the lowest due to lower rates and acceptance of smoking behaviors (1, 2). The highest incidence rate of lung cancer occurs in Chinese females who have rates as high as 21.3 cases per 100,000 (2). High rates in the female Chinese population are believed to reflect indoor air pollution from coal-fueled stoves or exposure to other known risk

factors such as occupational exposure to asbestos, arsenic, radon, as well as smoking (2, 10-12). The worldwide burden of lung cancer primarily results from smoking which accounts for 80% of the worldwide cases in males and roughly 50% in females, but death rates in Western countries are decreasing as a result of reduced acceptance and usage of tobacco (2, 13-16).

When considering liver cancer, 70-85% of all liver cancer cases are Hepatocellular Carcinomas (HCCs) (17). Roughly 750,000 new cases of liver cancer occurred in 2008 with a corresponding 695,900 cancer related deaths (1, 2). It is the fifth most commonly diagnosed cancer in men with a corresponding 2<sup>nd</sup> most frequently cause of cancer related death worldwide (1, 2). It is also the 7<sup>th</sup> most commonly diagnosed cancer in women and 6<sup>th</sup> leading cause of cancer related death (1, 2). The dispiriting fact is that half of all liver cancer cases and deaths worldwide occur in China (1). Chronic infection of Hepatitis B virus (HBV) has been identified as a primary effector in the development of HCC in populations of Asia or sub-Saharan Africa with 8% of the total population in these areas being chronically infected (2). Comparing developed to developing nations, HBV infection is responsible for 23% and 60% of total liver cancer cases respectively (18). Hepatitis C virus (HCV) infections lead to 33% and 20% of all HCC cases in developing and developed nations respectively (18).

## **1.2 HEPATOCELLULAR CARCINOMA**

HCC is a disease that affects many populations throughout the world, but has a higher incidence in underdeveloped regions due to a lack of infrastructure or resources to manage the disease (1, 19). In 2008 there were 748,000 new cases of HCC with corresponding 696,000 deaths (1, 19). 80% of all cases occurred in underdeveloped regions such as Eastern Asia or

Western Africa (1, 19). HCC is also present in developed nations, but at lower rates of incidence and mortality, as well as occurring under differing circumstances (2, 20). The difference in the observed incidences of HCC between developed and underdeveloped regions primarily stems from contrasting environmental and economic factors such as HBV and HCV infections, and establishment of effective medical practices for managing the disease (2, 18). Whereas underdeveloped nations are susceptible to HCC generation due do chronic HBV infection, Westernized areas of the world tend to be burdened by alcohol, obesity and diabetes related liver damage and hepatic fibrosis leading to chronic cirrhosis and ultimately HCC (21). The only known treatment of HCC, which provides significant health benefit, is liver transplantation, but unfortunately there is shortage of organs for transplantation (22, 23). Because of these statistics, HCC has become to be the seventh most common cancer in the world, as well as number three in cancer related deaths (1, 2, 19).

### **1.2.1 Major Global Risk Factors for HCC**

Most of the areas of the world that are underdeveloped have environmental risk factors which contribute to the high incidence of HCC. Many of these factors include increased incidence of HBV, HCV infections, or the presence of Aflatoxin B1 (AFB1), which are responsible for over 80% of all HCCs in these areas (1, 19, 24, 25). Chronic HBV is one of the major causes of HCC in underdeveloped areas of the world (18, 25). More than half of all HCC cases in the world are a result of HBV infection (18, 25). A study in Taiwan in the 1980s showed that men who are chronically infected with HBV are 98.4 times more likely to develop HCC than patients without the infection (26, 27). Just as well as HBV infection increases risk for development of HCC, HCV leads to chronic liver disease culminating in HCC. In another study,

12,008 men in Taiwan were observed over a period of 9.2 years that patients carrying the HCV virus had an increased risk of developing HCC about twenty times greater than individuals without the infection (28).

NAFLD is a major precursor to HCC development. It is similar to alcohol induced fatty liver damage, but can present in patients who do not readily abuse alcohol. Hepatic steatosis, or the accumulation of triglycerides in the hepatocytes, is a hallmark of NAFLD which is also strongly associated with obesity and metabolic syndrome (29). After analyzing 11 studies from countries such as the United States, Europe and Asia which contained 5,037 overweight and 6,042 obese individuals compared to normal-weight patients the odds ratios of developing HCC was 1.17 and 1.89 respectively indicating that body weight may correlate with an increased risk of developing HCC (29)

Typically subgroups of patients with NAFLD go on to develop inflammation which results in NASH. These events can further progress to fibrosis and cirrhosis that can evolve to HCC (30). When considering advanced fibrosis and cirrhosis as a result of NAFLD leading to HCC, there seems to be a dichotomy in the molecular pathogenesis of the disease depending on the environmental stimuli. Interestingly, patients with NAFLD alone have a lower risk of developing advanced cirrhosis or HCC compared to patients with chronic HCV infection with rates at 0.6% compared to 17% respectively according to a Japanese study (31). This was corroborated in another international study performed in the United Kingdom which showed HCC resulting from NAFLD related cirrhosis was 2% compared to chronic HCV induced cirrhosis at 7% incidence rates (32). However, liver cancer can also develop in NASH patients without advanced fibrosis (33, 34). A Japanese study examined patients who developed HCC as

a result of clinically diagnosed NASH and identified that 28% of 19 patients had significantly less advanced fibrosis at time of diagnosis of HCC (33).

NAFLD related HCC is increasing in Westernized nations leading to incidence rates between 17-24% (34-36). These statistics may be a result of many things, including the potential compounding effect of chronic hepatitis infection on fibrosis leading to HCC development in NASH. It has been identified that patients who present chronic HCV infections with NAFLD have a 2-3 fold greater risk of developing HCC compared to individuals without NAFLD (37-39). A study in Japan on incidence rates of patients with NAFLD alone as diagnosed by ultrasound, showed an annual rate of 0.043% and a 12 year incidence at 0.5% of HCC indicating rarity of NAFLD induced HCC, although patients with advanced fibrosis had a 25-fold increased risk of developing HCC (40). Corresponding to this, another study in the United States showed patients with NAFLD and advanced cirrhosis having increased incidence rates of HCC from 2% over 7 years to 13% over 3 years (41)

When considering the compounding effect chronic Hepatitis viral infections can have on the path to progression of HCC, obesity and other metabolic disorders, such as type 2 Diabetes, in conjunction with chronic HBV and HCV infections also increases the risk of developing HCC (42-47). A study that followed roughly 5,000 patients for 14 years with type 2 Diabetes and obesity which were chronically infected with HBV or HCV, indicated a 100-fold increased risk of developing HCC (48). Knowing that Diabetes in NAFLD patients is a prelude to HCC development, treatment with insulin-sensitizing drugs has been shown to improve hepatic histology including reducing steatosis and inflammation leading to reduced HCC risk (47, 49-51).

## **1.2.2 HCC in the United States**

Even though developing countries are at significant increased risk of developing HCC as a result of chronic HBV infection as opposed to HCV, Westernized nations such as the United States are more susceptible to hepatocarcinogenesis by chronic HCV infection rather HBV (24, 52-54). One of the causes for this is the presence of the HBV vaccination program, which exists in the United States to prevent chronic HBV infection. However, within a thirty year time span from 1975 to 2005 there was still an increase in incidence of HCC in the United States from 1.6 cases to 4.9 cases per 100,000 individuals (55). The major risk factor believed to be associated with this increased incidence of HCC in the United States is chronic HCV infection (56, 57). There are 3 million people in the United States who are chronically infected with HCV, many of whom were exposed during the 1960s as a result of poor quality blood transfusions or intravenous drug use (58, 59). Individuals carrying HCV develop chronic liver disease with 20 to 30 percent developing cirrhosis within 20 years of infection setting the stage for the development of HCC in 1 to 4 percent of individuals with cirrhotic livers every year (57, 60, 61). It is projected that the HCC patient population resulting from chronic HCV infection in the United States will increase and peak between 2015 and 2020 then gradually fall off (20, 53, 54). However, this drop off is expected to be met with an increase of incidence of HCC as a result of the growing epidemic of diabetes, obesity, and NAFLD/NASH in the United States which is still a reason for concern (62).

Cirrhosis as a result of NAFLD is predicted to surpass chronic HCV induced cirrhosis in the US within the next 5 years as the burden of HCV decreases and metabolic disorders become more prevalent (63). When considering the obesity epidemic, a study conducted on roughly 900,000 United States citizens over 16 years found that obesity will increase the risk of many

cancers, with the greatest effect being on HCC (64). Obesity also plays a role in the development of HCC in populations with advanced fibrosis or cirrhosis by about 3 to 11 fold when considering undefined cirrhosis or alcoholic induced cirrhosis respectively in a US study done on 19,271 transplant patients due to cirrhosis (65)

A population-based study using ultrasonography screens from 12,454 adults who participated in the Third National Health and Nutrition Examination Survey conducted in the United States from 1988 to 1994 on 20–74 year old individuals suggests that at least 25% of the population has NAFLD (66). The study indicated that the rates of hepatic steatosis and NAFLD in the United states were 21.4% and 19.0%, respectively, corresponding to an estimated 32.5 million adults with hepatic steatosis and 28.8 million adults with NAFLD nationwide (66). NAFLD incidence rates were highest in Mexican Americans (24.1%) followed by non-Hispanic whites (17.8%) and then non-Hispanic blacks (13.5%) with higher incidences in men (20.2%) than women (15.8%) (66). This is a large percentage of the United States population which could potentially further develop NASH followed by HCC. Studies have shown by using a liver injury marker aminotransferase that 6-8% of adults in the United States have NASH (67). 1.5-2% of the US population has cirrhosis due to NAFLD, and unfortunately 25% of patients with NASH will develop cirrhosis potentially leading to HCC causing them to succumb to liver related disease (30, 68, 69).

### **1.3 HEPATOCARCINOGENESIS**

HCC development is a process which involves multiple steps during a span of several decades (**Fig. 1**) (70). About 80% of all HCCs are a result of chronic insults to the liver from

HBV, HCV, AFB, NAFLD, or NASH resulting in hepatocyte damage, which can trigger pathways that induce fibrosis, cirrhosis and eventually lead to development of HCC (24). HBV and AFB act synergistically to alter the stability of genomic DNA causing rearrangements, breaks, and various mutations such as in the TP53 gene which interrupt the protective nature of the p53 protein (71-78). HBV along with HCV may also release viral particles that interrupt normal cell stability and metabolism (73, 74, 76). Oxidative stress, as well as nitric-oxide (NO) generation resulting from a chronic inflammatory response in the liver upon viral presentation, is also one of the underlying causes of mutations which lead to HCC development (52, 79).

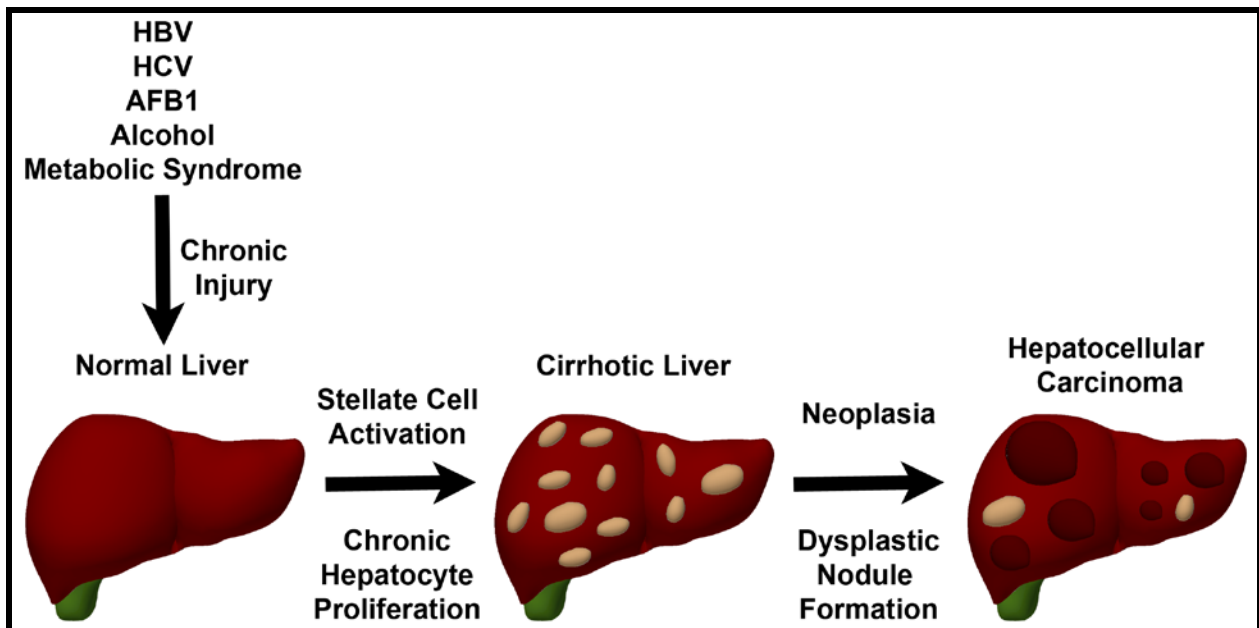


Figure 1. Pathological progression to HCC.

### 1.3.1 Stepwise process to hepatocellular oncogenesis

Identifying the causative factors of HCC requires deeper insight into the complex menagerie of signaling cascades that have an association with the aforementioned chronic

hepatitis, alcoholism, diabetes, obesity, metabolic disorders leading to oxidative stress. These underlying conditions typically lead to recurring cycles of proliferation, inflammation and necrosis that effects every cell in the liver from hepatocytes, endothelial cells, kupffer cells and activation of stellate cells which are responsible for the deposition of fibrotic matrix ultimately causing cirrhosis (80, 81). Stellate cells are the main source of matrix and collagen in the liver, and increased activation of these cells has been shown by oxidative stressors which will lead to the synthesis of collagen (82). The deposition of fibrotic matrix represents a wound healing response that eventually supports expansion of hepatocytes. Proliferating hepatocytes are easily susceptible to oncogenic mutations leading to dysplasia and onset of HCC (83). Oxidative stress can lead to hepatocarcinogenesis by several methods such as causing DNA damage and can also promote the development of fibrosis and cirrhosis. This has been corroborated in mice which overexpress PDGF-C causing the development of fibrosis and ultimately leading to HCC (84). Oxidative stress itself has been shown to be related to increased rates of oncogenic mutations such as in the p53 gene (85).

Chronic viral infection can be another mechanism which results in oxidative stress leading to HCC. It has been widely accepted that viral induced carcinogenesis is a precursor of HCC resulting from host-virus interactions, and are responsible for clearing the viral infection leading to enhanced T-cell responses contributing to hepatocyte necrosis, inflammation, and liver regeneration under chronic states which result in carcinogenesis (86-88). One potential mechanism may stem from endoplasmic reticulum (ER) stress ultimately inducing oxidative stress, and leads to activation of proliferation and survival signals thereby resulting in mutations via free radical generation culminating in stellate cell activation, which finally leads to matrix deposition and potentiation of fibrosis (89-91). HBV infection related carcinogenesis depends on

chronic versus acute infection states, of which 10% of individuals infected with HBV have a chronic response rather than acute (92). Chronic HBV infection results in continuous replication of hepatocytes leading to development and sustaining of oncogenic lesions in DNA and potential telomere erosion which all cause genomic instability. The Hepatitis B virus can also insert into host DNA and results in host microdeletions which can trigger loss of heterozygosity (LOH) in cancer relevant genes such as telomerase reverse transcriptase (TERT), platelet derived growth factor receptor  $\beta$  (PDGFR $\beta$ ), and mitogen activated protein kinase 1 (MAPK1) (93, 94).

HCV infection has a significant distinction compared to HBV infection in that chronic infection occurs in 60-80% of all cases compared to 10% in HBV (88, 95). HCV also more frequently leads to cirrhosis compared to HBV at a rate of 5-10% of cases after 10 years of chronic infection, which is 10-20 times higher than HBV (88). HCV being a chronic disease leads to constant waves of hepatocyte inflammation and necrosis leading to subsequent regeneration which tend to make cells more susceptible to developing oncogenic mutations.

The prototypical hallmarks of HCC generation such as chronic waves of inflammation, necrosis of hepatocytes, regeneration and stellate cell activation is not restricted to hepatitis infection, as can be observed in chronic alcohol consumption. In the presence of chronic alcohol, hepatocytes tend to be more sensitive to TNF $\alpha$  toxic effects which set the groundwork for the development of chronic hepatocyte cell death, regeneration, stellate cell activation, cirrhosis and ultimately HCC (96). Chronic alcohol intake has been implicated in causing the production of factors involved in inflammation and instigating increased levels of endotoxin which in turn activate kupffer cells that release chemokines and cytokines such as TNF $\alpha$ , interleukin-1 $\beta$  (IL-1 $\beta$ ), and IL6 among others which all play a critical role in hepatocyte survival (97). Alcohol also

causes oxidative stress on the liver as shown by clinicopathologic signs of alcoholic hepatitis indicated by elevated levels of isoprostane, a marker of lipid peroxidation (96).

Other environmental factors such as AFB1 have also been shown in the past to contribute to hepatocarcinogenesis by frequently causing DNA adducts, specific examples being the p53 gene as well as other well-known oncogenes such as HRAS (98-103). Counter to chronic hepatitis infection or alcohol consumption, there is little evidence that supports exposure to AFB1 leading to increased risk of developing fibrosis which will precede cirrhotic development and oncogenesis, leading to the justification that AFB1 is a primary mutagen responsible for these HCC cases. However, when HBV and AFB1 exposure coexist this leads to a 5-10 fold increased risk of developing HCC compared to exposure of only one of these factors (104). Mechanistic data in this field falls short, but it is reasonable to believe that the genetic mutations resulting from AFB1 exposure will give an oncogenic advantage to cells dividing in response to the chronic cell death from HBV infection.

### **1.3.2 Biochemical Pathways known to be involved in HCC**

Analysis of oncogenic biochemical pathways in a heterogeneous disease such as HCC leads to many challenges in deciding the significance of said pathways, but also indicates the importance of developing targeted therapies. For example, p53 is an antiapoptotic regulator, and although it is widely accepted that p53 mutations are relevant to hepatocellular oncogenesis, whether it plays a role in initiation or promotion of the disease remains less well defined. (105, 106). Depending on whether HCC development is in the context of HBV, HCV or AFB1, p53 LOH mutations give mixed results in determining its role as an initiator or an oncogenic promoter (98, 99, 107-110). p53 mutations occur at relatively low frequency in HCC, but is

frequently induced when underlying conditions exist such as AFB1 exposure is present at about 50% of all cases for example (100). p53 mutations can occur in HCV induced HCC versus HBV induced HCC at 13% and 53% respectively (111).

Underlying HBV infection can induce a multitude of signaling pathways which are all related to oncogenesis. The HBV Protein-X (HBx) can bind and inactivate the tumor suppressor p53 by sequestering it in the cytoplasm inhibiting its nuclear functions of promoting cell survival (98, 107, 112). HBx can also alter the expression of several important kinases such as Ras, Raf, MAPK, ERK, and JNK among others involved in cell survival and proliferation (113-115) (116-118). Increasing evidence has directly linked HBx protein to hepatocarcinogenesis by showing its overexpression can lead to HCC (107). Another specific pathway that HBx has been shown to influence is the Wnt/ $\beta$ -catenin signaling pathway (119, 120). Several studies have shown that HBx protein is capable of interrupting the E-cadherin- $\beta$ -catenin interactions at the membrane leading to subsequent induction of Wnt related pro-survival and proliferation genes (120-122).

Other etiologies of HCC, such as HCV and chronic alcohol consumption, result in aberrant signaling activation as well such as in the MAPK pathway components ERK, MEK and Raf. It can also activate other oncogenic signaling pathways such as the signal transducer and activator of transcription 1 (STAT1), which deregulates INF $\gamma$  activation, thus interfering with protective interferon signaling thereby contributing to increased risk of carcinogenesis (123) (124, 125). DNA methylation events have also been implicated in HCC development (126-129). Specific hypermethylation events in HCC have occurred in genes such as p16(INK4a), E-Cadherin, COX2 among others, which increase in expression once HCC cells in culture are treated with demethylating agents (130-132). These factors are specifically involved in the

regulation of cell senescence therefore suggesting epigenetic silencing via methylating events are very much apparent in HCC as they are in other cancers.

Even though diabetes and obesity have shown a significant correlation in NAFLD related liver disease, the molecular pathogenesis of the disease progression is not clearly understood. There is however a link between PI3K activity being activated by insulin (133, 134). PI3K is a signaling pathway which mediates cellular processes such as metabolism, growth, and survival. Amplification and enhanced signaling activity in the PI3K pathway are commonly found in many cancers which include HCC (135). With this being said, it is possible that increased insulin production in a diabetic state may intensify hepatocyte proliferation during steatosis potentially leading to the development of HCC.

Another molecular characteristic of NAFLD induced HCC is that levels of des- $\gamma$ -prothrombin tend to be higher compared to  $\alpha$ -fetoprotein (136). High  $\alpha$ -fetoprotein expression is a traditional hallmark of HCC, and this tells us that des- $\gamma$ -prothrombin might be a great indicator to differentiate NAFLD induced HCC for personalized therapy (137, 138). Identifying the molecular indicators leading to HCC are the most promising advances in terms of trying to develop an effective targeted therapy. For example, genome wide association studies have shown that the phospholipase domain containing 3 (*PNPLA3*) gene may lead to NAFLD induced HCC resulting from a genetic mutation in this protein which increases the risk of developing cirrhosis thereby increasing the risk of HCC (139).

NAFLD, obesity and diabetes all share in common a chronic inflammatory state during which NF- $\kappa$ B has always been known to be classically activated during chronic inflammatory states (140). NF- $\kappa$ B has been shown to have a hand in hepatic steatosis, insulin resistance, inflammation, fibrosis and cancer by the interaction of cofactors in the nucleus which induce the

production of specific cytokines and factors that play a role in chronic inflammatory responses (141-144). A study using mice deficient in NF- $\kappa$ B signaling and fed methionine and choline deficient (MCD) diet, which has been classically known to induce NASH, showed that mice lacking NF- $\kappa$ B signaling experienced exacerbated inflammation and fibrosis which were caused by an upregulation of interleukin-15 (IL-15) expression (145). In an independent study, mice deficient in NF- $\kappa$ B signaling specifically in hepatocytes strongly enhances the development of diethylnitrosamine (DEN), a known chemical carcinogen used to induce HCC, related liver cancer (146).

Another major molecular mechanism in liver biology is the folate driven one-carbon metabolism. One-carbon metabolism is a metabolic network of pathways which exists in different compartments within the cell which include the cytoplasm, mitochondria, and nucleus. One-carbon metabolism in the cytoplasm is required for the synthesis of purines and thymidylate and the remethylation of homocysteine to methionine. One-carbon metabolism in the mitochondria is required for the synthesis of formylated methionyl-tRNA; the catabolism of choline, purines, and histidine; and the interconversion of serine and glycine (147). One-carbon metabolism is regulated by intracellular levels of folate and methionine, and deregulation of this pathway has been linked to increased risk of developing cirrhosis leading to HCC as indicated by reduced levels of *S*-adenosylmethionine (SAME), the key methyl group donor in mammalian cells (148). The synthesis and activity of SAME are regulated by methionine adenosyltransferase (MAT) and glycine *N*-methyltransferase (GNMT), respectively (149-152). Knockout mice of either of these enzymes have been shown to be essential in the development of NAFLD related HCC (153-155). The MAT protein is encoded by two genes, *MAT1A* and *MAT2A*. Interestingly,

there is evidence that 60% of patients with cirrhosis have reduced expression of *MAT1A*, and it is also frequently silenced in HCC (156, 157).

#### 1.4 WNT/ $\beta$ -CATENIN SIGNALING

The canonical Wnt/ $\beta$ -catenin signaling pathway is an evolutionary conserved signaling pathway with many important functions during development and in adult homeostasis. Wnts are secreted cysteine rich glycoproteins from epithelial, mural, or endothelial cells, which bind to receptor Frizzled (Fzd) and co-receptor low-density lipoprotein receptor related protein (LRP) 5 or 6 (158). This initiates a cascade of events beginning with the activation of an intracellular protein called Disheveled (Dvl) which subsequently causes inactivation of a degradation complex composed of glycogen synthase kinase-3 $\beta$  (GSK-3 $\beta$ ), adenomatous polyposis coli (APC), and Axin (159-166). GSK-3 $\beta$  has been shown to be the gatekeeper of Wnt/ $\beta$ -catenin signaling, and once active it phosphorylates  $\beta$ -catenin at specific sites at the amino-terminus, targeting it for proteasomal degradation (161-163). However, in the presence of Wnt signal, the degradation complex is inactivated,  $\beta$ -catenin builds up in the cytoplasm and promptly translocates into the nucleus where it can interact with histone acetyl transferases such as cAMP response element-binding protein (CREB)-binding protein (CBP) and p300, transcription factors belonging to T-cell factor/lymphoid enhancing factor (TCF/LEF) family or co-factors such as B-cell CLL/lymphoma 9 (BCL-9) protein which in turn regulate the transcription of specific target genes (**Fig. 2**) (167-170). Several different factors have been shown to be subject to  $\beta$ -catenin regulation such as Cyclin D1, c-myc, glutamine synthetase (GS), and others that play a role in cell cycle, migration, survival and metabolism (171-173). In absence of Wnt signal,  $\beta$ -catenin is

phosphorylated at specific serine and threonine residues in exon-3, making it a target of ubiquitin-proteasome degradation.

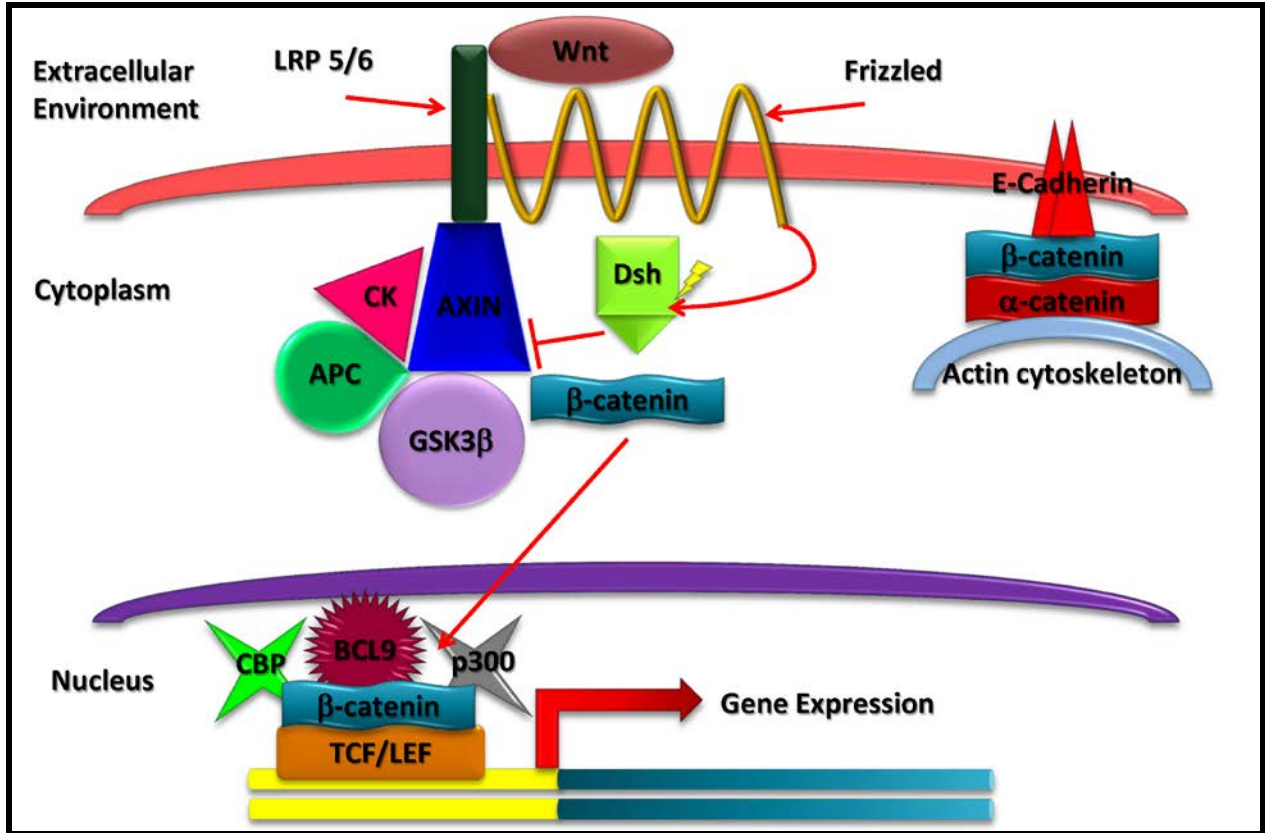


Figure 2. Schematic representation of Wnt/ $\beta$ -catenin signaling pathway.

#### 1.4.1 Wnt/ $\beta$ -catenin signaling in HCC

Understanding the molecular role Wnt/ $\beta$ -catenin signaling plays in HCC development is critical in the development of effective therapies against aberrant Wnt signaling. Because of the role  $\beta$ -catenin has in regulating cellular proliferation, it is considered an oncogene in specific cancers such as colorectal and HCC (163, 171, 173-175). Some studies indicate  $\beta$ -catenin overexpression and mutations are related to early onset HCCs, as well as its involvement in

disease progression (176, 177). With this being said,  $\beta$ -catenin activation seems to be playing an ambiguous role between disease initiation and disease progression, which is a field in need of deeper characterization. However, in terms of underlying HBV and HCV infection, overexpression and mutational changes in  $\beta$ -catenin occur more frequently in HCV related HCCs than HBV related HCCs (178-180). It has also been suggested that  $\beta$ -catenin mutations are typical in HCCs that are not characterized by genomic instability because studies have shown that HCCs possessing high rates of LOH exhibit low levels of  $\beta$ -catenin activating mutations (181, 182). This indicates the potential for deregulated  $\beta$ -catenin signaling to be a specific causative factor in the development of HCCs.

$\beta$ -catenin mutations and increased nuclear localization have been detected in human HCCs. In primary HCC, mutations in the *CTNNB1* gene leading to aberrant activation occur in about 10-30% of cases, while total upregulated Wnt signaling activation can occur in about 40-60% of all HCC cases (163, 175, 180, 183-190). Mutations in the *CTNNB1* gene which render  $\beta$ -catenin constitutively active occur due to either a mutation causing a truncation at the amino-terminus, or point mutations of critical serine/threonine residues, ultimately resulting in hypophosphorylated  $\beta$ -catenin (163, 175, 189, 190). The signaling pathway is highly regulated, but a mutation, alteration, or a truncation in specific parts of the gene lead to non-degradable  $\beta$ -catenin protein causing its constitutive activation, resulting in over-expression of downstream targets (163, 171-173, 175). Under specific conditions it is possible to selectively activate the Wnt/ $\beta$ -catenin signaling pathway such as in the case of c-myc and E2f1 transgenic mice (191). These transgenic mice have been shown to resemble human HCC, and frequently result in genetic mutations in  $\beta$ -catenin (191).

We have shown aberrant intratumoral  $\beta$ -catenin stabilization in 33% of HCC cases with 9% showing predominant nuclear with some cytoplasmic (N/C) localization and 24% displaying predominant cytoplasmic with occasional nuclear (C/N) localization (192). Identification of this aberrant  $\beta$ -catenin localization correlated with various tumor attributes such as reduced fibrosis, increased GS, increased inflammation and increased tumor cellular proliferation, making it an attractive target for treatment in a specific group of HCC patients.

## **1.5 CURRENT THERAPEUTIC STRATEGIES FOR HCC**

Current methods of treating primary HCC are slim with the majority of cases using a multi-tyrosine kinase inhibitor known as Sorafenib to combat the disease. Surgical resection including partial hepatectomy tends to be the most common method of treatment, and also potentially leads to disease regression with improved five years of disease-free survival (22). Orthotopic liver transplantation is another treatment modality when applicable. The only caveat to this procedure is the apparent lack of donor organs. As discussed in previous sections, HCC is a highly heterogeneous disease resulting from a multitude of aberrant signaling activations in part from etiological differences of underlying diseases. There are significant differences in progression to HCC between, for example, chronic HBV infection and NAFLD related HCCs, but the underlying molecular mechanisms leading to oncogenesis in each case do share some commonalities allowing for targeted therapies to be beneficial for all.

### 1.5.1 Sorafenib and TACE in HCC

Physicians have taken advantage of the fact that HCC is a highly vascularized tumor deriving its blood supply from chiefly the hepatic artery. Since liver has a dual blood supply with most of its supply from portal vein, a technique was developed which utilizes impeding the flow of the hepatic artery to the tumor called Trans-arterial Chemoembolization (TACE) (193). TACE delivers chemotherapy locally to the site of the primary HCC, and more frequently includes the use of beads laced with Doxorubicin to patients who have an unresectable HCC and patients ineligible for transplantation. TACE has been an effective means to control HCC. However, since TACE causes hypoxia in the tumor, these hypoxic events lead to production of angiogenic signals such as VEGF-A. These events occur temporarily after TACE as early as a few hours after intervention, which can ultimately reduce TACE's efficacy (194-197). Combined with the fact that HCCs show increased expression of VEGFRs and PDGFRs, which are involved in angiogenic signaling, clinicians suggest that anti-angiogenic intervention during TACE may be beneficial to its effectiveness (198-200).

Sorafenib is a multikinase inhibitor and targets these specific receptors, and has shown to be modestly effective in terms of increasing the survival of patients with HCC (201, 202). However, a Phase III clinical trial which included the use of traditional TACE followed by administration of Sorafenib 1-3 months following TACE failed to show any survival benefit (203). Only when Sorafenib was combined with TACE administered Doxorubicin-eluting beads (DEBs) in a Phase II clinical trial, it showed the first evidence that combined therapy is beneficial in HCC patients with unresectable cancer leading to a 95% disease control rate and roughly 60% of tumors responding to treatment (204). In fact combinatorial therapy of Sorafenib and TACE has been shown to increase tumor shrinkage from 29% to 62% in patients treated with

a placebo or Sorafenib respectively (205). Since Sorafenib has minimal efficacy where it only has a 3 month added median benefit to survival, more effective molecular therapeutic strategies are needed (201). Unfortunately in cancer, inhibition of one signaling pathway can potentially lead to feedback activation of another oncogenic pathway, which is why multidirectional therapeutics is potentially the best course of treatment (206).

Single agent therapies have modest disease control, but it is widely accepted that combination therapeutics may provide the best course of treatment. Combination therapies using TACE and anti-angiogenic therapies are becoming increasingly common in clinical trials. An example is the use of Axitinib, a multi-Tyrosine Kinase Inhibitor (TKI) of VEGFR1, VEGFR2, VEGFR3, PDGFRs, and c-kit in unresectable HCC (NCT01352728) (207). Sorafenib currently has been combined with a multitude of therapeutic agents in order to identify the most effective combinatorial avenue such as Erlotinib, an EGFR inhibitor, which are in different phases of clinical trials (NCT00901901) (205, 207-210).

### **1.5.2 Current clinical trial developments**

Granted that cirrhosis is a clinicopathologic precursor to HCC, this condition makes following HCC clinically difficult due to biological complications. A preliminary development in following HCC patients has shown that analysis of systemic alpha-feto protein (AFP), a serum glycoprotein secreted in approximately 70% of HCCs, following therapeutic intervention showed a 30% reduction in levels in serum and correlated with increased survival (211). Not only are better methods of detecting and mediating HCC, better methods of therapeutic intervention, many TKIs, are being developed during clinical trials for HCC intervention. Sunitinib is a multi-TKI receptor inhibitor that targets VEGFRs, PDGFRs and c-kit in Phase III of clinical trials

(212). Brivanib is a dual VEGFR and FGFR inhibitor which has moved into Phase III clinical trials as well for unresectable, advanced or metastatic HCC, and has shown to have a decent effect on increasing overall survival in HCC patients by about 10 months and the median progression free survival in patients was about 3 months (213, 214). Brivanib is currently undergoing deeper investigation into therapeutics compared to Sorafenib in an ongoing current clinical trial directly comparing the two systemic therapies (BRISK-FL NCT00858871) as well as being used in another clinical trial in patients who have failed with Sorafenib treatment (BRISK-PS NCT00825955) (207).

Anti-angiogenic therapeutics have also been explored as a possible treatment avenue for HCC patients. Bevacizumab, a monoclonal antibody targeting VEGF-A, has been used in Phase II clinical trials for HCC showing a response in 13% of cases, however complications arise using this type of treatment in patients with severe cirrhosis as they experience increased risk of hemorrhage leading to grade 3 toxicities (215). Ramucirumab is another monoclonal antibody however it targets VEGFR2, the active receptor for VEGF-A, which has been applied in HCC patients. In a Phase II clinical trial, Ramucirumab has shown a response in 43% of patients in the trial, as well as an increased progression free survival rate at 4.3 months with a median overall survival of 12 months (216). Currently a Phase III clinical trial using Ramucirumab is planned in patients who have already undergone Sorafenib therapy (NCT01140347) (207).

Targeting EGFR has been postulated to be an avenue to pursue in HCC therapeutics. However clinical trials using approved EGFR TKIs Gefitinib, Erlotinib, and Lapatinib in Phase II clinical trials only showed response rates ranging from 0%-9% with progression free survivals also minimally ranging from roughly 2-3 months (217-220). Another EGFR inhibitor, Cetuximab, showed no disease response as well as progression free survival at less than 2

months in Phase II clinical trials indicating that if an EGFR inhibitor were to be pursued for HCC it may be wise to validate the whether or not EGFR is playing a critical role in the disease prior to administration of an EGFR TKI (221). Combinatorial therapy using Bevacizumab and Erlotinib, which will target both VEGF-A and EGF signaling, have been investigated in HCC with differing results. One study has showed the combination results in 25% tumor response with average progression free survival at 9 months and overall survival benefit at roughly 16 months, but another study conducted in Asia with a significantly lower response, which may result from molecular differences of underlying chronic conditions leading to HCC development (222, 223).

c-Met is a surface receptor in hepatocytes which, when in the presence of hepatocyte growth factor (HGF), can activate intracellular kinase pathways to induce cellular proliferation. It is upregulated in roughly 20% of human HCCs (224, 225). ARQ197 is a TKI inhibitor of c-Met and has undergone Phase I clinical trials to show that inhibition of c-Met signaling results in HCC disease stabilization and some patients even continue to have disease stabilization after 4 months of therapy with minor toxicity and having a wide range of time to progression in disease ranging from 3 to 42 weeks (226). There is a current Phase II clinical trial ongoing comparing ARQ197 to placebo in patients with unresectable HCC who have previously failed other avenues of treatment (NCT00988741) (207). Another TKI inhibitor of c-Met which also targets VEGFR2 called Foretinib is undergoing Phase I safety trials for patients who have failed a first line method of treatment (NCT00920192) (207).

The PI3K/Akt/mTOR signaling cascade has been known to be oncogenically activated in multiple cancer types, and components of this pathway have been shown to be aberrantly activated in 40-50% of all HCCs (227, 228). An mTOR inhibitor, Everolimus, has undergone Phase I clinical trials in 28 patients with advanced HCC which have undergone previous

treatments. In these cases, disease control was 44% and median survival was 8.4 months after therapeutic intervention (229). Currently, Everolimus is undergoing Phase III clinical trials in individuals who have failed Sorafenib therapy (NCT01035229) (207). An additional mTOR inhibitor, Temsirolimus, is currently undergoing Phase II clinical trials in patients with histologically positive HCC (NCT01251458) (207).

Downstream signaling cascades resulting from aberrant RTK activity is critical to developing oncogenesis, and one significant pathway which is involved in a multitude of cancers is the Ras/Raf/MAPK pathway. It is aberrantly active in 50 – 100% of all HCCs, and when HCC cells in culture are treated with MEK1/2 specific inhibitors U0126 and PD98059 led to significant cell growth inhibition and apoptosis (230). A MEK1/2 inhibitor, Selumatinib, has undergone Phase II clinical trials where there was no response to the therapy as well as a depressing progression free survival of only 1.4 months indicating again that even though a critical RTK pathway may be targeted, the disease may progress to a point where it can rely on alternate pathways for survival (231).

Epigenetics studies the modification of gene expression occurring without mutagenic alteration in the nucleotide sequence. The two key epigenetic mechanisms are hypermethylation and histone acetylation (232). Specific underlying conditions such as chronic HBV infection has been associated with increase rates of hypermethylation in CpG islands in dysplastic, early onset HCCs leading to the realization that epigenetic changes are part of the oncogenic process in HCC development (233). Histone deacetylases (HDACs) are responsible for controlling the coiling and uncoiling of DNA via acetylation of the histones which condense the DNA. It is possible to control both methylation and acetylation events as shown in numerous preclinical models where use of HDAC inhibitors can lead to HCC cell death as a result of reactivation of tumor

suppressor genes (234-236). A Phase II clinical trial has been completed using the HDAC inhibitor Belinostat in patients with advanced HCC who have had another form of therapeutic intervention. Disease stabilization occurred in roughly 48% of patients in the trial, with a disease free progression of roughly 3 months while increase overall survival of about 7 months without major grade toxicities (NCT00321594) (237).

### **1.5.3 Preclinical Developments**

There are several additional TKIs in preclinical development that target VEGFRs, PDGFRs, and FGFRs such as SU6668/TSU-68 and Dovitinib, which have been shown to be effective in reducing angiogenesis as well as disease burden in preclinical tumor models (238-241). Dovitinib is currently being evaluated in comparison to Sorafenib therapy in phase II clinical trials (NCT01232296) (207). However, without molecular classification and identification of driver oncogenes in HCC effective therapies for controlling HCC are still beyond our reach (242).

Current therapeutic strategies are beginning to take advantage of specific pathways which are upregulated in HCC, such as the Wnt pathway, or pathways which lead to a biological event which HCC has become addicted to, such as angiogenesis. A current study done in vitro and in vivo showed that a combination therapy of interferon- $\alpha$  and 5-fluorouracil inhibited HCC tumor angiogenesis by reducing VEGF and angiopoietin 1 and 2 (Ang1 and Ang2) levels (243).  $\beta$ -catenin has been targeted by various groups in several different methods in vitro as well as in vivo (244-246). One study examined the role of cyclooxygenase-2 (COX-2) in inhibiting  $\beta$ -catenin activity in HCC cell lines (244). It was shown that in the presence of Celecoxib, COX-2 inhibitor, and R-Etodolac, a nonsteroidal anti-inflammatory drug, that Wnt signaling in HCC cell

lines was significantly diminished as well as the production of downstream targets of  $\beta$ -catenin (244). Another independent group has shown the development of a novel, small molecule, ICG-001, which was shown to significantly reduce  $\beta$ -catenin activity in colon cancer cell lines at 5  $\mu$ M doses (245). Currently, a second generation of ICG-001, PRI-724, is undergoing multiple Phase I and Phase II clinical trials for pancreatic adenocarcinoma, solid tumors, and for myeloid malignancies respectively (NCT01764477) (NCT01302405) (NCT01606579).

These studies elucidate and suggest the potential to utilize  $\beta$ -catenin as a potential therapeutic target in HCC. Considering that  $\beta$ -catenin highly regulates many factors which control angiogenesis, one might think that a therapy which targets  $\beta$ -catenin in HCC will not only slow down the proliferative potential of the tumor cells, but also inhibit the growth of new vasculature into the tumor, which will in turn choke the growth of HCC. All of these factors point to the strong idea that a therapy which will target  $\beta$ -catenin will also target angiogenesis in a growing HCC mass providing a multiple step therapy which in the end will be more effective than targeting a single therapeutic aspect.

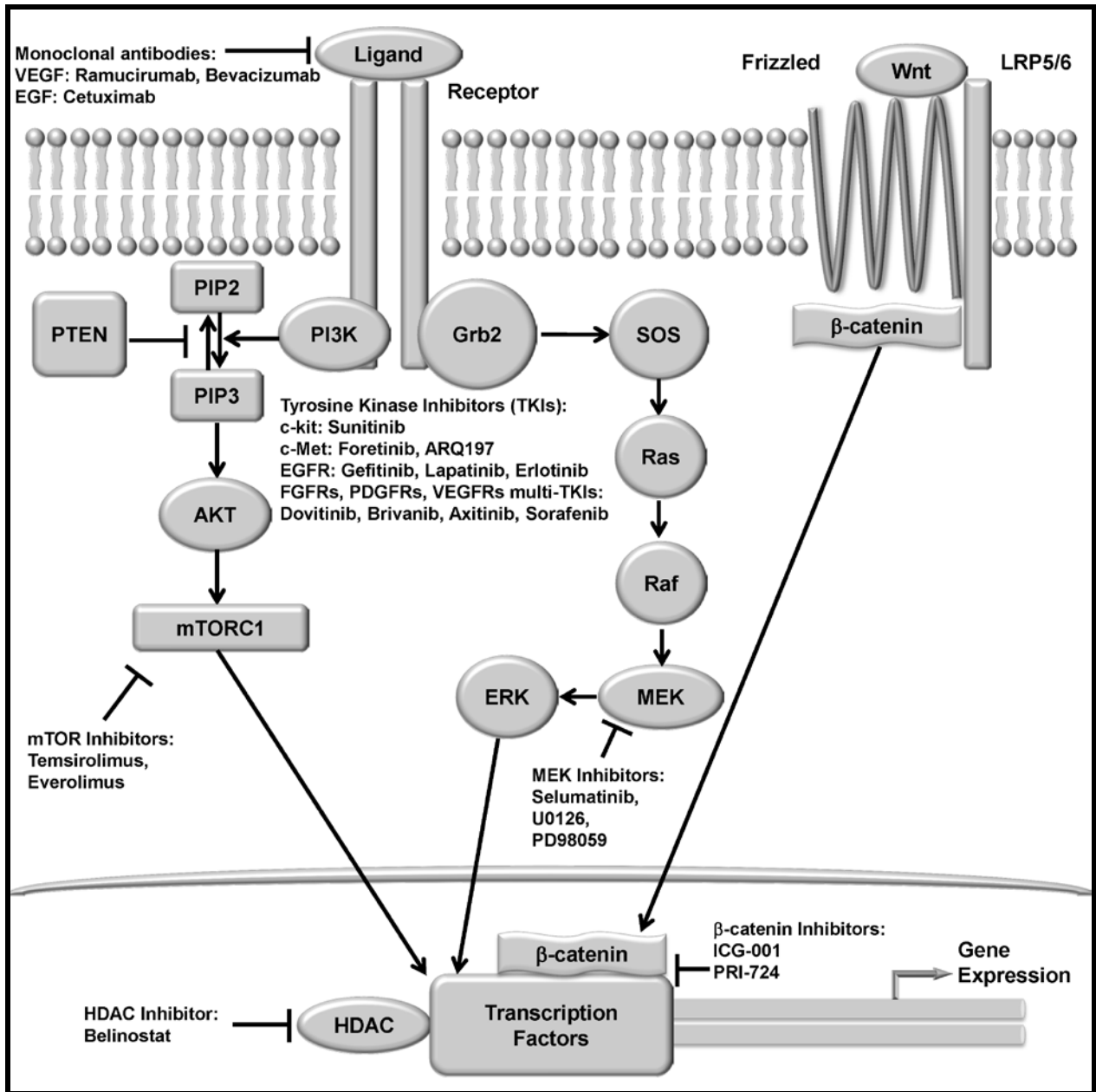


Figure 3. Outline of molecules and respective targeted sites of action currently under investigation for therapeutic benefit in clinical and pre-clinical models.

## 1.6 CURRENT CONTRIBUTIONS OF BETA-CATENIN TARGETED THERAPEUTICS IN HCC

With the current global prevalence and future trends in HCC incidence, a new modality of therapy is required to combat the disease. Knowing the importance and potential implications  $\beta$ -catenin directed therapeutics may have on HCC we were inspired to try multiple avenues in targeting  $\beta$ -catenin and aberrant Wnt signaling in HCC. Our lab has already shown that targeting  $\beta$ -catenin via silencing RNA (siRNA) leads to significant cell growth inhibition as well as apoptosis in HCC cells *in vitro* {Zeng, 2007 #131}. We now believe that targeting active Wnt signaling in HCC specifically is possible and will be a useful targeted therapy for a subset of tumors (247). Considering how there is no Wnt/ $\beta$ -catenin targeted therapeutic approved for use in the clinic, or even undergoing clinical trials for HCC, we believe there is a significant need to develop a therapy for the 40-60% of patients with aberrant HCC.

Chapter one will discuss the development of a SM inhibitor, which much like **ICG-001**, inhibits activated Wnt/ $\beta$ -catenin signaling in HCC cells as well as in zebrafish. This SM, **PMED-1**, inhibits  $\beta$ -catenin/CBP interaction, causing a decrease in  $\beta$ -catenin driven downstream targets leading to a significant inhibition of HCC cell growth and survival *in vitro*. The second chapter will discuss the synthesis, development, and characterization of a novel type of antisense nucleic acid called the peptide nucleic acids (PNAs). PNAs are unique in that they can enter into cells passively and affect target gene expression directly with little to no off target toxicity *in vitro* (248). We utilize PNA directed against  $\beta$ -catenin to diminish its expression in HCC cells, and much like the use of siRNA, HCC cells succumb to  $\beta$ -catenin knockdown secondary to decreased expression of its targets that in turn led to reduced survival and proliferation. Finally,

chapter three discusses another antisense technology for targeting  $\beta$ -catenin *in vivo* in HCC. Locked Nucleic Acids (LNAs) are a timely and novel means that very effectively affect gene expression and have the advantage of being stable and specific and currently in various phases of clinical trials for genes such as miRNA-122. We, for the first time show that an LNA-directed against  $\beta$ -catenin dramatically decreased tumor burden in mice in a model where HCC occurred secondary to  $\beta$ -catenin gene mutations. Altogether, these data demonstrate the significant potential and need for  $\beta$ -catenin directed therapeutics for patients with activated Wnt signaling. Development of agents targeting  $\beta$ -catenin may pave the way towards personalized therapies in HCC patients who specifically have aberrantly active Wnt signaling.

## **2.0 IDENTIFICATION AND CHARACTERIZATION OF A NOVEL SMALL MOLECULE INHIBITOR OF BETA-CATENIN SIGNALING IN HEPATOCELLULAR CANCER CELLS**

The following body of work focuses on identifying a novel small molecule inhibitor that resembles **ICG-001**, a previously described SM inhibitor of Wnt signaling, to target  $\beta$ -catenin in HCC cells. By applying a cost-effective, efficacious, and simplistic method of SM identification rather than traditional high-throughput screening we show that based solely on the structure of **ICG-001**, we were able to identify two SMs that significantly inhibit  $\beta$ -catenin activity. One of these compounds labeled hereon as **PMED-1** showed no toxicity to primary human hepatocytes and lacked any off target effects. We further show that **PMED-1**, like **ICG-001**, inhibits  $\beta$ -catenin signaling by not altering  $\beta$ -catenin expression but rather by impeding  $\beta$ -catenin-CBP interactions, which in turn affects tumor cell proliferation and viability in multiple HCC cell lines. Thus our findings highlight the relevance of similarity searches in streamlining drug discovery and at the same time report discovery of a prospective SM that may be effective against  $\beta$ -catenin in HCC cells.

## 2.1 IDENTIFICATION OF SMALL MOLECULES TARGETING WNT/BETA-CATENIN SIGNALING

**ICG-001** is a SM, which significantly reduces  $\beta$ -catenin activity in colon cancer cell lines at 5  $\mu$ M concentration (245). **ICG-001** and its next generation derivative PRI-724, which is in phase I clinical trials, inhibits  $\beta$ -catenin signaling by blocking  $\beta$ -catenin-CBP interactions (249). Using an agent similar to **ICG-001** will be of high relevance in 30% of HCCs where point mutations in exon-3 of the *CTNNB1* gene affect key serine/threonine residues rendering  $\beta$ -catenin stable and constitutively active (163, 175, 189, 190). In this subset, mutant  $\beta$ -catenin targeting in the nuclei to impair its interactions with CBP to impair expression of several target genes in the tumor will be of high therapeutic relevance.

### 2.1.1 Structural similarity search reveals ICG-001 analogs

Recognition of small molecules by proteins is largely mediated by molecular surface complementarities. Structure-based drug design approaches use this as the fundamental guiding principle, i.e., closely related molecules will elicit similar activity in a biological assay (250, 251). Our starting point was to identify compounds similar to **ICG-001** that would serve as structural analogues by screening the drug-like subset of the ZINC 8.0 database (approximately 3.5 million compounds) (**Fig. 4A**) (252). This search yielded a large number of around 13,400 compounds, which were sorted by similarity score. We retained 24 compounds that showed a similarity score of almost 70%.

### 2.1.2 *In silico* toxicity prediction reveals promising small molecules

Since most failures in clinical trials result from issues related to drug pharmacodynamics and pharmacokinetics, all state-of-the-art drug discovery strategies and programs now incorporate the evaluation of absorption, distribution, metabolism and excretion (ADME) and toxicological (Tox) properties early in the discovery process to mitigate this risk. Next, we applied an *in silico* ADME/Tox filtering to prioritize the compounds for purchase and further characterization. Twenty out of the 24 compounds passed all the ADME/Tox filters and the structure of the top 2 molecules labeled as **PMED-1** and **PMED-2** along with the structure of **ICG-001** are shown (**Fig. 4B-D**).

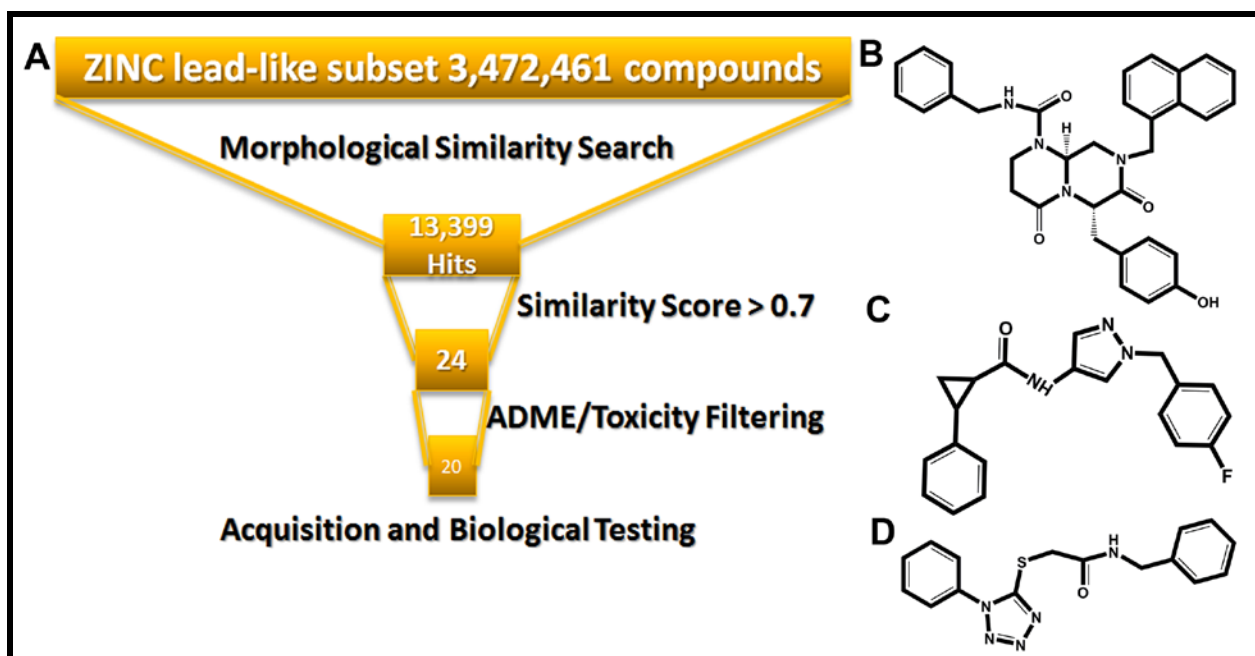


**Figure 4. Computational approach and structures of investigated small molecules.** (A) Using the ZINC 3.0 database we were able to identify 13,399 small molecules structurally similar to **ICG-001** available for purchase. A similarity score of 70% restricted the hits to 24 molecules, of which 20 passed *in silico* ADME/Toxicity

filtering, which were subsequently purchased for biological testing. **(B)** Chemical structure of **ICG-001**. **(C)**

Chemical structure of **PMED-1**. **(D)** Chemical structure of **PMED-2**.

## 2.2 BIOLOGICAL VALIDATION OF LEAD SMALL MOLECULES

To generate a biologically active complex that can regulate expression of downstream target genes such as Cyclin-D1, c-myc, GS, and VEGF-A, (171-173, 253)  $\beta$ -catenin not only must interact with transcription factors like TCF4, but recruits other essential transcriptional regulators such as histone acetyl transferases, one specifically being CBP.  $\beta$ -catenin signaling is active in a significant subset of HCC patients due to multitude of causes various proof of concept studies have shown therapeutic efficacy of inhibiting  $\beta$ -catenin as a treatment strategy for this tumor type, both in vitro and in vivo (244, 246, 248, 254). However, developing an effective small molecule from *in silico* to bench to bedside all has its challenges due to complexity of biological systems. In the current study, we took an *in silico* approach to identify **PMED-1** to then validate in HCC cells and eventually tested its efficacy *in vivo* in zebrafish to discover a novel SM that effectively inhibits Wnt/ $\beta$ -catenin.

### 2.2.1 Identifying small molecules capable of inhibiting Wnt/ $\beta$ -catenin signaling *in vitro*

In order to characterize the effectiveness of the top two SMs in inhibiting  $\beta$ -catenin/TCF activity, we utilized human hepatoblastoma cell line (HepG2), which harbors constitutively active  $\beta$ -catenin due to monoallelic deletion in exon-3 of *CTNNB1*, by TOPFlash luciferase reporter assay (255). HepG2 cells were treated with 2% **DMSO**, 200  $\mu$ M **PMED-1**, or 200  $\mu$ M

**PMED-2** for 24 hours. A 50% or 80% decrease in TOPFlash reporter activity was observed following **PMED-1** or **PMED-2** treatment respectively (**Fig. 5A**). When primary hepatocytes were treated with 200  $\mu$ M of either **PMED-1** or **PMED-2** in comparison to 2% **DMSO** control for 18 hours, there was no change observed in cell viability as assayed by MTT assay (**Fig. 5B**). However at 48 hours, while **PMED-1** showed no toxicity, **PMED-2** led to a significant decrease in hepatocyte viability by MTT assay (**Fig. 5B**).

### **2.2.2 Toxicity studies reveal PMED-1 to be top candidate**

Since **PMED-1** was non-toxic to primary human hepatocytes, we further assessed its impact on HepG2 cells. Treatment of these cells with 200  $\mu$ M **PMED-1** led to a significant cell death as observed by live cell imaging showing normally spread viable hepatocytes in control versus clumped, rounded cells in **PMED-1** treated cultures (**Fig. 5C**). This was further validated at a lower dose when 100  $\mu$ M **PMED-1** treatment of HepG2 cells for 24 or 48 hours led to around 30-35% reduction of viability by MTT assay (**Fig. 5D**). These results indicate that although both **PMED-1** and **PMED-2** decrease  $\beta$ -catenin activity, only **PMED-1** is selectively toxic to HepG2 cells and not primary hepatocytes.

## **2.3 INVESTIGATING TIME AND DOSE DEPENDENCY OF PMED-1**

Drug stability and activity is full of complex intricacies which make identifying the true effectiveness of a SM challenging. In order to tease out the possible effectiveness of a SM, dose dependency and time course studies are the traditional way to figure out how long a molecule

will retain its activity, as well as the optimal dose. The ideal goal in this aspect is to reach what is now known as the half maximal inhibitory concentration ( $IC_{50}$ ). The  $IC_{50}$  will give an idea of what concentration and how long the duration of treatment will be resulting in 50% reduction in a specific characteristic of interest such as activity or viability.

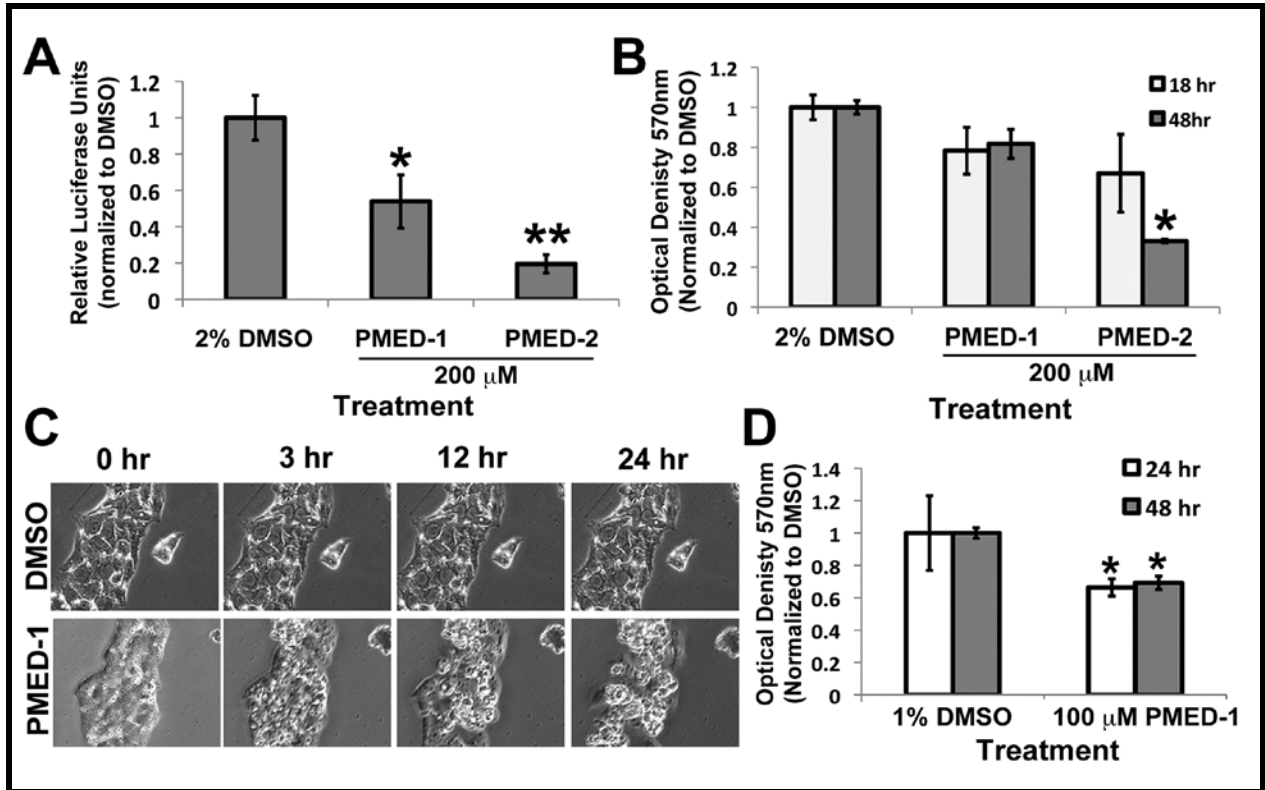


**Figure 5. Effect of PMED-1 and PMED-2 on HepG2 cell line and normal human hepatocytes.** (A) HepG2 cells treated with 200  $\mu$ M PMED-1 or 200  $\mu$ M PMED-2 for 24 hours show significant decrease in TOPFlash luciferase reporter activity as compared to 2% DMSO treatment. (B) Primary hepatocytes treated with 2% DMSO, 200  $\mu$ M PMED-1 or 200  $\mu$ M PMED-2 for 18 or 48 hours show a significant decrease in viability by MTT assay only after PMED-2 treatment for 48 hours. (C) HepG2 cells treated with 200  $\mu$ M PMED-1 for 24 hours monitored by live cell imaging using Nikon Eclipse Ti live cell imager shows notable morphological changes reminiscent of cell death as early as 3 hours after treatment when compared to the 2% DMSO-treated controls. (D) HepG2 cells treated for 24 or

48 hours with 100  $\mu$ M **PMED-1** leads to a significant decrease in cell viability as assessed by MTT assay as compared to 1% **DMSO** control.

### 2.3.1 Wnt/ $\beta$ -catenin activity assay studies **PMED-1** efficacy

We performed dose response of **PMED-1** using the TOPFlash reporter activity in HepG2 cells. HepG2 cells were treated with **PMED-1** for 24 hours at a concentration ranging from 200  $\mu$ M to 500 nM. A significant decrease in TOPFlash reporter activity was only observed at a concentration of 25  $\mu$ M or higher (data not shown). Intriguingly when HepG2 cells were treated for 24 and 48 hours, TOPFlash reporter activity was decreased significantly at both times, although the extent of decrease at 48 hours was less than 24 hours, suggesting metabolic inactivation of the SM (**Fig. 6A**). Thymidine incorporation, which is a measure of DNA synthesis, however showed significant decrease at both 24 and 72 hours after **PMED-1** treatment when compared to **DMSO** control (**Fig. 6B**). This was also verified by immunofluorescence for Ki-67, an S-phase marker of cell cycle, which showed a notable decrease after **PMED-1** as compared to **DMSO** treatment of HepG2 cells for 24 hours (**Fig. 6C**).

### 2.3.2 Inhibiting cell cycle progression and growth supports activity assay

Since a significant decrease in TOPFlash reporter activity in HepG2 cells was observed at 24 hours after **PMED-1** treatment at 25  $\mu$ M, we next examined the status of  $\beta$ -catenin and protein expression of some of its downstream targets. As seen in **Figure 6D**, while no change in total  $\beta$ -catenin was evident, a notable decrease in GS, Cyclin-D1, c-myc, and Regucalcin protein levels was evident. Thus treatment with **PMED-1** impedes  $\beta$ -catenin signaling in HepG2 cells.

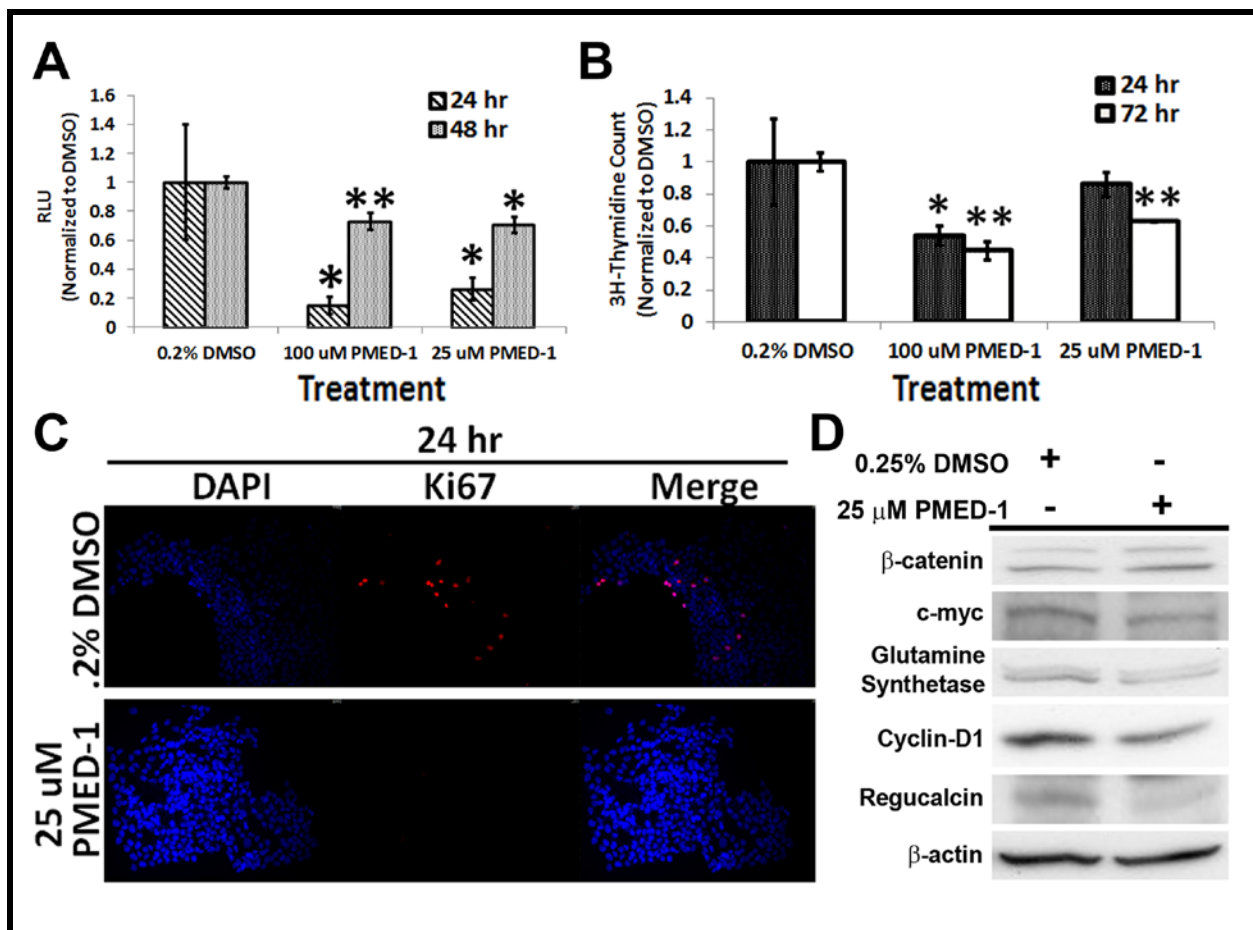


**Figure 6. PMED-1 targets  $\beta$ -catenin signaling to affect cell proliferation in HepG2 cells.** (A) HepG2 cells treated with 100  $\mu$ M or 25  $\mu$ M for 24 hours with **PMED-1** showed a more significant decrease in TOPFlash reporter activity assay than at 48 hours. (B) DNA synthesis in HepG2 cells measured by thymidine incorporation shows a significant decrease in response to 24 or 72 hour treatment with 100  $\mu$ M or 25  $\mu$ M of **PMED-1** when compared to 0.2% **DMSO**. (C) Decrease in Ki-67 positive cells (red) was noticed after treatment of HepG2 cells with 25  $\mu$ M **PMED-1** as compared to 0.2% **DMSO**. (D) Western blots with whole cell lysates from HepG2's treated with 25  $\mu$ M **PMED-1** show a notable decrease in  $\beta$ -catenin targets without affecting its protein expression when compared to the **DMSO** control.  $\beta$ -actin verified comparable protein loading.

## 2.4 HCC CELL LINE SPECIFICITY OF PMED-1 EXAMINED

Many times when an experimental SM is developed, its activity and metabolism differ when used in different cell types or cell lines. This is possible due to the fact that in culture, mutations may frequently occur during passaging of the cell line leading to resistances or susceptibilities to specified treatments. Cell line/type specificity can also occur especially in cases where specific cell lines don't even express proteins which a SM therapy is targeted.

### 2.4.1 Multiple HCC cell lines are susceptible to PMED-1 via TOPFlash assay

In order to further substantiate the anti- $\beta$ -catenin effect of **PMED-1**, we treated various HCC cell lines that express endogenous wild-type (WT)  $\beta$ -catenin (Snu-449, Huh7, Hep3B), endogenous mutated  $\beta$ -catenin (Snu-398) or a stable cell line expressing either WT- $\beta$ -catenin (Hep3B-WT) or constitutively active mutated  $\beta$ -catenin (Hep3B-S33Y) (248, 256, 257). Twenty-four hour treatment of all cell lines with 25  $\mu$ M **PMED-1** led to a significant decrease in TOPFlash reporter activity ranging from 15% to 50% as compared to **DMSO** treatment (**Fig. 7A**). **PMED-1** treatment also led to a significant decrease in cell viability in various HCC cell lines at the corresponding times when compared to the **DMSO** controls (**Fig. 7B**). As shown in a representative analysis, **PMED-1** treatment also led to a significant decrease in thymidine incorporation in Snu-398 cells at both 24 and 72 hours (**Fig. 7C**).

## **2.4.2 PMED-1 causes consistent inhibition of Wnt target gene expression in multiple HCC cell lines**

To further demonstrate the impact of **PMED-1** on  $\beta$ -catenin signaling in these HCC cell lines, we analyzed whole cell lysates for the protein expression of  $\beta$ -catenin and some of its known targets. A notable decrease in GS, Cyclin-D1, and VEGF-A was observed after 24 hours of **PMED-1** treatment on various HCC cells without any impact on total  $\beta$ -catenin levels (**Fig. 7D**). Taken together, this data supports that **PMED-1** is indeed effective in targeting  $\beta$ -catenin activity in multiple HCC cells and thus has significant biological implications.

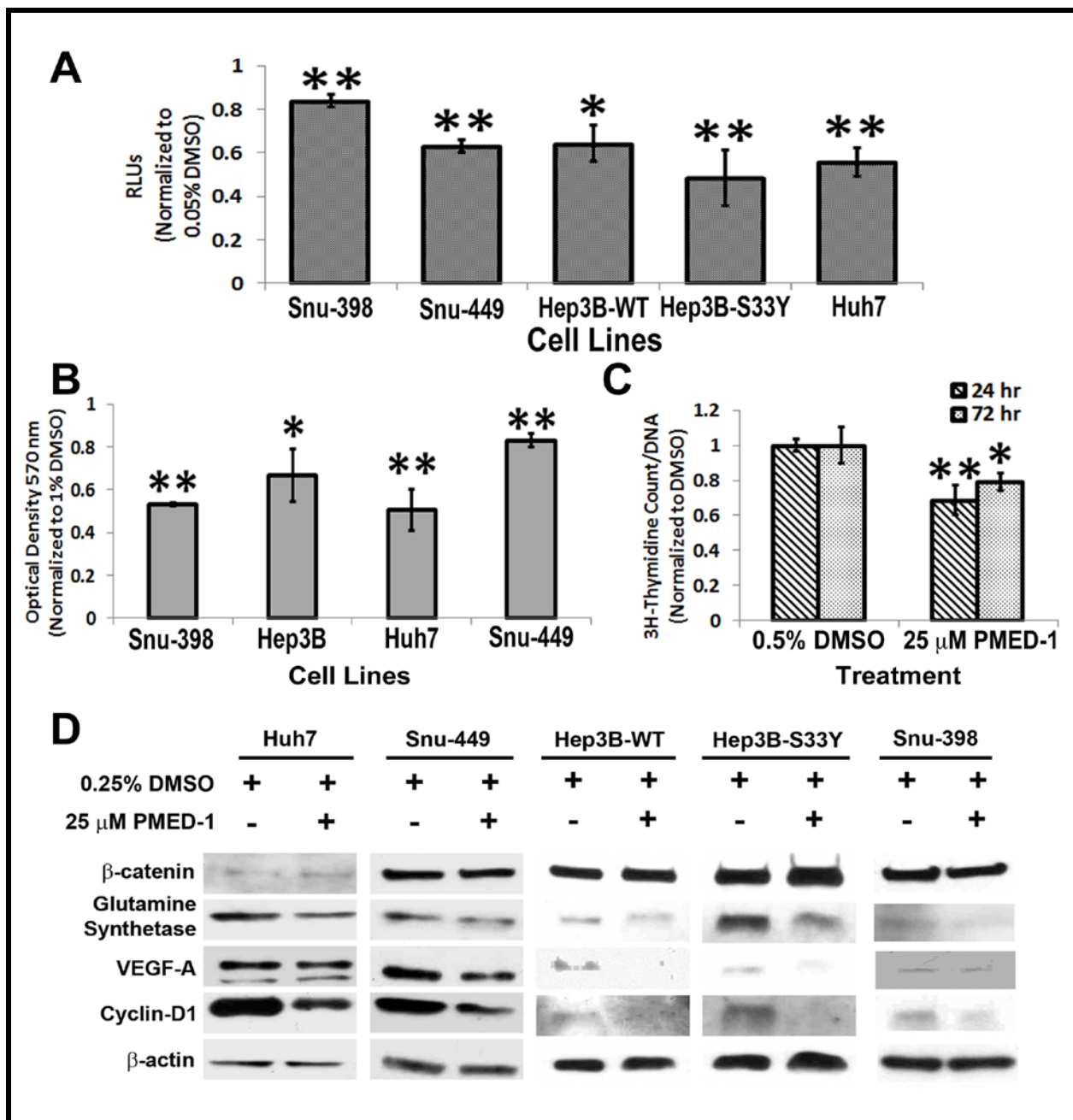


**Figure 7. PMED-1 targets  $\beta$ -catenin effectively in multiple HCC cell lines.** (A) TOPFlash luciferase assay conducted in Snu-398, Snu-449, Hep3B-WT, Hep3B-S33Y, and Huh7 HCC cells after 25  $\mu$ M **PMED-1** treatment for 24 hours shows a significant and consistent decrease although the extent of decrease varied among various cell lines. (B) MTT assay shows a significant decrease in viability of Snu-398, Hep3B, and Huh7 HCC cells after 24 hour of 25  $\mu$ M **PMED-1** as compared to 1% **DMSO**. (C) DNA synthesis measured by thymidine incorporation is significantly reduced in Snu-398 HCC cells treated for 24 or 72 hours with 25  $\mu$ M **PMED-1** as compared to 0.05%

**DMSO.** (D) Western blots using whole cell lysates from Huh7, Snu-449, Snu-398, Hep3B-WT, and Hep3B S33Y HCC cells treated with 25  $\mu$ M **PMED-1** show notable decreases in  $\beta$ -catenin downstream targets without affecting total  $\beta$ -catenin levels when compared to 0.05% **DMSO** control.  $\beta$ -actin verified comparable protein loading.

## 2.5 ACTIVITY SPECIFICITY OF PMED-1 MIMICS ICG-001

Identifying an active SM which inhibits Wnt signaling that is structurally similar to **ICG-001**, a known  $\beta$ -catenin inhibitor, through *in silico* techniques is hypothetical at this point in time. In order to validate the hypothesis, studying the specific activity of **PMED-1** versus **ICG-001** is required. Also, we wanted to make sure that **PMED-1** was not having any adverse off target effects against any other critical signaling pathway in the cell which could have been giving us false positive results. Target specificity is of utmost importance when developing a novel therapy from bench top to bedside in order to reduce any toxicity a patient would potentially experience.

### 2.5.1 Co-immunoprecipitation of CBP/ $\beta$ -catenin shows **PMED-1** activity

In order to address the molecular basis of  $\beta$ -catenin inhibition by **PMED-1**, we verified the mechanism of  $\beta$ -catenin inhibition brought about by **ICG-001**. In agreement with the previously published studies, treatment of HepG2 and Snu-398 cells for 24 hours with **ICG-001** led to a notable decrease in CBP- $\beta$ -catenin association as demonstrated by immunoprecipitation studies (**Fig. 8A**). Since **PMED-1** was identified by structure-function based computational search, an evident decrease in the association of these two proteins when compared to no

treatment or **DMSO** control validated our computational search (**Fig. 8A**). This data suggests that our computational strategy successfully yielded a SM having structure-function similarity to **ICG-001**.

### **2.5.2 PMED-1 does not show off target kinase inhibition**

To further verify if **PMED-1** could potentially affect additional kinases that may be resulting in some of the observed biological effects, we compared its efficacy to a multi-kinase inhibitor H89 in inhibiting key kinases including AKT, PKD, CAK, Plk1 and Plk2. While in response to H89, a dose-dependent inhibition of AKT (**Fig. 8B**), CAK (**Fig. 8D**), PKD (**Fig. 8F**), Plk1 (**Fig. 8H**) and Plk2 (**Fig. 8J**) was observed, no inhibition of these kinases was evident after **PMED-1** treatment (**Fig. 8C, 8E, 8G, 8I and 8K**). Intriguingly low doses of **PMED-1** showed 60% (-2.5 to -1.0 log  $\mu\text{M}$  representing 0.003  $\mu\text{M}$  to 0.09  $\mu\text{M}$ ) showed an inverse decrease in Plk1 kinase, however at higher dose, this activity was lost (**Fig. 8I**). It should be noted that 25  $\mu\text{M}$  equivalent of **PMED-1**, which significantly decreased  $\beta$ -catenin-TCF activity in HCC cells showed no inhibition of any of the 5 kinases tested at that concentration, which equates to 1.39 log  $\mu\text{M}$ . This analysis shows that **PMED-1** does not seem to be promiscuous by inadvertently effecting major kinase pathways at doses that effectively blocked  $\beta$ -catenin activity.

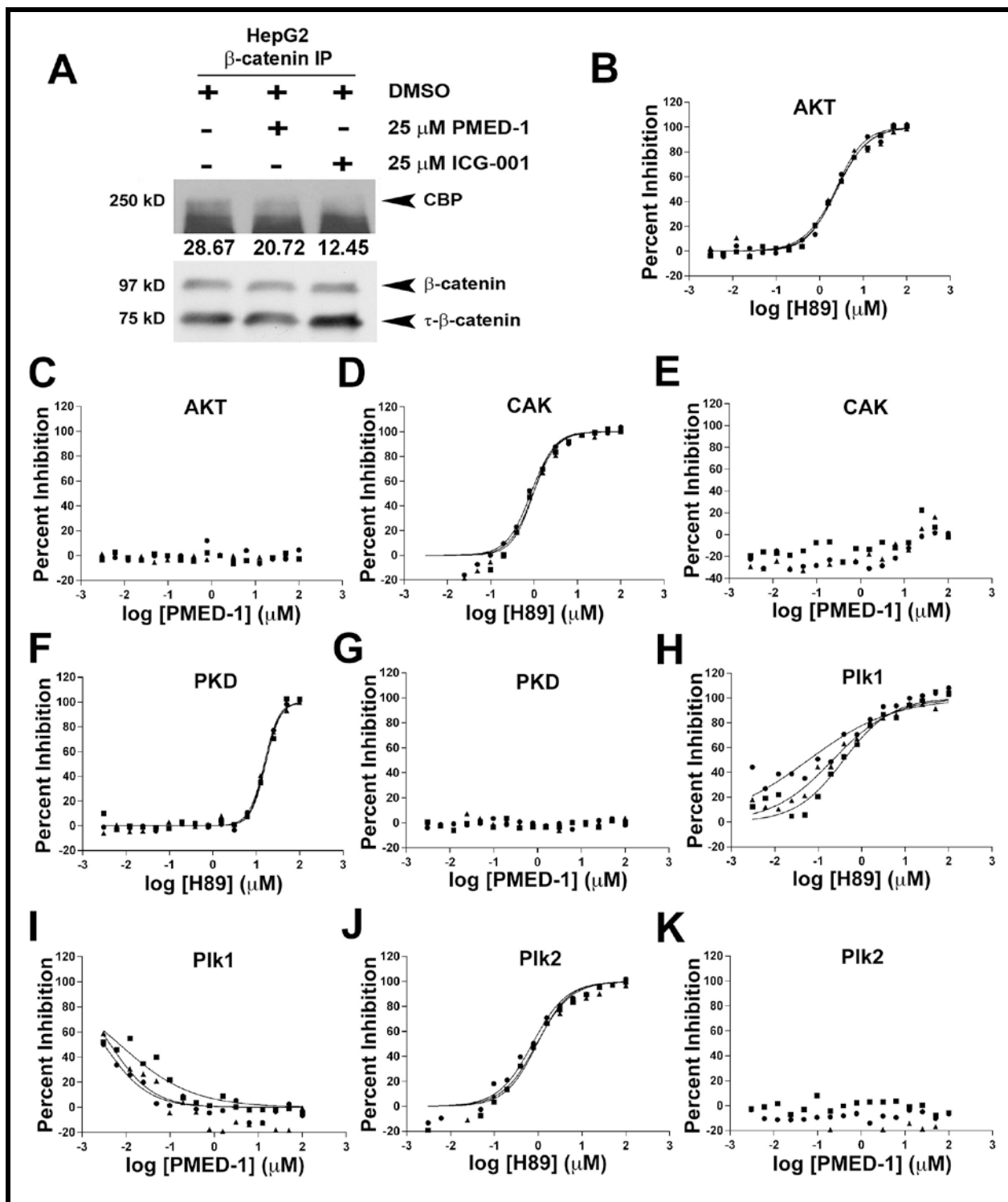


**Figure 8. PMED-1 specifically inhibits β-catenin-CBP interactions and does not impact other common kinases.** (A) Whole cell lysates from untreated HepG2 cells or HepG2 cells treated for 24 hours with either 2% DMSO, 25 μM PMED-1 or 25 μM ICG-001 used for immunoprecipitation show significantly less CBP pull down

with anti- $\beta$ -catenin antibody only in **PMED-1** and **ICG-001** treated cells by western blot analysis. (Densitometry for CBP provided under each band) **(B)** H89 decreases AKT activity in a dose dependent manner as assessed by IMAP-based AKT FP assay. Three replicates are shown. X-axis is in log scale. **(C)** **PMED-1** does not affect AKT activity. **(D)** H89 decreases CAK activity as assessed by IMAP-based CAK TR-FRET assay. Three replicates are shown. X-axis is in log scale. **(E)** **PMED-1** does not affect CAK activity. **(F)** H89 decreases PKD activity as assessed by IMAP-based PKD FP assay. Three replicates are shown. X-axis is in log scale. **(G)** **PMED-1** does not affect PKD activity. **(H)** H89 decreases Plk1 activity as assessed by IMAP-based Plk1 TR-FRET assay. Three replicates are shown. X-axis is in log scale. **(I)** **PMED-1** showed inhibitory effect on Plk1 up to  $-1 \mu\text{M}$  log scale ( $0.097 \mu\text{M}$ ), however no decrease is evident at higher concentrations. **(J)** H89 decreases Plk2 activity as assessed by IMAP-based Plk2 TR-FRET assay. Three replicates are shown. X-axis is in log scale. **(K)** **PMED-1** does not affect Plk2 activity.

## 2.6 POSSIBLE *IN VIVO* APPLICATION FOR **PMED-1**

When developing a novel therapeutic for possible clinical applications, there is only so much evidence *in vitro* assays can provide about *in vivo* efficacy and activity. Just because a SM does not appear to have any overt toxicity or off target effects *in vitro* in cell culture studies does not necessarily mean that the molecule will either retain its activity, or be inert considering other pathways in a living model. There is only so much biological function cell culture studies can reveal, and the only true way to ascertain the true impact a SM may have on all organ systems is to use *in vivo* models.

### 2.6.1 Addressing stability of **PMED-1** *in vitro*

To address the stability of **PMED-1** in culture and *in vivo*, we treated Hep3B cells that are stably transfected with constitutively active S33Y- $\beta$ -catenin mutant with single dose of

**PMED-1** at 25  $\mu$ M for 3 hours to 48 hours as described in methods and compared its effect on TOPFlash reporter activity at each of these times as compared to vehicle only treatment. As seen in **Figure 9A**, beginning at 12 hours inhibition of  $\beta$ -catenin activity in comparison to **DMSO** control was observed. However, statistically significant, 50% inhibition of  $\beta$ -catenin activity was evident at 18-24 hours post **PMED-1** treatment. At 36 hours TOPFlash activity was coming back to baseline. Thus, a single treatment with 25  $\mu$ M **PMED-1** decreased  $\beta$ -catenin activity as early as 12 hours which progressively decreased  $\beta$ -catenin activity until 24 hours in cell culture.

## 2.6.2 Inhibition of Wnt signaling in Zebrafish with **PMED-1**

To determine whether **PMED-1** can inhibit Wnt/ $\beta$ -catenin signaling *in vivo*, we used the *Tg(OTM:d2EGFP)* zebrafish line which expresses destabilized GFP under the promoter containing six copies of Tcf/Lef binding sites (258). For a positive control, a potent Wnt/ $\beta$ -catenin signaling inhibitor, XAV939 (259), was used. GFP expression was greatly reduced in 91% of the *Tg(OTM:d2EGFP)* embryos (20 out of 22) treated with XAV939 from 40 to 55 hours post-fertilization (hpf) and weakly reduced in the remaining embryos compared to **DMSO**-treated controls (**Fig. 9B**). Importantly, GFP expression was greatly reduced in 48% of the embryos (12 out of 25) treated with **PMED-1** compared to the controls although it appeared unaffected in the remaining embryos. Here, only 50% of embryos were affected by **PMED-1** likely due to its extremely hydrophobic nature which decreases its bioavailability. These data indicate the *in vivo* efficacy of **PMED-1** as a Wnt/ $\beta$ -catenin signaling inhibitor and suggest that the Wnt/ $\beta$ -catenin inhibitory activity of **PMED-1** may be weaker than that of XAV939.

### 2.6.3 Characterizing duration of Wnt signaling inhibition *in vivo*

To determine how long **PMED-1** can inhibit Wnt/ $\beta$ -catenin signaling *in vivo*, we examined GFP expression at multiple time points after **PMED-1** treatment. To better reveal GFP expression in *Tg(OTM:d2EGFP)* embryos, we used homozygous *Tg(OTM:d2EGFP)* embryos in which GFP expression is much stronger than in the hemizygous embryos. Strong GFP<sup>+</sup> *Tg(OTM:d2EGFP)* embryos were treated with **DMSO**, XAV939 or **PMED-1** at 48 hpf; 6, 12 or 24 hours later, their GFP expression was examined (**Fig. 9C**). 6 hours later, at 54 hpf, most embryos treated with XAV939 (10 out of 12) or **PMED-1** (15 out of 18) exhibited reduced GFP expression compared to controls. 12 hours later, at 60 hpf, GFP expression was further reduced in XAV939-treated embryos; it was still, but not further, reduced in **PMED-1**-treated embryos (11 out of 15). Interestingly, 24 hours later, at 72 hpf, GFP expression was significantly restored in **PMED-1**-treated embryos (8 out of 12), whereas it was still reduced in XAV939-treated embryos. These data indicate that the Wnt/ $\beta$ -catenin inhibitory activity of **PMED-1** lasts shorter than that of XAV939.

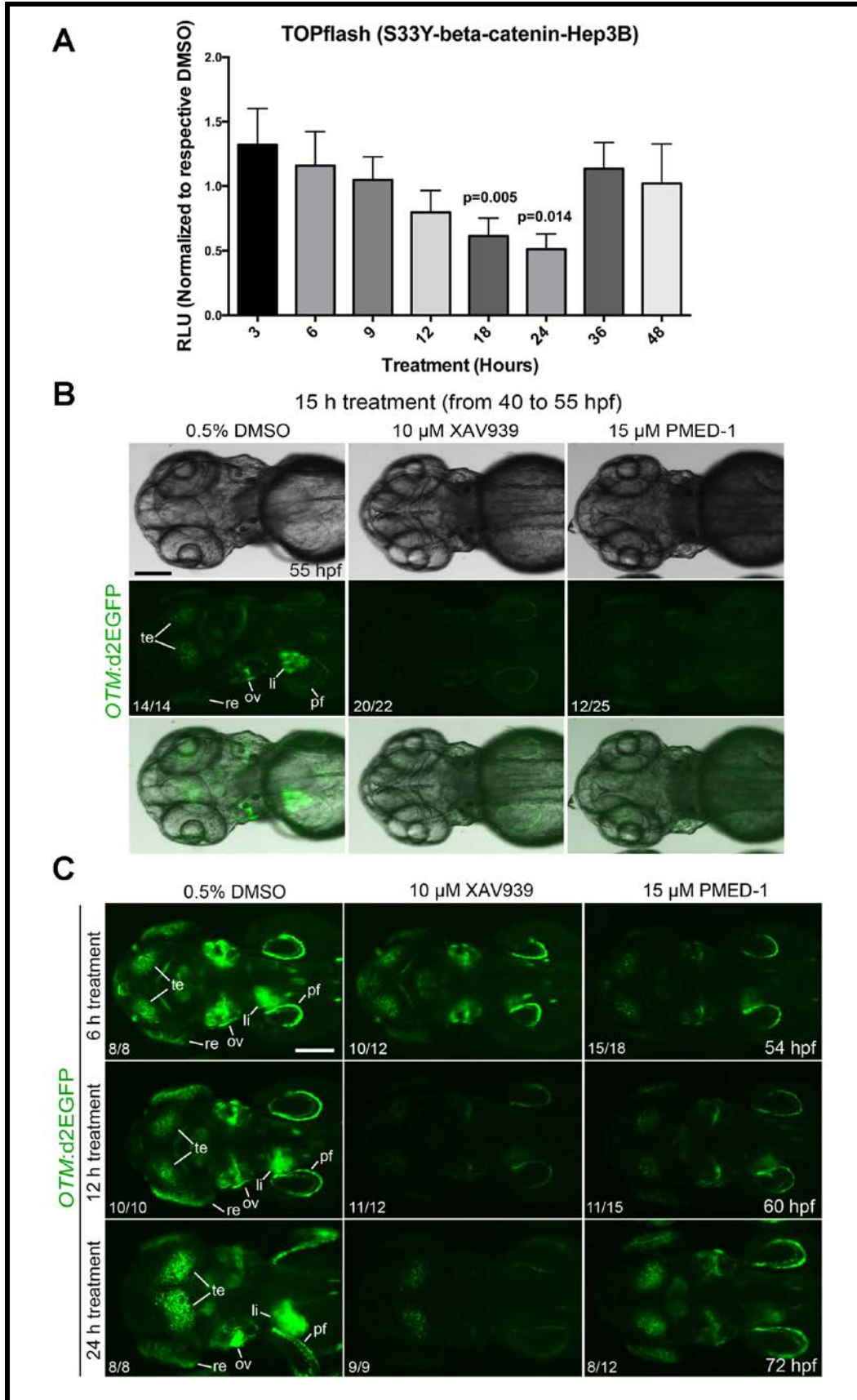


**Figure 9. Efficacy and duration of PMED-1's effect on  $\beta$ -catenin activity in vivo and in vitro.** (A) Stably transfected Hep3B cells with S33Y- $\beta$ -catenin, treated with a single dose of **PMED-1** at 25  $\mu$ M, shows gradual decrease in TOPFlash reporter activity becoming significant ( $p \leq 0.05$ ) at 18 and 24 hours after treatment with rebound at 36 and 48 hours. (B) GFP+ embryos obtained from outcrossing Tg(OTM:d2EGFP) zebrafish were treated with **DMSO**, XAV939, or **PMED-1** from 40 to 55 hpf, and their GFP expression was assessed under a fluorescence microscope. The bottom row shows the merged images of bright field and GFP fluorescence (green) images. Numbers indicate the proportion of embryos showing the corresponding GFP expression. Tectum (te), retina (re), otic vesicle (ov), liver (li), and pectoral fin (pf). All images are dorsal view with anterior to the left. Scale bar, 100  $\mu$ m. (C) Epifluorescence images showing GFP expression in Tg(OTM:d2EGFP) embryos. Strong GFP+ embryos obtained from incrossing Tg(OTM:d2EGFP) zebrafish were treated with **DMSO**, XAV939, or **PMED-1** from 48 hpf. 6, 12 or 24 hours later, these embryos were harvested and their GFP expression was assessed under a fluorescence microscope. Numbers indicate the proportion of embryos showing the corresponding GFP expression. Tectum (te), retina (re), otic vesicle (ov), liver (li), and pectoral fin (pf). All images are dorsal view with anterior to the left. Scale bar, 100  $\mu$ m.

## 2.7 DISCUSSION OF APPLICABILITY OF PMED-1

Developing a drug from bench to bedside is an arduous and slow process. High-throughput screens assess SMs for potential efficacy against a desired target however the eventual effect may be due to an off-target effect since there is little to no selectivity or specificity in these screens (260). The intention in these studies is to discover a molecule that will cause cell death in culture with little to no knowledge of the mechanism, which can then be tested for its efficacy in vivo. We took a novel approach by basing our drug discovery on a previously established SM inhibitor of  $\beta$ -catenin-**ICG-001**. Based on the premise of structure-function similarity, we show that the **PMED-1**, a SM resembling the structure of **ICG-001**,

shows similar function in inhibiting  $\beta$ -catenin in multiple HCC cell lines although at a higher concentration. Like **ICG-001**, **PMED-1** also inhibits  $\beta$ -catenin and CBP interactions and thus impedes downstream signaling. CBP is a histone acetyl transferase and interacts with  $\beta$ -catenin in the nucleus once it has been activated and has been shown to be critical for  $\beta$ -catenin-dependent target gene expression (252). In addition **PMED-1** did not show any off-target kinase inhibition against AKT, PKD, CAK, and Plk2. We also checked the quality of **PMED-1** by high performance liquid chromatography (HPLC) and nuclear magnetic resonance (NMR) to verify if any contaminant or a degradation product could be responsible for inhibiting  $\beta$ -catenin-TCF activity. However **PMED-1** used in our studies was greater than 95% pure (data not shown). A major limitation with the current study was the issue of solubility of **PMED-1**. Being a hydrophobic SM, it could be only dissolved in **DMSO** and limited our ability to perform in vivo studies in orthotopic HCC models in mice. However, we were able to demonstrate its efficacy in a zebrafish model indicating that it is a potent  $\beta$ -catenin inhibitor in vivo as well. Additional studies will be necessary to address if modifications would be possible in **PMED-1** to enhance its solubility and hence deliver in vivo.

Targeting Wnt/ $\beta$ -catenin signaling in tumors has shown to be efficacious in preclinical models including use of **ICG-001** in colorectal carcinoma and AV-65, another SM, in multiple myeloma (245, 261). In the current study we demonstrate **PMED-1**, another novel SM, which has the potential for future therapeutics in HCC or other tumors. Targeting  $\beta$ -catenin by **PMED-1** in HepG2 and Snu-398 cells is highly relevant because these cells have constitutively active  $\beta$ -catenin owing to deletion or point mutation, respectively. **PMED-1** successfully affected  $\beta$ -catenin activity along with suppression of downstream Wnt targets and ensuing compromise in tumor cell proliferation and survival. It was interesting to note that at 48 hours HCC cells regain

$\beta$ -catenin activity, which may suggest that half-life of **PMED-1** due to its metabolism/inactivation or which may be due to re-growth of cells in culture that escape  $\beta$ -catenin inhibition. Indeed in a time-course study both *in vitro* and *in vivo*, **PMED-1** showed peak downregulation of  $\beta$ -catenin activity at 18-24 hours in cell culture and between 6-12 hours in zebrafish embryos. However the effects of the initial treatments can be observed in the lingering delay of DNA synthesis even up to 72 hours indicating that a single dose of **PMED-1** is sufficient to interrupt the  $\beta$ -catenin signaling cascade and in impairing the associated downstream biological processes. Indeed similar prolonged biological effect has been observed using other modalities like PNA despite recovery of some  $\beta$ -catenin activity (248).

Ultimately, our work shows the practical application of *in silico* screening in effective identification of a specific molecule against  $\beta$ -catenin driven HCC with future therapeutic implications. For **PMED-1** to be developed into an FDA approved compound that is clinically effective further investigation and optimization of its activity is required. Identifying other potential molecular targets of **PMED-1** is crucial to our understanding of the activity and specificity of this compound. Biotinylating **PMED-1** on an inactive subgroup will allow us to treat cells in culture and pull out the biotinylated **PMED-1** along with any complexed molecules. Mass spectrometry can then be used in order to characterize what other proteins **PMED-1** may be interacting with other than CBP. This type of investigation will also allow us to identify the functional group responsible for interacting with CBP to block its interaction with  $\beta$ -catenin. Knowing the functional group responsible for inhibiting CBP/ $\beta$ -catenin interaction is critical when trying to understand the activity of **PMED-1**. We have conducted preliminary experiments treating C57BL6 mice with **PMED-1** in order to better understand maximum tolerated doses. However, the hydrophobic nature of the SM did not lend to it being readily absorbed *in vivo*.

This is where understanding the specific functional group responsible for the major activity of **PMED-1** is important because we can then alter the chemical structure to make the SM more hydrophilic without inhibiting the activity of **PMED-1**. Making **PMED-1** hydrophilic will increase the bioavailability in culture, as well as *in vivo* therefore increasing the efficacy of **PMED-1** directed CBP/ $\beta$ -catenin inhibition. An additional method of increasing the bioavailability of a SM such as **PMED-1** is by loading it onto nanoparticles which can be functionalized specifically to target hepatocytes (262, 263). Though the technology for nanoparticle based delivery systems exists, the efficacy and applicability of this type of method has been poorly characterized.

Little is known about the consequences of CBP/ $\beta$ -catenin directed transcription. There is evidence that differential Wnt target gene expression may be a result of specific interaction of transcription factors and  $\beta$ -catenin in the nucleus (264, 265). In order to understand this more clearly, cells treated with **PMED-1** can be harvested for gene array analysis which will allow us to understand the importance of CBP/ $\beta$ -catenin interaction to cellular biology. Even though through structural similarity searches we have been able to discover **PMED-1** as an effective SM that inhibits CBP/ $\beta$ -catenin interaction, it is important to understand the full mechanism of **PMED-1** in order to develop a clinically applicable SM for future therapeutic implications.

### **3.0 $\beta$ -CATENIN KNOCKDOWN BY CELL PERMEABLE GAMMA GUANIDINE-BASED PEPTIDE NUCLEIC ACID REVEALS ITS NEW ROLES IN HEPATOCELLULAR CANCER**

When considering the development of targeted, personalized medicine in cancer, genetic therapies directed against an activated oncogene would be the most direct and effective method for an anti-tumorigenic effect. In this chapter, we report the application of second-generation PNA to target  $\beta$ -catenin. As a proof of concept, we show that targeting  $\beta$ -catenin not only impacts HCC cell proliferation and viability, which we initially show in **Chapter 2**, but also demonstrate another function of  $\beta$ -catenin knockdown in reducing tumor angiogenesis. This was shown by decreased downstream target gene expression and concomitant biological consequences. We show for the first time that several factors that are involved in angiogenesis are regulated by  $\beta$ -catenin signaling in HCC cells, and PNA-mediated  $\beta$ -catenin knockdown in HCC cells impairs secretion of factors that in turn affect tubulogenesis and spheroid formation by the HCC-associated endothelial cells. The results presented herein have important implications in HCC treatment and in countering drug resistance.

### 3.1 DEVELOPING AN ANTISENSE AGAINST BETA-CATENIN

PNA is a promising class of nucleic acid mimic developed in the last two decades in which the naturally occurring sugar phosphodiester backbone is replaced with *N*-(2-aminoethyl) glycine units (266). PNA has many appealing features, as compared to the natural counterparts, including strong binding affinity and sequence selectivity towards DNA and RNA, and resistance to enzymatic degradation by proteases and nucleases. These properties, along with the ease of synthesis, make PNA an attractive molecular platform for regulating gene expression; however, a drawback is that it is not cell-permeable (267, 268). Previously we have shown that installation of a guanidinium group at the  $\alpha$ -backbone significantly improves the cellular uptake of PNA (269). This new class of guanidine-based PNA (GPNA) has been successfully employed in the selective knockdown of E-cadherin (270, 271). More recently we reported the synthesis of a second-generation  $\gamma$ GPNA, in which the guanidinium group is incorporated at the  $\gamma$ -backbone, with improved hybridization properties and economy of synthesis. Here we wanted to combine our experience targeting E-cadherin with the optimization of the  $\gamma$ GPNA by targeting the  $\beta$ -catenin gene in human hepatocellular carcinoma.

#### 3.1.1 Design and synthesis of Peptide Nucleic acids

Inspired by the effectiveness of  $\alpha$ GPNA in knocking-down E-cadherin in our previous study, we decided to target  $\beta$ -catenin, a well-described oncogene highly expressed in hepatoma cells by using the second-generation  $\gamma$ GPNA with improved hybridization properties. We designed and synthesized two specific PNA sequences against the  $\beta$ -catenin gene, one against the transcription start site, called **T1**, and the other against the translation start site, labeled as **T2**

(**Fig. 10A-C**). Both **T1** and **T2** contain regular PNA units with inserted  $\gamma$ GPNA monomer units (5 units) to increase its cellular uptake properties. In order to demonstrate the selective binding of **T1** a control PNA containing mismatch binding sites, **MM** was also synthesized. In order to examine the cellular uptake properties of designed PNA, we fluorescently labeled **T1** with TAMRA dye.

### **3.1.2 Uptake of Peptide Nucleic Acids Leads to Inhibited Wnt/ $\beta$ -catenin Signaling in HCC cells**

The human hepatoma cell line HepG2 was cultured in media containing Hoescht nuclear dye and 1  $\mu$ M of **T1**  $\gamma$ GPNA tagged with TAMRA dye for a period of 19 hours under live cell imaging (**Fig. 10D**). Within 3 hours of **T1**-TAMRA treatment, a red signature appeared within cells. At 19 hours, **T1**-TAMRA was present in punctate structures, as well as within the nuclei of HepG2 cells. This result indicates that  $\gamma$ GPNA is able to traverse the extracellular membrane of hepatoma cells on its own without the aid of a transfection reagent, or any other mechanical or electrical means.

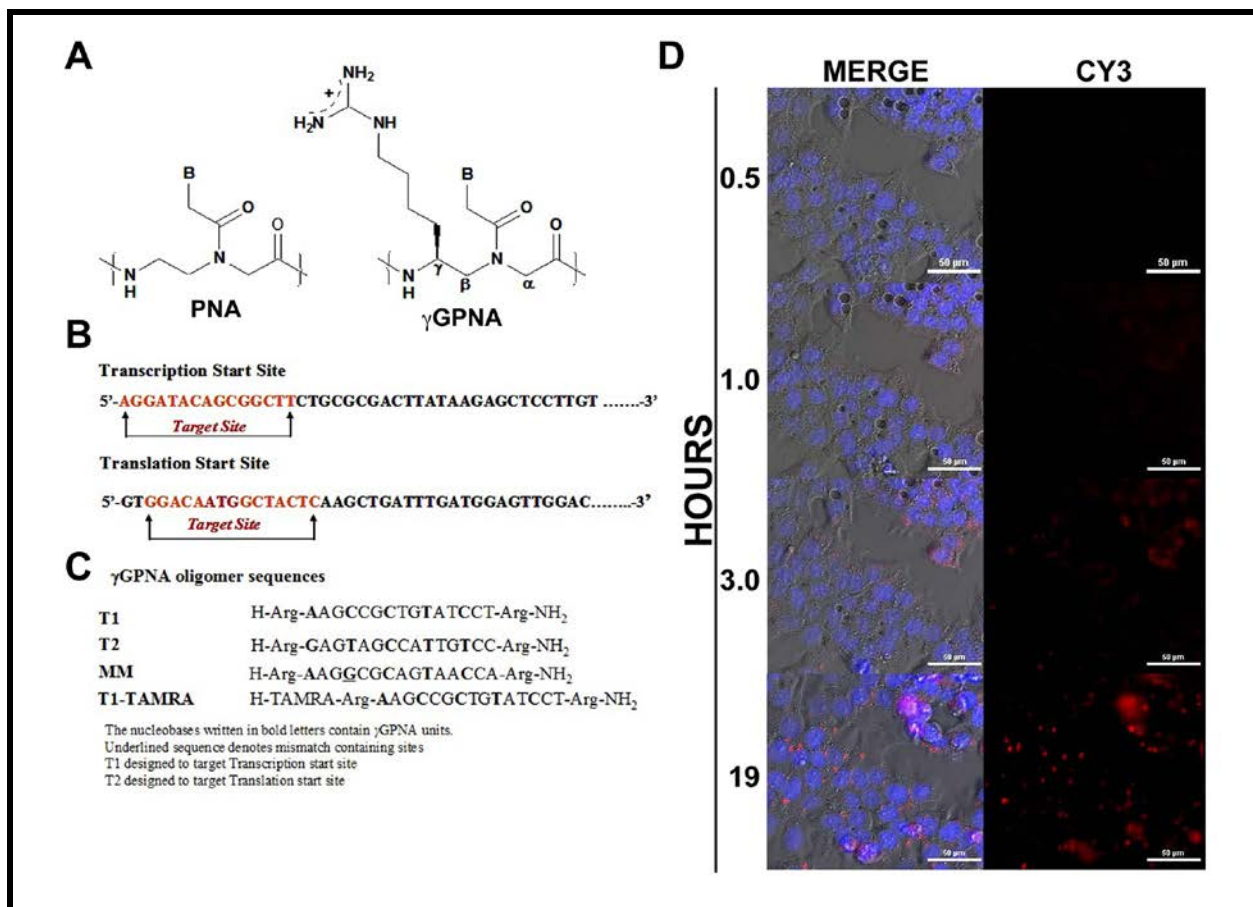


**Figure 10. Structure and sequence of antisense oligonucleotides and controls that show an unaided cellular uptake.** (A) Chemical Structures of PNA and  $\gamma$ GPNA. (B) Human beta-catenin (CTNNB1) gene transcript and location of targeted sequence and (C) Sequence of  $\gamma$ GPNA Oligomers employed for study. (D) Human hepatoma cells (HepG2) were cultured in the presence of TAMRA-labeled **T1**  $\gamma$ GPNA for a period of 19 hours and the fluorescent dye was tracked by live cell imaging. Within 3 hours of treatment, TAMRA-**T1** increased significantly within the cells without the aid of a transfection reagent. Cells were also incubated with Hoechst nuclear stain for nuclear visualization. Scale bars indicate 50  $\mu\text{m}$ .

Next, we assessed the antisense activities of  $\gamma$ GPNAs against the transcription and translation start sites of  $\beta$ -catenin. To address this, we utilized the TOPFlash luciferase reporter to assess  $\beta$ -catenin-TCF activity. HepG2 cells were treated with either **T1** or **T2** at 5  $\mu\text{M}$  for 24 hours, 15 minutes after transfection. A 90% or 50% decrease in TOPFlash reporter activity was

observed after **T1** and **T2** treatment, respectively (**Fig. 11A**). In fact **T1** treatment for 24 hours demonstrates a dose-dependent decrease in TOPFlash reporter in HepG2 cells (**Fig. 11B**). This result shows that while both  $\gamma$ GPNA inhibit  $\beta$ -catenin, **T1** is more potent than **T2** and was used for additional investigations.

To determine the specificity of **T1**  $\gamma$ GPNA, we designed a mismatch  $\gamma$ GPNA (**MM**) control, which differed from **T1** by four base pairs (**Fig. 11C**). We utilized two liver tumor cell lines that have distinct modes of  $\beta$ -catenin activation. HepG2 cells harbor a deletion in exon-3 in  $\beta$ -catenin, while Snu-449 cells have a point mutation in exon-3 of *CTNNB1*, a common occurrence in human HCC (255, 257). Both cell lines were treated with 1 $\mu$ M of **T1** for 72 hours to determine  $\beta$ -catenin inhibition over a prolonged duration. As compared to the MM control, **T1** treatment reduced TOPFlash activity significantly in both cell types (**Fig. 11C-D**).

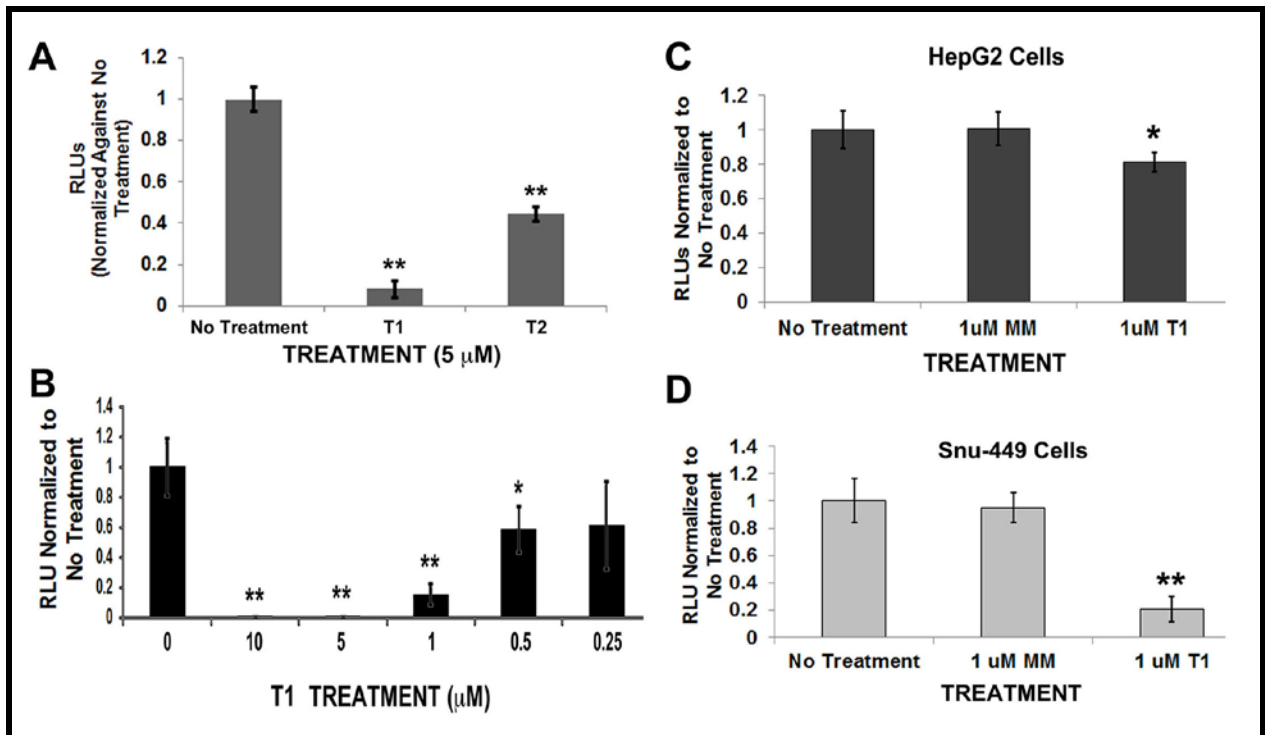


**Figure 11.  $\gamma$ GPNA designed against  $\beta$ -catenin decreases its reporter activity in hepatoma cells with T1's impact being more pronounced.** (A) T1- and T2-targeted against  $\beta$ -catenin gene transcription and translation start site respectively, when incubated with HepG2 cells at 5  $\mu$ M for 24 hours, reduced TOPFlash reporter activity, although T1 had a significantly stronger effect than T2. (B) Twenty-four hour exposure of HepG2 cells to T1 ranging from 5  $\mu$ M to 50 nM exhibits a dose-response in reducing TOPFlash activity represented as ratio of Firefly to Renilla luciferase that in turn was normalized to no treatment control. Error bars represent standard deviation. (\*P<0.05, \*\*P<0.01) (C) HepG2 cells were incubated for 72 hours with 1  $\mu$ M MM or T1 that led to a significant, sustained inhibition of  $\beta$ -catenin activity when analyzed by TOPFlash reporter assay. (D) Snu-449 cells, also treated with 1  $\mu$ M MM and T1 for 72 hours, showed a reduction in  $\beta$ -catenin activity as assessed by TOPFlash assay.

### 3.2 ANTISENSE TARGETING OF $\beta$ -CATENIN AGAINST HCC *IN VITRO*

As indicated in **Chapter 2**, targeting a signaling pathway such as the Wnt/ $\beta$ -catenin may lead to off target effects. In order to identify if T1  $\gamma$ GPNA treatment of HCC cell lines is as specific as we intend on our antisense technology to be, we can take advantage of  $\gamma$ GPNA activity. Counter to the activity of **PMED-1** where  $\beta$ -catenin activity is inhibited, but total protein levels remain the same, T1  $\gamma$ GPNA targets  $\beta$ -catenin at the genetic level leading to a reduction of protein levels and thereby a subsequent reduction in Wnt target genes. Here we identify this to be true by analyzing the protein and mRNA levels of  $\beta$ -catenin, as well as the downstream consequences of Wnt signaling inhibition.

### 3.2.1 PNA results in reductions of $\beta$ -catenin downstream targets

We next assessed the effects of **T1**  $\gamma$ GPNA on  $\beta$ -catenin gene expression and protein levels of  $\beta$ -catenin and its targets in HepG2 cells treated with 1  $\mu$ M **T1** or **MM** for 72 hours. Real-time PCR normalized to GAPDH showed a significant decrease in  $\beta$ -catenin mRNA as compared to **MM** control ( $p < 0.05$ ) (**Fig. 12A**). Western blot shows that **T1** effectively reduces full-length and truncated forms of  $\beta$ -catenin in HepG2 cells and full-length form in Snu-449 cells (**Fig. 12B**). Respective lysates were also assessed for several known targets of the Wnt signaling pathway. A decrease in the protein expression of GS, Cyclin-D1, c-Myc, Axin-2, Regucalcin, and VEGF-A were evident in **T1**-treated HepG2 and Snu-449 cells as compared to **MM** control as shown in representative western blots (**Fig. 12B**). These findings further validate the efficacy of **T1**  $\gamma$ GPNA to successfully target  $\beta$ -catenin signaling in liver tumor cells.

### 3.2.2 Targeting $\beta$ -catenin via PNA effects HCC cell biology

The impact on tumor cell proliferation and survival was next analyzed following **T1**  $\gamma$ GPNA-mediated  $\beta$ -catenin suppression. [ $^3$ H]-Thymidine incorporation assay in 1  $\mu$ M **T1**-treated HepG2 cells for 72 hours showed a 20% decrease in DNA synthesis or mitosis when compared to **MM** treatment indicating a significant decrease in cell proliferation ( $p < 0.05$ ) (**Fig. 12C**). Immunofluorescence for Ki-67 (not shown), a measure of cells in S-phase of cell cycle was reduced by a staggering 75% ( $p < 0.05$ ) after **T1** as compared to the **MM** treatment (**Fig. 12D**), indicating  $\beta$ -catenin's role in G1 to S phase transition by regulating expression of Cyclin-D1.

Mitochondrial activity as a measure of cell metabolism and viability, was assessed by the MTT assay. It showed a notable decrease after 72-hour **T1**-treatment of HepG2 cells (**Fig. 12E**). In addition, number of apoptotic nuclei reflecting oncotic or apoptotic cell death as assessed by TUNEL immunohistochemistry, was significantly higher ( $p < 0.01$ ) after **T1** treatment when compared to the **MM** group (**Fig. 12F**). Thus successful inhibition of  $\beta$ -catenin expression and activity by  $\gamma$ GPNA in HepG2 cells affected tumor cell proliferation and viability.

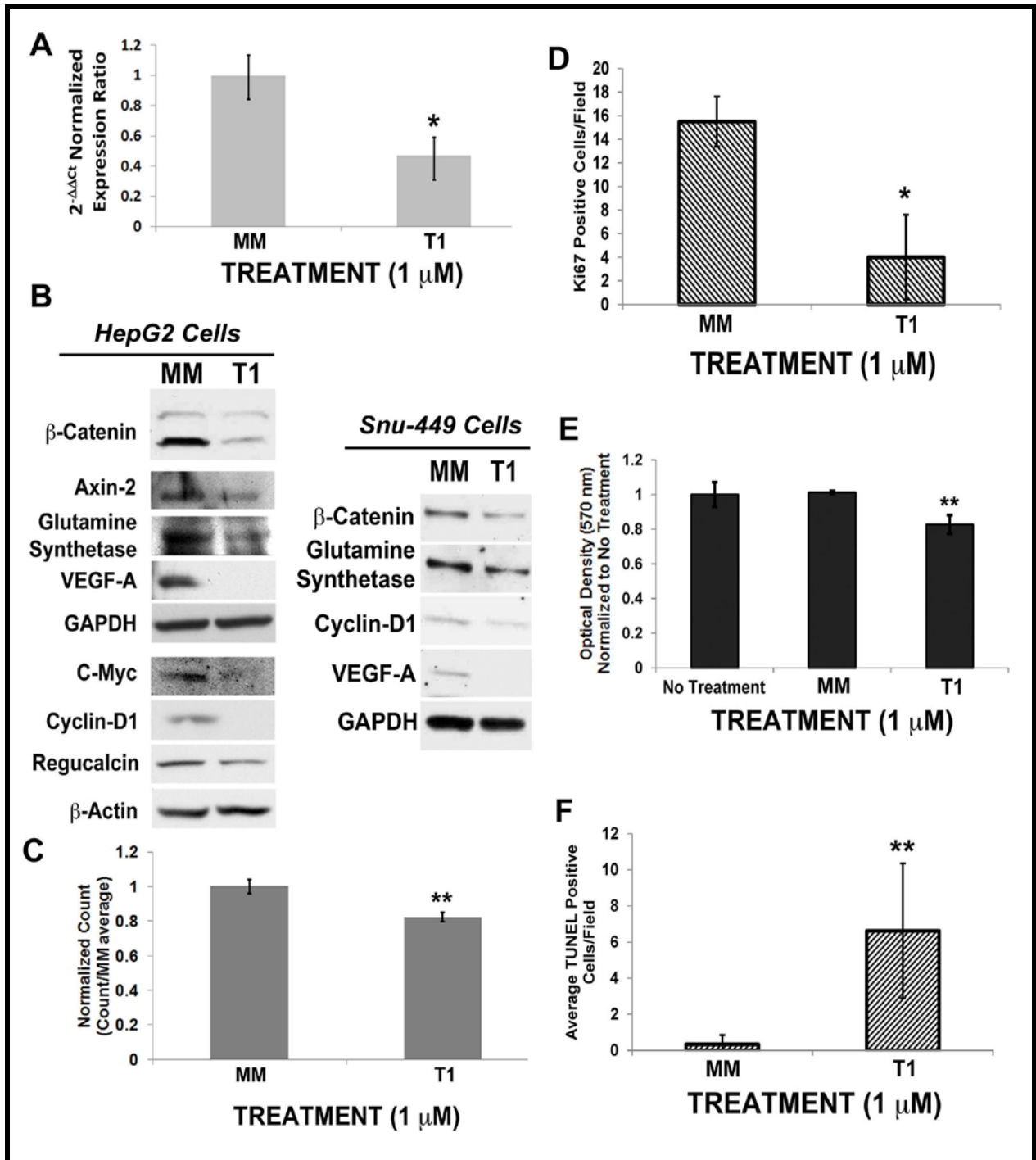


**Figure 12.** T1 PNA treatment affects expression of  $\beta$ -catenin gene and Wnt target expression to impair HCC cell proliferation and survival. (A) When compared to MM control, the T1 treatment of HepG2 cells at 1 $\mu$ M for 72 hours resulted in greater than 50% and significant (\* $p$ <0.05) decrease in  $\beta$ -catenin mRNA expression as seen by Real-Time PCR. (B) Western blots with whole cell lysates from HepG2 and Snu-449 cells treated similarly with T1

show decrease in  $\beta$ -catenin protein expression along with several of its targets as compared to MM control. **(C)** HepG2 cells incubated with 1  $\mu$ M **T1** or MM for 72 hours and exposed to 2.5  $\mu$ Ci of [5'-<sup>3</sup>H]-Thymidine for 48 hours showed a significant decrease in DNA synthesis in **T1** group. **(D)** HepG2 cells incubated with 1  $\mu$ M **T1**, MM or no  $\gamma$ GPNA for 72 hours and stained for Ki-67 shows a dramatic decrease in Ki-67 positive cells after **T1** treatment only. **(E)** A significant decrease in HepG2 viability by MTT assay was also evident after 72 hours of 1  $\mu$ M **T1** treatment as compared to MM. **(F)** Increased numbers of apoptotic nuclei were evident in 1  $\mu$ M **T1**-treated HepG2 after 72 hours as compared to MM only. All error bars represent standard deviation. (\*P<0.05, \*\*P<0.01).

### **3.3 SECONDARY ANTI-ANGIOGENIC EFFECTS DUE TO TARGETING BETA-CATENIN IN HCC VIA PNA**

The process of angiogenesis is indispensable to tumor growth and progression. While Wnt signaling has been shown to be contributing to this process by mechanisms such as by regulating the expression of vascular endothelial growth factor (VEGF), its role in angiogenesis in HCC remains unexplored (253). VEGF is classically known to be a stimulator of angiogenesis, and has seven consensus binding sites on its promoter for the  $\beta$ -catenin/T-cell factor (TCF) complex (272). Several studies indicate the importance of VEGF in HCC progression and show overexpression of VEGF, and its respective receptors VEGFR-1 and VEGFR-2, in the tumors (200, 273). However, a direct study that investigates  $\beta$ -catenin signaling to address any impact on angiogenesis, molecularly and functionally, in HCC is lacking. Here we intend to answer this enigma by utilizing our optimized **T1**  $\gamma$ GPNA against  $\beta$ -catenin in HCC cells.

### 3.3.1 Inhibition of $\beta$ -catenin in HCC leads to inhibited expression of molecules involved in angiogenesis

Wnt/ $\beta$ -catenin signaling is known to regulate VEGF expression in colorectal cancer (253, 272). Indeed VEGF expression was notably downregulated after **T1** treatment of HepG2 cells (**Fig. 12B**). We next interrogated if Wnt/ $\beta$ -catenin may be regulating other angiogenic factors in liver tumor cells and utilized a quantitative Real-Time PCR angiogenesis array. Intriguingly, **T1**  $\gamma$ GPNA treatment of HepG2 cells for 72 hours led to decrease in expression of several angiogenic factors including CXCL5, Ephrin-A1, FGF2, IL-1b, Midkine, Placental Growth Factor (PGF), and SERPINF1 when compared to **MM** treatment (**Fig. 13A**). In fact, fifteen secreted pro-angiogenic factors showed significant differences with  $\beta$ -catenin inhibition with the exception of Heparan sulfate-cleaving enzyme heparanase (HPSE). Changes in  $\beta$ -catenin, VEGF-A, and FGF2 mRNA expression were also validated by Real-time PCR using mRNA from HepG2 cells treated with either 1  $\mu$ M **MM** or **T1** for 72 hours, or 50 nM of negative control or  $\beta$ -catenin siRNA for 48 hours that showed successful  $\beta$ -catenin knockdown along with a significant ( $p < 0.01$ ) decrease in the expression of VEGF-A and FGF2 (**Fig. 13B-C**).

To further validate that VEGF-A was a major target of  $\beta$ -catenin in liver tumor cells we assessed its expression in another HCC cell line Hep3B that was stably transfected with either wild-type or serine-33 to tyrosine (S33Y)-mutated  $\beta$ -catenin. A robust increase in the expression of VEGF-A was evident in Hep3B cells harboring S33Y mutant  $\beta$ -catenin (**Fig. 13D**). Thus VEGF-A expression is regulated by  $\beta$ -catenin in HCC cells.

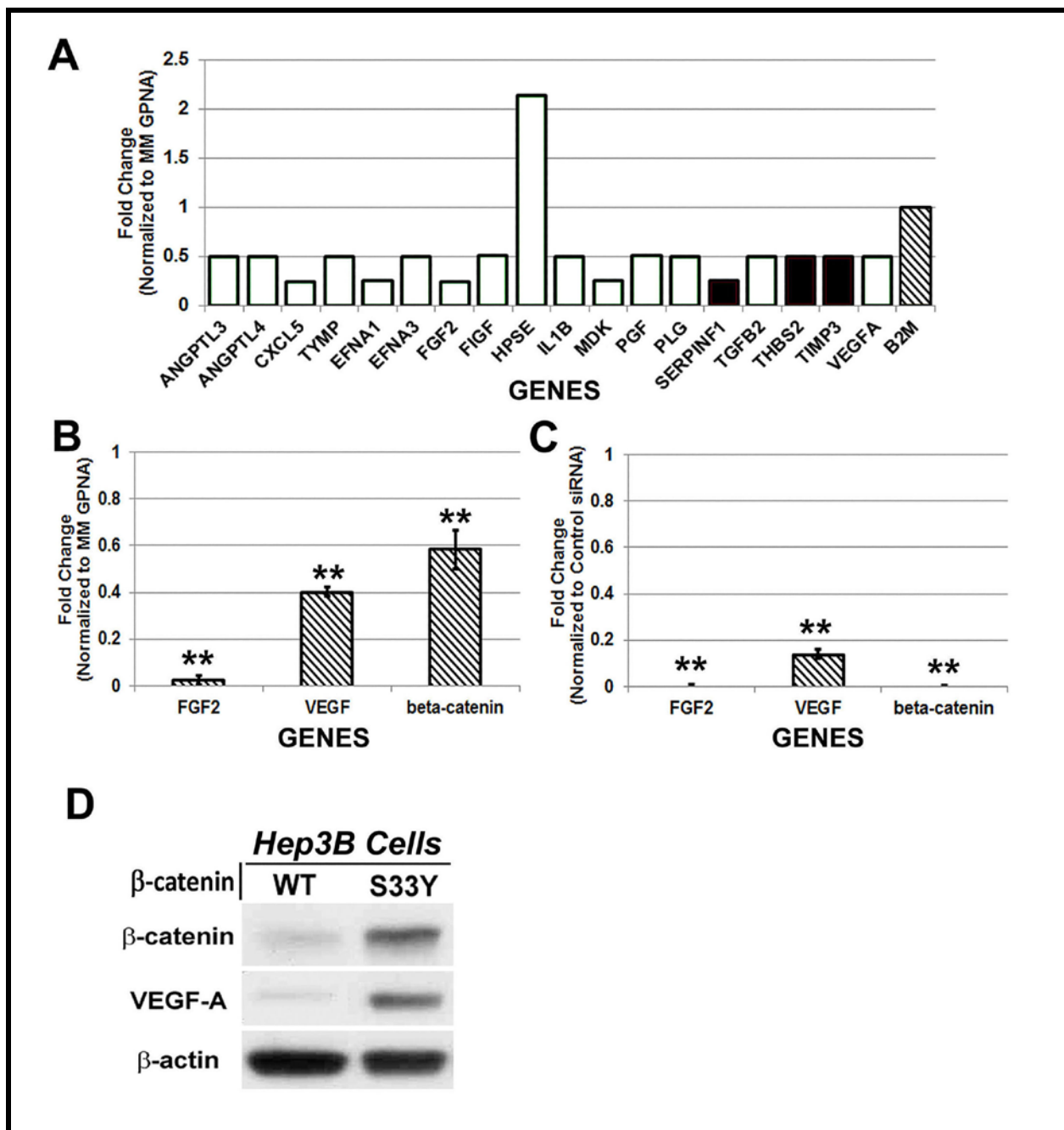


**Figure 13. Modulation of  $\beta$ -catenin regulates expression of angiogenic factors in HCC cells.** (A) Quantitative RT-PCR angiogenesis array on mRNA isolated from HepG2 cells treated with 1  $\mu$ M MM or **T1** for 72 hours reveals a notable decrease in expression of several secreted pro-angiogenic factors. (B) Additional validation by Real-Time PCR shows significant decreases in the expression of  $\beta$ -catenin and concomitantly of FGF2 and VEGF-A ( $p < 0.01$ ) after **T1** and not MM treatment of HepG2 cells. (C) Results were also verified by Real-Time PCR on mRNA from HepG2 cells transfected with  $\beta$ -catenin or control siRNA that showed significant decreases in  $\beta$ -catenin, FGF2 and

VEGF-A expression ( $p < 0.01$ ). **(D)** Hep3B cells stably transfected with S33Y-mutated and not wild-type (WT)  $\beta$ -catenin shows notable increase in  $\beta$ -catenin and VEGF-A expression.

### **3.3.2 Reduced expression of angiogenic factors due to $\beta$ -catenin directed PNA treatment leads to inhibition of angiogenesis in endothelial cells**

We next investigated if decreased expression of various angiogenic factors observed after  $\beta$ -catenin inhibition is functionally relevant and could hinder HCC-associated angiogenesis. We utilized SK-Hep1 cells, an endothelial cell line derived from a hepatic adenocarcinoma (274). We generated endothelial spheroids which, after embedding in collagen gels, were grown in conditioned media taken from HepG2 cells after either **MM** or **T1**  $\gamma$ GPNA treatment as described in methods (**Fig. 14A**). A significant decrease in the numbers of tubes sprouts ( $p < 0.01$ ) from the SK-Hep1 spheroids was evident when cultured in **T1**-conditioned media as compared to the **MM** control for 24 hours (**Fig. 14B**). Likewise, the tube sprouts that did form from the spheroids in the **T1**-conditioned media showed a significant decrease ( $p < 0.05$ ) in length as compared to the **MM** control (**Fig. 14C**). Additionally, SK-Hep1 cells were cultured on an extracellular matrix that promotes tubule formation of endothelial cells. When SK-Hep1 cells were grown for 3 hours in the conditioned media from **T1**-treated HepG2 cells, there was a dramatic decrease in tube formation as compared to the ones cultured in the conditioned media from **MM** treated HepG2 cells (**Fig. 14D**). We next assessed the tube length from each condition. There was a statistically significant decrease in average tube length in **T1** group versus **MM** ( $p < 0.05$ ) (**Fig. 14E**). Additionally, number of tubes that were 4  $\mu$ m in length or more

was significant fewer ( $p < 0.05$ ) when cultured in conditioned media from **T1**-treated HepG2 cells (**Fig. 14F**).

In order to address if the conditioned media used in spheroid and tubulogenesis assays could have any leftover  $\gamma$ GPNA, which may directly affect  $\beta$ -catenin activity in the endothelial cells, HepG2 cells were transfected with TOPFlash and cultured for 24 hours in the same conditioned media used in assays above. Comparable TOPFlash activity verified an absence of any residual **T1**  $\gamma$ GPNA in the conditioned media (**Fig. 14G**). Thus,  $\beta$ -catenin suppression in liver tumor cells impairs growth and development of tumor-associated endothelial cells in a paracrine manner.

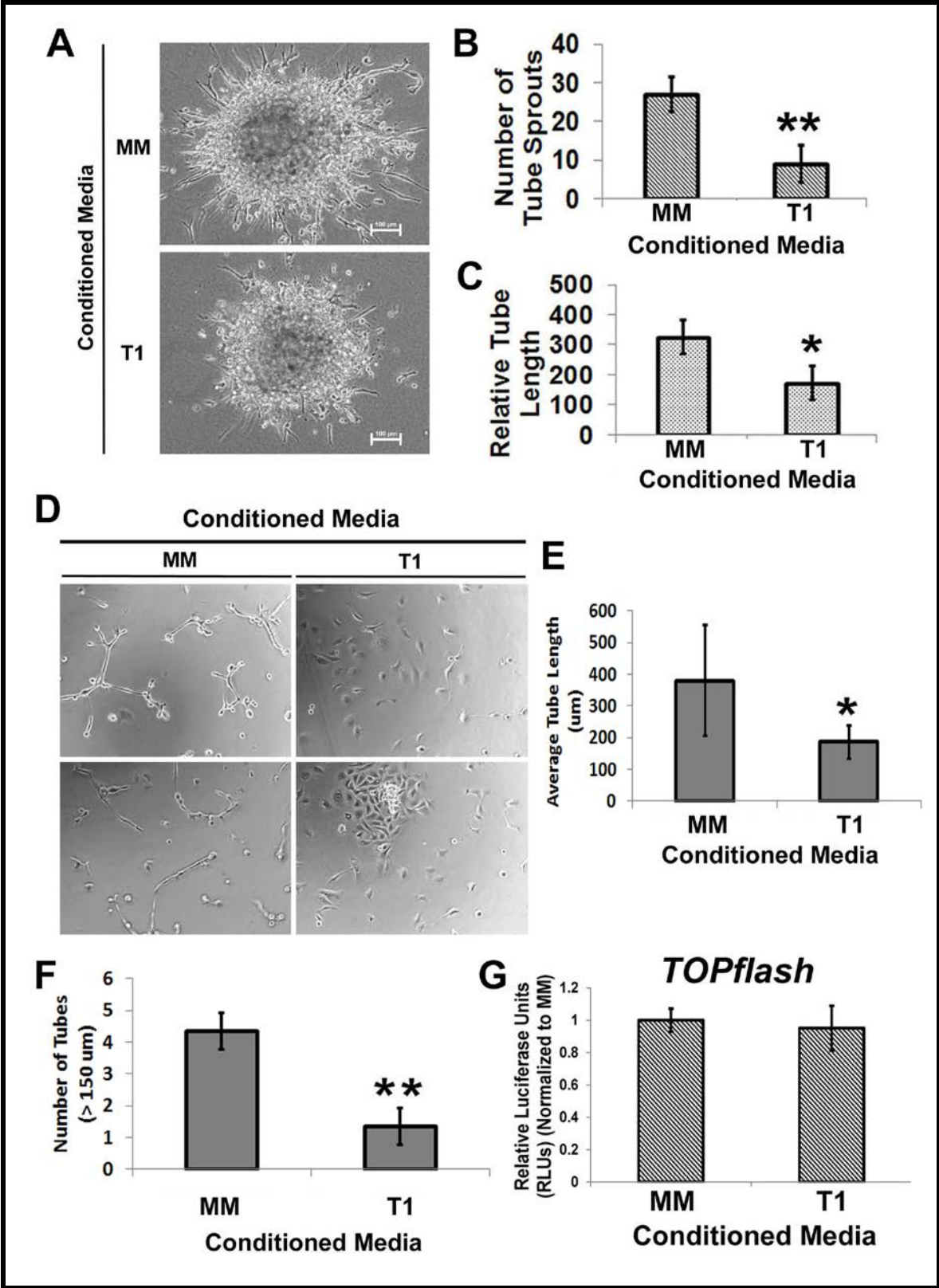


**Figure 14. Conditioned media from single T1 treatment of HepG2 cells collected after 72 hours diminished angiogenesis in SK-Hep1 cells.** (A) SK-Hep1 endothelial spheroids incubated with conditioned media obtained from HepG2 cells cultured in the presence of **T1** or MM for 72 hours show dramatically less branching in **T1**. (B) Numbers of tube sprouts from each spheroid were counted. Comparison of averages (MM  $n=3$ ; **T1**  $n=4$ ) (+/-SD) showed a significant decrease in number of sprouts in the **T1** group (\*\* $p < 0.01$ ). (C) Average tube length (+/-SD) from SK-Hep1 endothelial spheroids (MM  $n=3$ ; **T1**  $n=4$ ) also showed a significant less length in **T1** group (\* $p < 0.05$ ). (D) Two representative phase contrast images each from SK-Hep1 cells incubated for 3 hours on extracellular matrix while cultured in either conditioned media from HepG2 cells treated with MM  $\gamma$ GPNA or **T1**  $\gamma$ GPNA for 72 hours, show a noteworthy inhibition in tube formation and connections in the presence of **T1**-conditioned media only. (E) Quantification of tube length from conditions described in D shows a significant decrease in average length of tubes formed by SK-Hep1 cells when cultured in conditioned media from HepG2 cells treated with **T1**  $\gamma$ GPNA (\* $p < 0.05$ ). (F) Number of tubes measuring greater than 150  $\mu$ m were also significantly lower in **T1** as compared to the MM group (\*\* $p < 0.01$ ). (G) The same conditioned media used for A and D, when utilized to culture HepG2 cells showed comparable and low TOPFlash activity indicating lack of unused **T1**  $\gamma$ GPNA in the media that could have influenced endothelial cell function to confound angiogenesis assays.

### **3.4 DISCUSSION OF THE SIGNIFICANCE FOR DEVELOPMENT OF ANTISENSE FOR THERAPEUTICS**

PNA is a particularly promising class of nucleic acid analogue, developed in early 1990's, in which the natural sugar-phosphodiester backbone is substituted with achiral *N*-(2-aminoethyl) glycine units (266). The neutral backbone contribute the outstanding features to PNA which include 1) strong hybridization with complementary DNA and RNA with high affinity (and sequence selectivity) through Watson-Crick base pairing and 2) resistance to enzymatic degradation by proteases and nucleases (275, 276). These significant properties have

made PNA an attractive reagent for many applications in biology and medicine. However, poor cell-permeability remains a challenge for PNA (267, 268). Our group has reported a second-generation  $\gamma$ GPNA, which can be prepared from a relatively cheap L-arginine and exhibits better hybridization and cellular uptake properties (277). These  $\gamma$ GPNA oligomers are already conformationally pre-organized into a right-handed helix and are capable of binding DNA and RNA with high affinity and sequence selectivity, and we have already demonstrated that these can be taken-up by cells. Our studies indicate that within the first few hours of treatment,  $\gamma$ GPNA localizes to both nucleus and cytoplasm, where it can interact with mature mRNA.

Utilizing this new class of antisense molecules, we demonstrate a clear efficacy of  $\beta$ -catenin  $\gamma$ GPNA, both directed against the transcription start site (**T1**) as well as against the translational start site (**T2**) of *CTNNB1*. The effect of **T1** was greater than **T2** and is in agreement with previous studies (278). Using two liver tumor cell lines that harbors either a  $\beta$ -catenin gene deletion or a point mutation we demonstrate the efficacy of **T1** to inhibit  $\beta$ -catenin gene expression, protein and activity. The effect of  $\gamma$ GPNA treatment on tumor cells in culture was more robust at 24 hours than 72 hours. This is likely due to the lack of uptake of the  $\gamma$ GPNA by all cells in culture, giving such cells a growth and survival advantage over 72 hours. However, overall impact on tumor cell proliferation, viability and apoptosis was significant as has also been reported previously (Reviewed in (183)). The suppression of  $\beta$ -catenin activity after 72 hours of  $\gamma$ GPNA treatment on HepG2 cells was less robust as compared to Snu-449 cells. HepG2 HCC cells have a monoallelic, truncated  $\beta$ -catenin, which lacks exon-3 that contains all phosphorylation sites (serine 33, 27, 45 and threonine 41) required for degradation of  $\beta$ -catenin by the ubiquitin proteasome. Snu-449 cells have a single point mutation affecting serine 37, which also renders  $\beta$ -catenin stable. It is likely that the difference in stability of truncated versus

point-mutant  $\beta$ -catenin may be accounting for the difference in extent of decrease in  $\beta$ -catenin activity in response to the  $\gamma$ GPNA mediated  $\beta$ -catenin knockdown. Thus, we have developed  $\gamma$ GPNAs as a class of novel agents that could have significant therapeutic efficacy in targeting a specific molecule and at the same time have characterized a link between Wnt/ $\beta$ -catenin signaling and tumor angiogenesis in liver cancer.

In the current study we show that  $\beta$ -catenin suppression in HCC cells impairs the expression of several secreted pro-angiogenic factors that may be released by the tumor cells to influence angiogenesis in a paracrine manner. We identified decrease in various factors such as VEGF-A, Ephrin, FGF2, and CXCL5 after  $\beta$ -catenin suppression in liver tumor cells that are known to be relevant in HCC tumor angiogenesis (279). VEGF-A has been noted to be a direct target of  $\beta$ -catenin in colorectal cancer (253). It was interesting to note that FGF2 was decreased by both  $\beta$ -catenin-directed siRNA and  $\gamma$ GPNA to the same extent, although  $\beta$ -catenin suppression was much more robust in the former modality. This could be due to an autoregulation by FGF2 that has been described previously (280). Intriguingly, we saw an increase in HPSE expression after  $\beta$ -catenin knockdown by **T1** PNA treatment for 72 hours. Since this enzyme cleaves heparan sulfate in extracellular matrix, it has been associated with increased metastasis and angiogenesis. However, several other pro-angiogenic secreted factors were decreased as a result of  $\beta$ -catenin inhibition. This demonstrates a paracrine mechanism by which  $\beta$ -catenin activation in HCC could be supporting tumor growth and progression. Indeed the conditioned media from HCC cells cultured in the presence of **T1**  $\gamma$ GPNA was insufficient to support the growth and development of HCC-associated endothelial cells. An earlier study has also shown adenoviral mediated inhibition of Wnt signaling by Wnt inhibitory factor 1 (WIF1) and secreted frizzled-related protein 1 (sFRP1) overexpression in endothelial cell progenitors

impacted their differentiation and induced apoptosis (281). Thus, we conclude that  $\beta$ -catenin inhibition may in fact have dual impact on angiogenesis by not only interfering with growth and differentiation of endothelial progenitor cells directly but also via inhibiting paracrine signaling emanating from HCC cells.

When considering novel therapeutics, antisense technologies are among the most specific. Our PNA antisense is stable, effective and specific enough to reduce  $\beta$ -catenin protein expression in HCC cells leading to compromised cell growth and survival. There are several studies that indicate specific mutations in the DNA encoding for  $\beta$ -catenin which result in constitutive activation in HCC patients (163, 175, 189, 190). We have an HCC cell line with one of these genetic mutations cloned and being stably expressed utilized in this study, Hep3B-S33Y. In order to validate the specificity of our PNA antisense, we can clone out other known  $\beta$ -catenin mutations observed in HCC patients and create stable cell lines with these mutations as well. This will allow us to engineer PNA against these specific genetic mutations and can be tested by using the TOPflash luciferase assay. We could then analyze for off target effects of specific engineered PNA which may target a genetic mutation that it initially was not designed for. Ultimately, utilizing these PNAs in an *in vivo* model of HCC where activating  $\beta$ -catenin mutations drive the disease would be monumental achievement. However, what limits developing PNA for biological applications is the lack of optimized techniques for large scale synthesis of PNA. It is a very cost inefficient and labor intensive process to construct PNA oligonucleotides, and biological characterization will be slow until effective synthesis techniques for producing large quantities of PNA is developed.

#### 4.0 ANTISENSE LOCKED NUCLEIC ACIDS TREAT BETA-CATENIN DRIVEN HEPATOCELLULAR CARCINOMA IN MICE

Personalized medicine is beginning to make a significant presence in the battle against cancer. It is defined by the identification of a specific cause of a patient's disease, which can be precisely targeted resulting in a reduction of disease burden without overt toxicity. When considering the future of cancer therapeutics, the ideal method of therapy would be to specifically identify one or several factors driving the disease and target only these aberrations. Currently, groups including ours, such as in **Chapter 3**, have been pursuing antisense technologies for their potential to be tailored against a specific gene of interest. An interesting form of antisense oligonucleotide currently emerging is the Locked Nucleic Acids (LNAs). In this chapter we report the utilization of a novel LNA directed specifically against  $\beta$ -catenin in mouse models of HCC. Using a mouse model, which results in hepatocarcinogenesis secondary to activated  $\beta$ -catenin activation, we demonstrate that administration of LNA against the  $\beta$ -catenin gene to mice with established tumors resulted in a significant decrease in downstream Wnt target gene expression along with a notable reduction in tumor burden. The results presented here provide the final proof-of-concept therapeutic implications of targeting activated  $\beta$ -catenin in cancers like HCC for personalized medicine, to hence pave the way for the use of antisense oligonucleotides as a practical therapeutic modality.

#### 4.1 USE OF LNA LEADS TO REDUCED WNT/BETA-CATENIN SIGNALING

Two independent groups were responsible for the initial synthesis and characterization of LNA oligonucleotides in the late 1990's to early 2000's. As opposed to normal DNA or RNA nucleotides, LNA nucleotides have a methylene bridge that “locks” the 2P-oxygen in the ribose backbone to the 4P-carbon (**Fig. 15**) (282-284). The bridge created actually stabilizes the position of the phosphate backbone in an LNA oligonucleotide resulting in superior hybridization with DNA or RNA (282-284). Because LNA can easily hybridize with an intended DNA or RNA target of interest, inhibition of gene expression can occur via the activation of the RNase H recognition and degradation pathway (285, 286). The activation of the RNase H pathway gives LNA its antisense effect, and we have shown in **Chapter 3** the applicability of  $\gamma$ GPNA as an antisense technology used to block  $\beta$ -catenin protein expression in HCC cell lines leading to inhibited cell viability. However, compared to  $\gamma$ GPNA synthesis, an attractive aspect about LNA is the synthesis of LNA is identical to the polymerization of DNA or RNA only differing in the locked monomeric units. This can allow for large-scale synthesis of LNA that is relevant especially for *in vivo* use. In this section we characterize the impact of  $\beta$ -catenin directed LNA *in vivo* in normal and tumor-bearing mice to assess and optimize its efficacy in reducing  $\beta$ -catenin expression and activity.

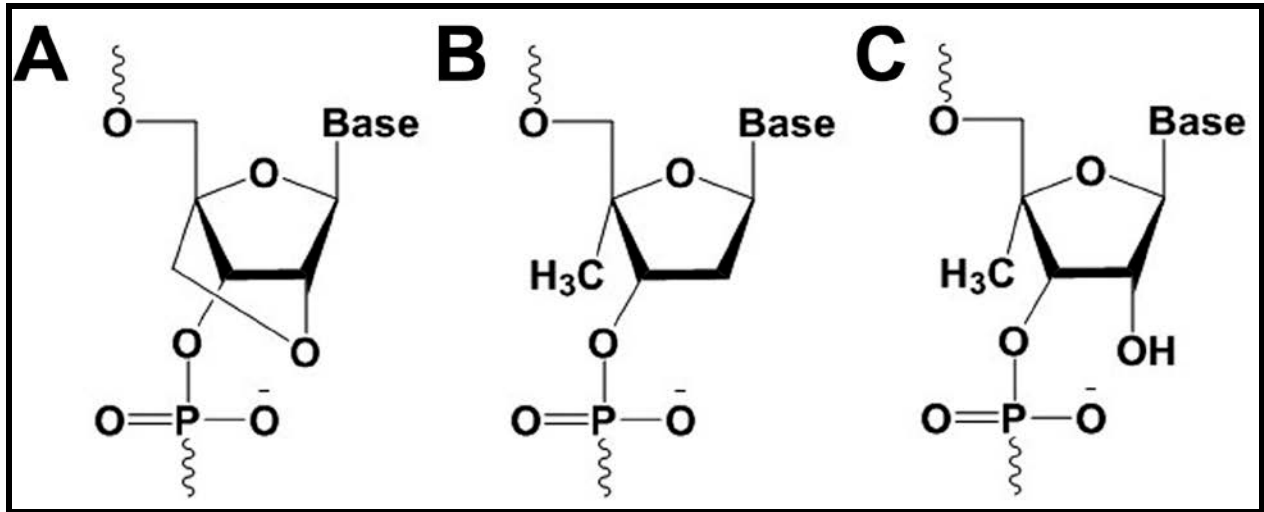
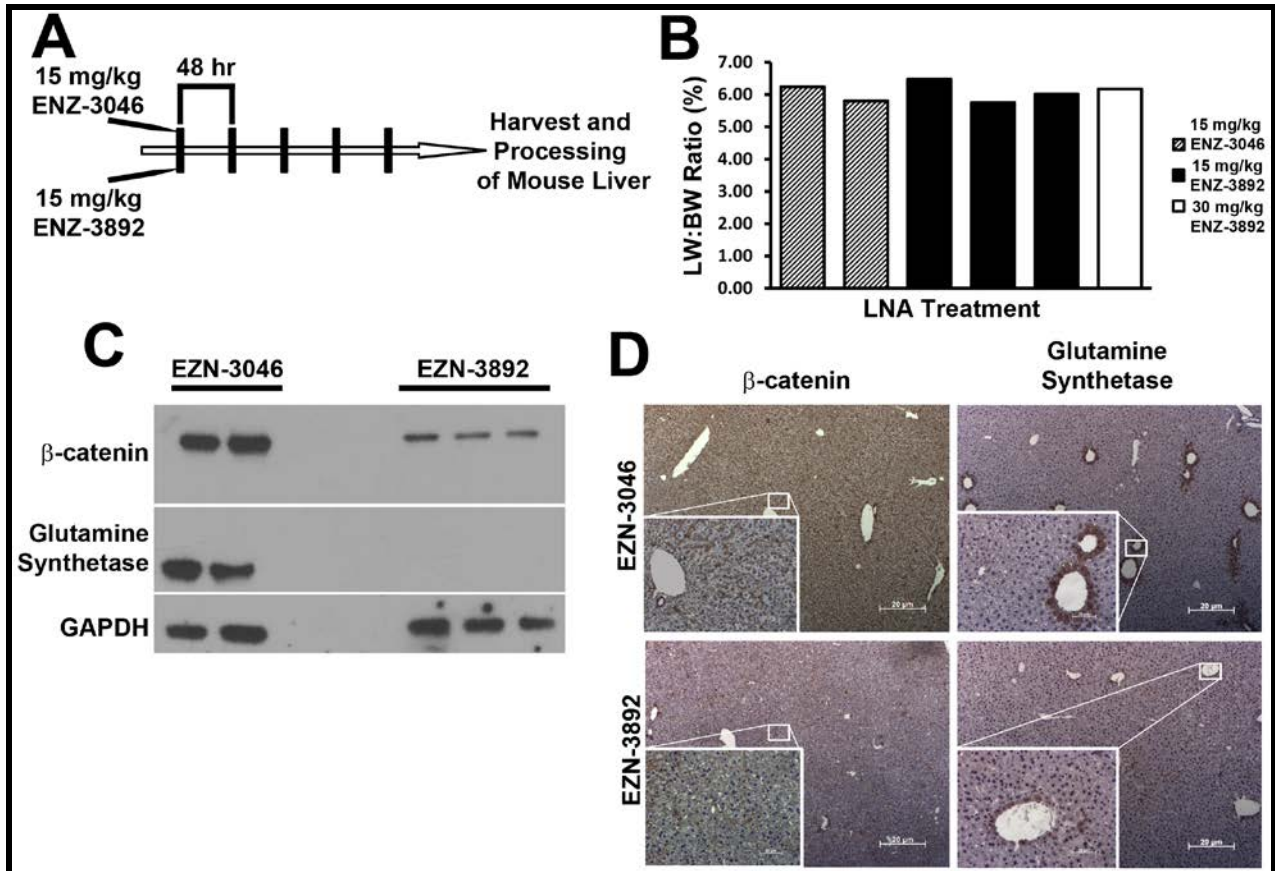


Figure 15. Nucleotide structures for LNA (A), DNA (B), and RNA (C).

#### 4.1.1 Optimization of LNA treatment *in vivo* in mouse liver

In order to assess the efficacy of LNA treatment *in vivo*, we treated wild type C3H/He mice with 15 mg/kg (n=3) or 30 mg/kg (n=1) **EZN-3892** (directed against  $\beta$ -catenin), and compared these mice to 15 mg/kg **EZN-3046** (directed against a scrambled sequence of survivin gene) treated mice (n=2) (**Fig. 16A**). Mice were treated every other day for a total of five times and monitored for toxicity. End of study liver weight to body weight (LW:BW) ratio showed no significant difference between the control and experimental group (**Fig. 16B**). Total  $\beta$ -catenin protein expression in whole liver lysates was significantly inhibited after **EZN-3892** LNA treatment compared to the control group with contaminant reduction of GS protein expression, the hallmark indicator of  $\beta$ -catenin co-transcriptional activity in the liver (**Fig. 16C**). Immunohistochemical (IHC) analysis of liver sections confirmed a visible decrease in total  $\beta$ -catenin levels throughout the liver as well as notably lower GS expression in the pericentral zone

of the liver (**Fig. 16D**). Thus, our analysis indicates that **EZN-3892** ( $\beta$ -catenin antisense LNA) treatment is a suitable tool to reduce  $\beta$ -catenin expression in mice leading to significant inhibition of Wnt/ $\beta$ -catenin activity.



**Figure 16. LNA administration significantly reduces  $\beta$ -catenin and GS levels in normal mice.** (A) Schematic representation of LNA administration. Mice were given 15 mg/kg of either **ENZ-3046** (Scrambled Survivin) or **ENZ-3892** ( $\beta$ -catenin) directed LNA five times every 48 hours prior to harvesting and processing for analysis. (B) Following LNA administration, mice livers when compared to their respective body weights did not differ when considering 15 mg/kg of **ENZ-3046**, 15 mg/kg **ENZ-3896**, or a high dose of 30 mg/kg **ENZ-3896** indicating no significant gross toxicity. (C) Protein levels for  $\beta$ -catenin and GS were significantly reduced following **EZN-3892** administration. (D) Immunohistochemistry also shows reduced levels of  $\beta$ -catenin and GS especially around the pericentral regions of the liver.

## 4.2 ESTABLISHING A WNT/ $\beta$ -CATENIN DRIVEN HCC MODEL *IN VIVO*

There are many mouse models of HCC currently available to researchers, but there are only few which represent clinically observed  $\beta$ -catenin activation in patients (189, 246, 287-291). The most clinically relevant mouse model which gives an accurate representation of the steps to carcinogenesis leading to activated  $\beta$ -catenin driven HCC is one which is induced by a chemical carcinogen called DEN, and then carcinogenesis is promoted by an activator of the constitutive active androstane receptor (CAR) called Phenobarbital (PB) leading to increased hepatocyte proliferation (173, 287, 292). DEN is bioactivated by two enzymes present in pericentral hepatocytes, Cytochrome P450 enzyme 2E1 (CYP2E1) and 2A6 (CYP2A6), causing its subsequent hydroxylation and oxidation, respectively, leading to the generation of genotoxic products which initiate DNA adducts and potentiate mutagenesis (293-297). PB is a barbiturate traditionally used as an antiepileptic. When administered orally, PB is absorbed through the portal circulation where it binds to Epidermal Growth Factor Receptor (EGFR) and blocks Epidermal Growth Factor (EGF) signaling, subsequently promoting the activating dephosphorylation of CAR which stimulates its transcriptional activity in hepatocytes (298-301). In this section we recapitulate the combination of DEN and PB mouse model *albeit* with administration at later stages and prove its quintessential use as a model of clinically observed, activated  $\beta$ -catenin in HCC.

### 4.2.1 Characterizing biological impact of DEN with PB in mouse liver

C3H/He mice were stratified into four groups of three mice each, Wild Type (WT), DEN only, PB only, and DEN+PB (DP), and were administered DEN and PB as indicated in methods

following which the mice were housed for roughly six additional months (**Fig. 17A**). During the course of the model there were some fatalities of unknown causes resulting in groups of mice being 2, 3, 2, and 2 respectively at the end of the study. After analysis of LW:BW ratio, the mice under the DP model had a higher LW:BW compared to the other three groups although statistics could not be done due to low numbers (**Fig. 17B**). Gross morphology of DP mouse livers reveals significant tumor burden as well compared to WT, DEN, or PB groups thus proving the efficacy of this model to induce hepatocarcinogenesis in mice under a relatively reasonable time frame (**Fig. 17C**).

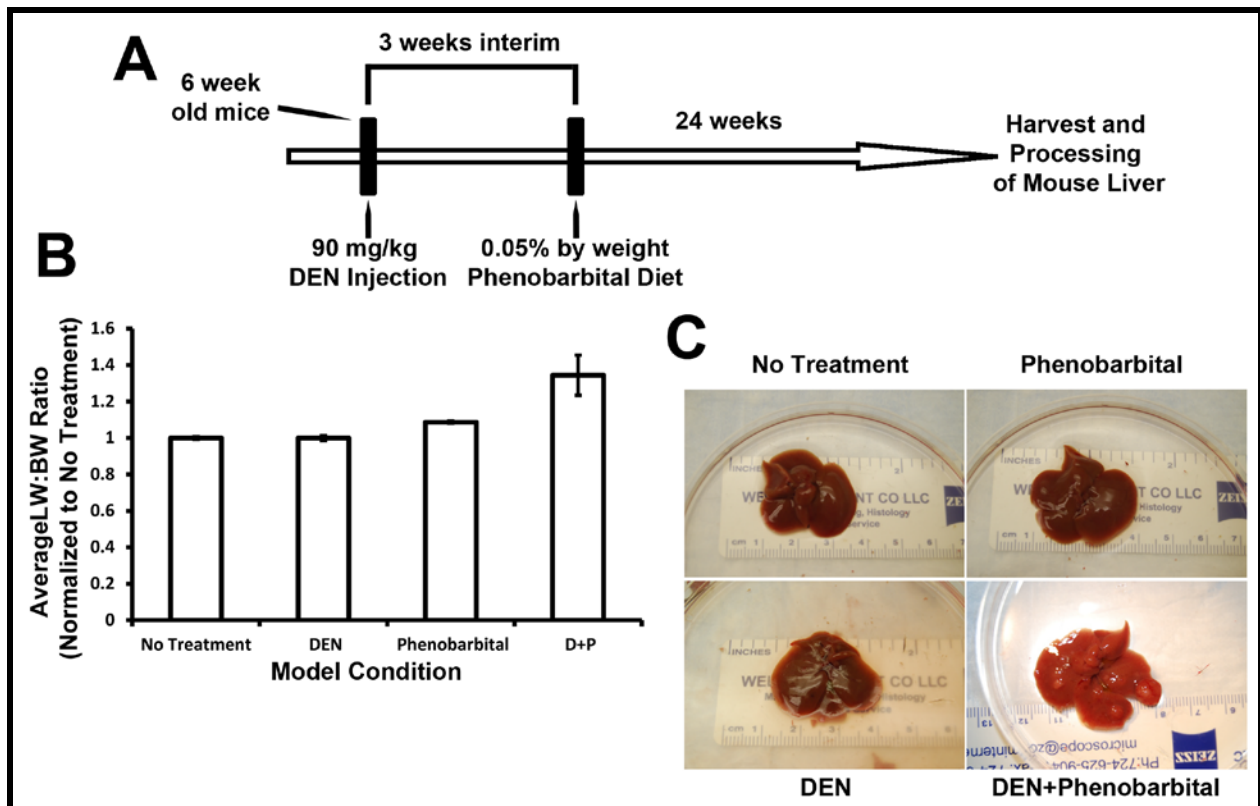


**Figure 17. Successful recapitulation of DP model leads to HCC tumor burden.** (A) Schematic representation of tumor model. 6 week old mice were injected with 90 mg/kg DEN followed by 3 weeks of rest. After, mice were put on 0.05% Phenobarbital diet for 24 weeks and mouse livers were harvested for analysis. (B) Average mouse

LW:BW ratio as compared to No Treatment group showed increase in liver weight in DP model as a result of tumor burden. (C) Representative gross images of mouse livers show DP group with significant HCC tumor burden.

#### **4.2.2 Histological and protein confirmation of activated $\beta$ -catenin in carcinogenesis model**

Upon histological investigation of the  $\beta$ -catenin status in each group of mice, the DEN+PB group showed prototypical hallmarks of  $\beta$ -catenin activation such as cytoplasmic and nuclear localization in tumor nodules (**Fig. 18A**). Concomitantly, nodules present in DP mice were all significantly positive for GS staining, with exception to two nodules visibly negative for GS, indicating activated Wnt/ $\beta$ -catenin signaling in majority of the tumor nodules (**Fig. 18B**). Indeed this protocol was shown to select for  $\beta$ -catenin-activation in 90% of HCCs (173). GS positive nodules were quantified per slide section per mouse and further indicate significant tumor burden from Wnt/ $\beta$ -catenin activation in DP mice (**Fig. 18C**). Data not shown here verified presence of S33Y mutations in many tumor nodules in this model. This data indicates our ability to successfully reestablish a model of HCC where Wnt/ $\beta$ -catenin seems to be the driving oncogenic signaling pathway.

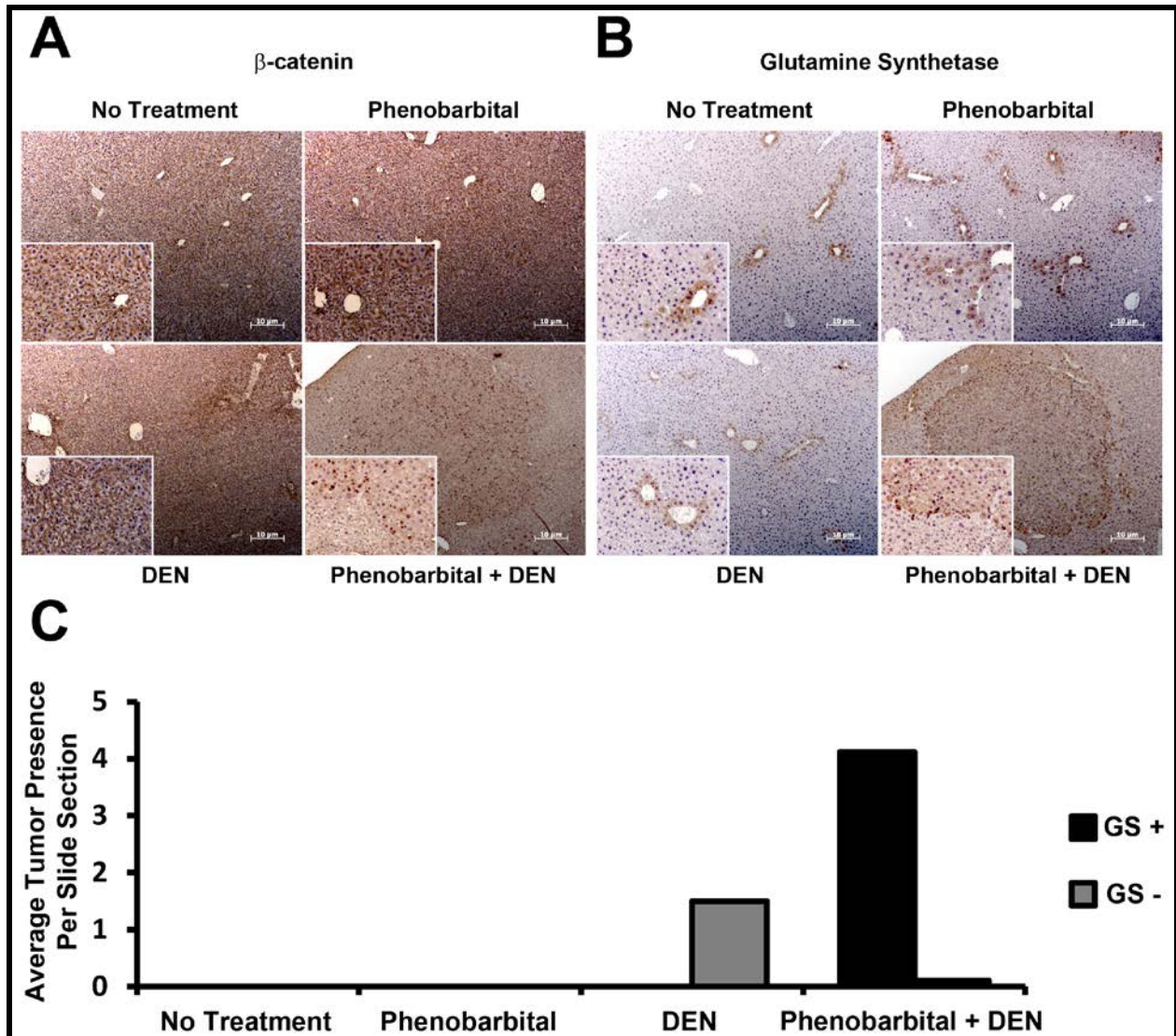


**Figure 18. Histological analysis of  $\beta$ -catenin driven HCC in DP murine model. (A)** IHC for  $\beta$ -catenin indicates nuclear/cytoplasmic presence in DP group only. **(B)** IHC for GS indicates tumors positive for nuclear/cytoplasmic  $\beta$ -catenin are also positive for GS staining. **(C)** Quantification of the number of GS positive and GS negative tumors per slide section in each group indicates GS positive nodules are exclusive to DP group.

### 4.3 USE OF LNA IN HCC MODEL LEADS TO REDUCED WNT/ $\beta$ -CATENIN SIGNALING AND TUMOR BURDEN

We have previously demonstrated the utilization of antisense oligonucleotides, which significantly inhibits HCC cell survival and subsequent secondary pathways such as those with effect on angiogenesis after targeting  $\beta$ -catenin in **Chapter 3**. Other studies have also proven the usefulness of antisense such as morpholinos in targeting Wnt/ $\beta$ -catenin signaling in culture as well as during rat liver regeneration (302). No such technology has been successfully been applied against Wnt/ $\beta$ -catenin driven HCC *in vivo*. Here we show for the first time that solely targeting  $\beta$ -catenin with antisense LNA in a mouse model of HCC with activated Wnt/ $\beta$ -catenin suppresses established tumor burden leading to significant disease regression.

#### 4.3.1 Baseline characterization of livers following LNA treatment under DEN + Phenobarbital model

C3H/He mice were stratified into 7 groups as summarized in **Appendix C**. Briefly, these included WT given 15 mg/kg ENZ-3046 (WTC) (3), WT given 15 mg/kg ENZ-3892 (WT $\beta$ ) (3), DEN+PB (DP) (5), DEN+PB given 15 mg/kg ENZ-3046 (DPC) (7), DEN+PB given 0.03 mg/kg ENZ-3046 (DPCL) (5), DEN+PB given 15 mg/kg ENZ-3892 (DP $\beta$ ) (8), and DEN+PB given 0.03 mg/kg ENZ-3892 (DP $\beta$ L) (4) (**Fig. 19A**). Mice were treated ten times every other day and monitored for toxicity. One mouse in group WT $\beta$  died from unknown causes, while two mice, one each in groups DPC and DP $\beta$ , died from anesthesia following the 8<sup>th</sup> injection of LNA. Baseline characterization began with identifying the  $\beta$ -catenin and GS expression in each group

(**Fig. 19B**). Histological examination of livers showed some heterogeneity in tumor development in the control groups whereas other show mostly homogeneous nodules in the DPC and DPCL groups as noted by uniformly GS positive nodules. One mouse each from DPC and DPCL groups did not present obvious GS positive nodules and therefore were omitted from further analysis. Remaining mice after omission in DPC (5) and DPCL (4) were considered together because regardless of dose, administration of scrambled control antisense oligonucleotides did not affect hepatocarcinogenesis or tumor biology. Also, tumor burden in DP $\beta$ L group as identified by GS and nuclear/cytoplasmic  $\beta$ -catenin presence did not reduce under IHC when compared to DP, DPC, or DPCL groups (data not shown) therefore the DP $\beta$ L group was also omitted from future quantitation and analysis. Ultimately, tumor burden as quantified by the presence of GS positive nodules was significantly reduced in the DP $\beta$  group compared to the DP and DPC groups (**Fig. 19B**).

Following administration of  $\beta$ -catenin-directed LNA, significant decreases in expression of both  $\beta$ -catenin and GS was observed in the DP $\beta$  group as compared to DPC or DP groups by Western Blot analysis (**Fig. 19C**). Tumor burden was assessed by H&E to analyze the presence of HCC tumors, which were significantly reduced in the DP $\beta$  group only (**Fig. 19D**). The most striking observation was absence of GS-positive nodules in the DP $\beta$  group by IHC as compared to DP and DPC groups (**Fig. 19D**). This indicates a inhibition of Wnt/ $\beta$ -catenin activation in DP $\beta$  group as shown by IHC (**Fig. 19E**). These data together suggest that  $\beta$ -catenin directed LNA alone is not only sufficient to reduce protein levels but also its activation, leading to decreased expression of GS, subsequently leading to regression of established HCC tumors *in vivo*.

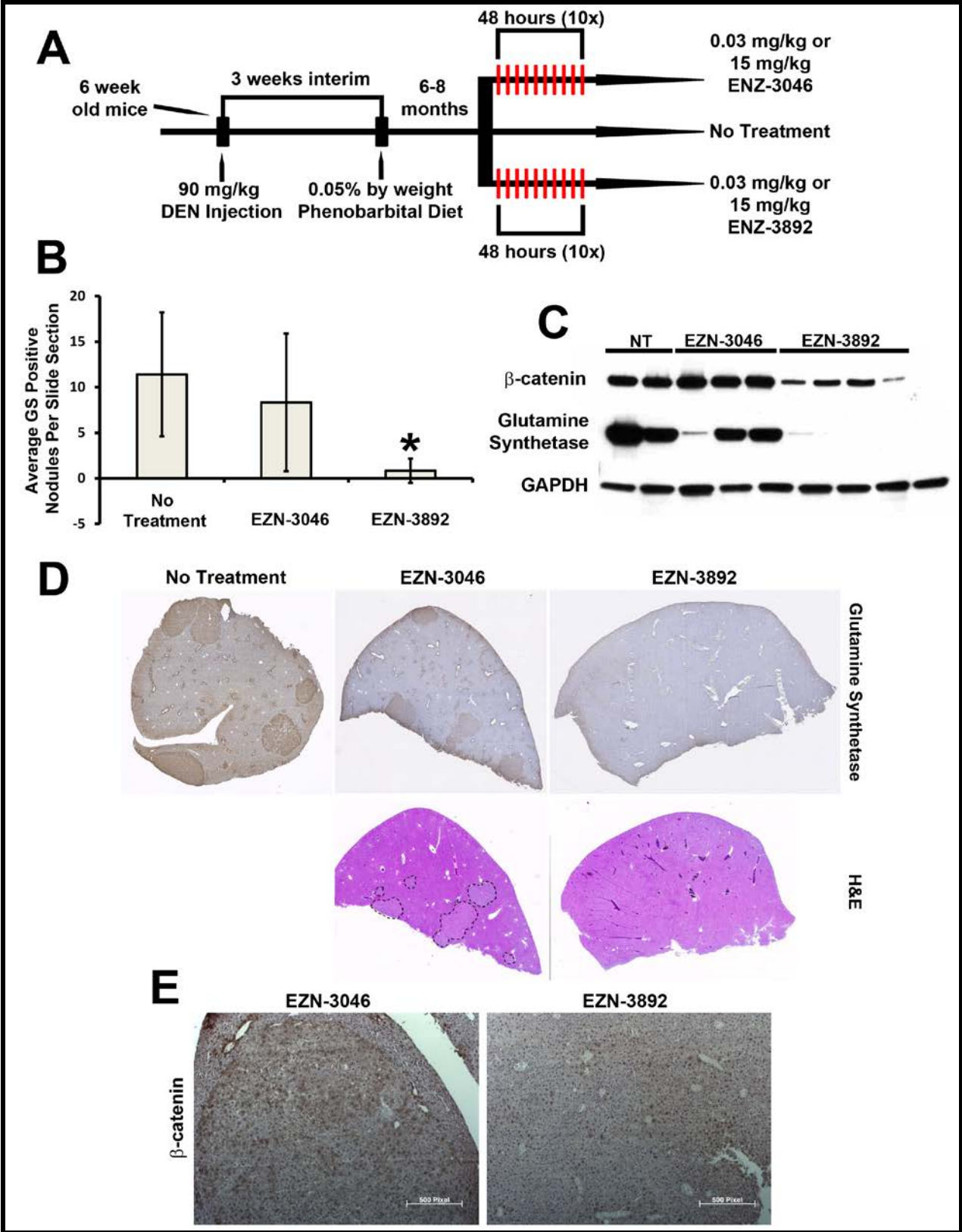


**Figure 19. Inhibiting  $\beta$ -catenin expression via LNA treatment reduces tumor burden following DEN+PB carcinogenesis model.** (A) Schematic representing LNA treatment after DEN+PB tumorigenesis. C3H/He mice injected at 6 weeks old with 90 mg/kg of DEN followed by a 3 week reprieve which led to 6-8 months on 0.05% PB diet. Mice were then categorized in 5 groups representing 0.03 or 15 mg/kg of **EZN-3046** or **EZN-3892**, as well as a group not treated with LNA. Injections occurred 10 times every 48 hours leading to harvesting of mouse livers for examination. (B) Tumor burden is quantified as average number of GS positive nodules per slide section per group. (C) Western blot for  $\beta$ -catenin and GS protein expressions compared to GAPDH in whole liver lysates showing significant reductions following **EZN-3892** LNA administration in mice under DEN+PB model. (D) H&E and GS immunohistochemistry of whole liver sections shows significant reductions in GS tumor burden following **EZN-3892** LNA administration compared to no treatment, or **EZN-3046** LNA. (E) IHC for  $\beta$ -catenin indicates significantly reduced nuclear/cytoplasmic  $\beta$ -catenin presence following **EZN-3892** LNA administration.

#### **4.4 DISCUSSING POSSIBLE THERAPUTIC IMPLICATIONS OF LNA ANTISENSE IN LIVER CANCER**

Originally, LNA oligonucleotides were used as molecular probes for microarray gene analysis because of their high binding affinity to DNA and RNA (303-305). Researchers began to test biological applications of LNA in cells such as inhibiting expression of telomerase showing not only their efficacy *in vitro*, but that they can easily transfected into cells by known lipophilic methods (306). Eventually chemotherapeutic implications were realized when *in vivo* experiments were performed targeting a subunit of RNA polymerase and showed that mice treated with LNA against this gene resulted in reduced tumor burden (307). As far back as 2001 LNA and antisense technology was proposed for possible chemotherapeutic applications (308).

Currently there are several companies dedicated to developing LNA antisense technologies for therapeutics, and several clinical trials are underway (309). The ease of LNA synthesis and its mass production makes it an attractive modality for specifically targeting known oncogenes driving cancer progression for personalized medicine. Indeed, concepts of personalized medicine have been applied from thyroid cancer treatment to antiretroviral medicines for HIV, and even in regenerative medicine (310-312). In the current study we show that targeting active Wnt/ $\beta$ -catenin signaling in HCC using LNA antisense technology may be another relevant application personalized medicine.

Activation of Wnt/ $\beta$ -catenin signaling pathway in primary HCC is heterogeneous making its targeting a challenge (254, 313). However, we have indicated in the previous chapters that inhibiting  $\beta$ -catenin activity in HCC cells either by reducing its nuclear activity by SM, or inhibiting its expression by antisense  $\gamma$ GPNA, leads to significant impact on tumor cell survival, proliferation and other processes such as angiogenesis (248). In this current study, we use LNA antisense in a successfully recapitulated *in vivo* model of HCC where  $\beta$ -catenin mutations drive tumorigenesis. Ablation of  $\beta$ -catenin expression alone was able to dramatically lower tumor burden in this model (**Fig. 19**).

We know through our studies that inhibiting  $\beta$ -catenin protein expression via LNA antisense technology leads to a reduction in HCC disease burden in mice. What we currently do not understand are the consequences which follow after  $\beta$ -catenin protein expression is reduced in these HCC tumors. What we do know is that  $\beta$ -catenin in hepatocytes is responsible for regulating the expression of GS and proteins involved in angiogenesis as previously described in **Chapter 3**. GS and angiogenesis are critical to cell viability and survival, therefore animals with HCC treated with antisense LNA against  $\beta$ -catenin should experience significant levels of

apoptosis leading to a potential inflammatory response to clear the dead cells. Apoptosis can be evaluated by TUNEL staining while the type of inflammatory response can be assessed for TH1/TH2/TH17 by analyzing interferon- $\gamma$ , IL4/5, or IL17 presence respectively by PCR, immunohistochemistry, or by fluorescence-activated cell sorting (FACS) analysis.

An additional question our DEN+PB model can be used to address is the origin of the  $\beta$ -catenin driven tumor cells which lead to their significant expression of GS. Interestingly, it is well known that the only cells that express GS at detectable levels by immunohistochemistry are those in the pericentral zone of the liver (314). Additionally, evidence suggests the pericentral hepatocytes are the only cells in the liver which express the necessary CYPs which metabolize and activate DEN, and express targets related to Phenobarbital administration (293-297, 301). With this being said, *in situ* hybridization of  $\beta$ -catenin through the duration of tumorigenesis under DEN+PB will allow us to observe if cells in the liver have copy number variations in the  $\beta$ -catenin gene. Analysis of loss of heterozygosity (LOH) will also give information when genetic aberrations become present.

While the precise mechanism of how  $\beta$ -catenin ablation leads to reduced tumor burden is currently not known, it is likely that through regulation of its downstream targets, it may have a multitude of effects on tumor cell proliferation and viability due to effects on metabolism, angiogenesis and even cancer stem cell expansion. Considering how other forms of LNA antisense therapy are in clinical trials, for example in castration-resistant prostate cancer, LNA-based anti  $\beta$ -catenin therapy may be feasible in a subset of HCC cases (309).

## 5.0 CONCLUSIONS AND FUTURE PROSPECTS

### 5.1 TARGETING $\beta$ -CATENIN IN HCC: A SAFE BET?

Identification of signaling pathways that are aberrantly active in tumor cells only, form the basis of personalized therapy and hold promise of fewer side effects. However, a lingering concern remains whether pathway like Wnt/ $\beta$ -catenin signaling that is critical in so many aspects of normal biology ranging from maintenance of the stem cell niche, to retention of cell-cell adhesions, could be druggable (315, 316). This is also a plausible concern since  $\beta$ -catenin is all part of the adherens junctions assembly. There are several theoretical arguments that demonstrate the safety of  $\beta$ -catenin inhibition especially in the liver. Liver-specific  $\beta$ -catenin conditional KO mice are viable and show no overt phenotype (317). Acute or chronic loss of  $\beta$ -catenin in liver or HCC cells is spontaneously compensated by  $\gamma$ -catenin albeit only at the adherens junctions (316, 318). Furthermore, liver is a unique organ in its dual blood supply that is derived from portal vein (~75%) and hepatic artery (25%). Interestingly, most HCCs are fed by the hepatic artery making loco-regional procedures such as TACE, viable and safe therapeutic modalities. Hence one can envision use of anti- $\beta$ -catenin agent to be delivered via such a procedure. Additionally, nanoparticle-based delivery or another method may have its own advantage to reduce any systemic toxic effects (319). Another caveat to this type of directed therapy is the fact that tumor cells may be able to activate alternate mechanisms of escape or resistance to a directed therapy.

We have shown that another oncogenic pathway, PDGFR $\alpha$ , is upregulated in HCC when Wnt/ $\beta$ -catenin signaling is suppressed (198, 320). And in such a case a sequential or combinatorial therapy may be useful. Thus, targeting activated Wnt/ $\beta$ -catenin signaling in HCC is plausible and may be safe and beneficial at least in a major subset of tumors.

## 5.2 USING SMALL MOLECULES FOR HCC THERAPY

HCC has a 90% fatality rate worldwide due to lack of an effective treatment (1, 19). HCC is currently the seventh most common cancer in the world and number three in cancer-related deaths (1, 19). With the current global burden of HCC, it is paramount to develop an effective therapy to treat the disease. Surgical resection and liver transplantation is a desirable therapeutic approach as it may be curative and also replaces cirrhotic liver with disease-free donor liver (22, 23). However, due to lack of resources, not every HCC patient can receive a liver transplant.

As discussed above, being a highly vascularized tumor, TACE is also useful in delivering chemotherapeutic agents in select patients with unresectable HCC (193). Eventually, owing to increased expression of VEGFR and PDGFR signaling, HCC has been shown to be somewhat susceptible to multi-TKIs (198-200). Sorafenib, a prototypical kinase inhibitor is used currently to treat unresectable primary HCC, with some therapeutic benefit (321). Sorafenib use in HCC patients has been shown to improve overall survival in advanced HCC patients, although it has limited efficacy especially in Child Pugh B and is often not well tolerated by patients (321, 322). Additionally Sorafenib targets multiple receptor tyrosine kinases including VEGFR, PDGFR and also Raf serine/threonine kinases eventually impacting the MAPK signaling. However, a distinct pathway implicated in hepatocarcinogenesis is the Wnt/ $\beta$ -catenin signaling pathway, which is

active in a significant subset of HCC due to various reasons. Thus, developing targeted therapies for HCC could significantly benefit patients with unresectable, primary HCC. Perhaps the most functional mechanism leading to constitutively active  $\beta$ -catenin in HCC is mutations in CTNNB1 and AXIN1/2, which interfere with its degradation resulting in nuclear translocation and increased target gene expression. These targets play various roles in tumor cell biology including regulation of tumor cell proliferation, survival, angiogenesis, and metabolism. Therefore inhibition of  $\beta$ -catenin in a subset of HCC is expected to be of significant therapeutic relevance. However, there are no effective inhibitors of  $\beta$ -catenin approved for clinical use and hence there is a need to drug discovery against this molecule.

We have developed a novel Wnt/ $\beta$ -catenin signaling inhibitor based off the structure of a known  $\beta$ -catenin inhibitor, **ICG-001**. Our SM is capable of inhibiting  $\beta$ -catenin driven downstream target expression which leads to subsequent inhibitions in cell survival and proliferation. Even though our SM has a limited efficacy observed *in vitro*, the potential for this molecule to be delivered through TACE is high. TACE delivers chemotherapeutic agents directly to the site of the lesion in the liver, allowing us to deliver **PMED-1** directly to the site of interest. **PMED-1**'s 24 hour activity is a benefit in this situation because while most of the SMs effect will be on the local area, once the SM disseminates systemically most of its activity will be gone indicating low to moderate off target toxicities. **PMED-1** may have applications in other pathologies with activated Wnt/ $\beta$ -catenin signaling such as colorectal carcinoma and certain melanomas. With further optimization and characterization, **PMED-1** may be a new therapeutic SM targeting Wnt signaling in diseases.

### 5.3 ANTISENSE THERAPY TARGETING $\beta$ -CATENIN IN HCC

Heterogeneity in signaling mechanisms among individuals is the thought behind personalized medicine. Several classes of signaling pathways have been identified to be aberrantly active in HCC making them attractive therapeutic targets. Wnt/ $\beta$ -catenin signaling is considered to be one of those pathways (183). While multiple modes of  $\beta$ -catenin activation have been reported in HCC, a major mechanism is mutations in *CTNNB1*, which leads to formation of stable  $\beta$ -catenin protein and has been shown to be associated with tumor proliferation, invasion, growth and viability (254, 313). In addition, based on the premise that cancer stem cells in HCC demonstrate active  $\beta$ -catenin signaling, its inhibition will impair the major cell source responsible for resistance, recurrence and metastasis (323-325). Concomitantly, based on the role of mutated- $\beta$ -catenin in making a subset of HCCs glutamine-addicted,  $\beta$ -catenin inhibitors may impair tumor metabolism to eventually affect tumor growth and survival (326). Thus, any strategy that would suppress  $\beta$ -catenin expression may have a therapeutic benefit in HCC. Indeed anti- $\beta$ -catenin therapies are being increasingly discussed and some agents are in various stages of preclinical and clinical development (327, 328). The role of  $\beta$ -catenin signaling however remains unexplored in HCC tumor angiogenesis and we now report regulation of several key angiogenic factors by the Wnt signaling, broadening the advantages of targeting  $\beta$ -catenin therapy in this tumor type. In fact we use a novel and timely modality, a new generation of  $\gamma$ GPNA, to inhibit  $\beta$ -catenin signaling and demonstrate its impact on angiogenesis.

As an added effect of inhibiting  $\beta$ -catenin activity in HCC cells, the expression of several targets involved in angiogenesis, were significantly inhibited leading to suppression of angiogenesis in SK-Hep1 endothelial cells which has never been shown before. Like many other

solid tumors, angiogenesis is also relevant in HCC. Growth and progression of hepatic tumors requires formation of new blood vessels as a source of nutrients and for effective metabolism (279). One of the potential mechanisms of the approved drug Sorafenib for stage IV unresectable HCC is its impact on angiogenesis through inhibition of certain receptor tyrosine kinases such as VEGFR2 (Flk1), platelet derived growth factor receptor (PDGFR) and others (329). However, angiogenesis inhibitors by themselves have had a limited impact on clinical outcome of HCC, which has been blamed on tumor heterogeneity in terms of areas of hypovascularity and hypoxia within tumors, and also on the hypoxia induced by the anti-angiogenic therapy. Hypoxia indeed has been shown to be a major driver of HCC growth as well as in imparting chemoresistance. Intriguingly, judicious use of anti-angiogenesis inhibitors as an adjuvant therapy has been shown to improve overall outcome in HCC patients. Similarly, agents such as Sorafenib, which impact multiple aspects of tumorigenesis including growth and viability of cancer cells and tumor angiogenesis has already shown a promise in HCC treatment. Our current study shows that therapeutic targeting of  $\beta$ -catenin may also have a similar broader impact in select HCC patients with activating mutations in *CTNNB1* or other mechanisms that lead to  $\beta$ -catenin activation by not only directly targeting cell viability, but also inhibiting angiogenesis by affecting angiogenic mediators downstream of hyperactive  $\beta$ -catenin.

Since  $\beta$ -catenin signaling can become activated due to many mechanisms, its inhibition from any antisense modality may have therapeutic benefit. We have shown both  $\gamma$ GPNA and LNA have anti-HCC effect through induction of cell death, inhibition of proliferation, anti-tumor angiogenesis effects, and eventually increased regression of disease. Antisense technology also has an added benefit in that it can be customized and made very specific to a gene of interest. Both  $\gamma$ GPNA and LNA have the potential to be targeted specifically against a mutation leading

to  $\beta$ -catenin activation in HCC. Clinically, there are specific  $\beta$ -catenin gene mutations observed that affect only a single allele (163). Antisense has the potential to target only the mutated gene of interest while resulting in no off target effects against wild-type  $\beta$ -catenin in other organ systems. If a biopsy of the lesion is feasible, tissue can be tested through genetic analysis for  $\beta$ -catenin gene mutation. Once the exact mutation in HCC is identified, devising an antisense against the specific mutation by utilizing either  $\gamma$ GPNA or LNA technologies will be a relevant personalized approach. We have shown the utilization of both  $\gamma$ GPNA and LNA, and these tools have the ability to passively diffuse through cellular membranes leading to significantly reduced toxicities which would be associated by agents used to force these oligonucleotides into cells. Also, because of their specificity, antisense oligonucleotides used, as a therapeutic intervention would show significantly less off target effects experienced by current chemotherapy. It would be an important task for future development to demonstrate the efficacy of these modalities to inhibit only the mutated  $\beta$ -catenin gene sequence to truly personalize treatment specific to a patient.

#### **5.4 $\beta$ -CATENIN BIOMARKERS FOR PERSONALIZED MEDICINE**

The molecular basis of HCC is heterogeneous and may partially reflect the varying underlying etiologies such as HBV, HCV, AFB1, chronic alcohol intake or NAFLD/NASH. The key for personalized medicine in HCC will be to identify a subset of patients with specific ‘driver’ mutations and target those for effective and safe treatment. Wnt/ $\beta$ -catenin signaling activation is one such mechanism of oncogenesis that appears to be critical in a major subset of

HCCs and developing an effective therapy will be of essence. However, can  $\beta$ -catenin be a global therapeutic target in HCC? The answer may be 'No' only because when hepatocyte-specific  $\beta$ -catenin conditional KO were subjected to DEN-induced carcinogenesis, a paradoxical increase in tumor burden became evident, which was associated with increased injury, inflammation, fibrosis and oxidative stress (317). Thus  $\beta$ -catenin should be targeted only when there is evidence of its activation. Thus specific biomarkers of aberrant  $\beta$ -catenin signaling in HCC are required to accurately diagnose a subset of HCCs that clearly demonstrate its activation. To date, the only effective way of identifying mutation is by genetic analysis of tumor upon its excision. Also,  $\beta$ -catenin activity is identifiable through analysis of biopsy by IHC (192). Others and we have identified nuclear and cytoplasmic  $\beta$ -catenin localization as well as tumor-wide staining of GS, which is a good indicator of aberrant Wnt activation. However, biopsies may not be feasible in majority of HCC patients since these patients have significant fibrosis or cirrhosis. Thus ideal way to detect  $\beta$ -catenin activation in HCC for clinical use may be through identification of a secreted biomarker in plasma. Another innovative means may be through assessment of genetic mutation in circulating tumor cells that may have recapitulate aberrations of the primary tumor. In the current study, we were able to successfully reproduce a model of  $\beta$ -catenin-driven HCC, which can be used to identify novel biomarkers of  $\beta$ -catenin activation (173). In the future it may be possible to determine the secretome in these mice to identify novel biomarkers of  $\beta$ -catenin that may be of significance for diagnostics as well as a tool to assess treatment response. Similarly, circulating tumor cells will be assessed to determine such procedure for diagnosing  $\beta$ -catenin gene mutations. Thus, biomarker discovery in this model may have important translational implications in the clinic and may be applied to the patients in the future.



## 6.0 MATERIALS AND METHODS

### 6.1 DEVELOPMENT OF $\gamma$ GPNA AND SMALL MOLECULES

#### 6.1.1 Oligomer Synthesis

All Boc/Z protected PNA monomers and Boc-<sup>L</sup>Arg-OH were purchased from Applied Biosystems and used without further purification. All  $\gamma$ GPNA monomers were synthesized by methods reported by Sahu and coworkers (277). All commercial reagents were used without further purification. MALDI-TOF experiments were performed on a Perceptive Biosystems Voyager STR MALDI-TOF mass spectrometer using a 10 mg/ml solution of  $\alpha$ -hydroxycinnamic acid in ACN-water (1:1) with 0.1% TFA. UV-Vis measurements were taken on a Varian Cary 300 Bio spectrophotometer equipped with a thermoelectrically controlled multi-cell holder.

All  $\gamma$ GPNA oligomers were synthesized on solid-support according to standard protocol using standard Boc chemistry (330). The oligomers were purified by reverse-phase HPLC and characterized by MALDI-TOF. All GPNA stock solutions were prepared using nanopure water and the concentrations were determined at 90°C using the following extinction coefficients for GPNA monomers: 13,700 M<sup>-1</sup> cm<sup>-1</sup> (A), 6,600 M<sup>-1</sup> cm<sup>-1</sup> (C), 11,700 M<sup>-1</sup> cm<sup>-1</sup> (G), and 8,600 M<sup>-1</sup> cm<sup>-1</sup> (T).

### 6.1.2 Small Molecule Similarity Search

The structural similarity is a similarity technique dependent only on surface shape and charge characteristics of ligands (331). Structural similarity is defined as a Gaussian function of the differences in the molecular surface distances of two molecules at weighted observation points on a uniform grid. The computed surface distances include both distances to the nearest atomic surface and distances to donor and acceptor surfaces. This function is dependent on the relative alignment of the molecules, and consequently their alignment and conformation must be optimized. The conformational optimization problem is solved by fragmentation, conformational search, alignment, and scoring, followed by incremental reconstruction from high-scoring aligned fragments. The alignment problem is addressed by exploiting the fact that two unaligned molecules or molecular fragments that have some degree of similarity will have some corresponding set of observers that are seeing the same things. Optimization of the similarity of two unaligned molecules or molecular fragments is enabled by finding similar sets of observers of each molecule that form triangles of the same size (331).

### 6.1.3 *In silico* ADME and toxicity screening of projected SMs

Computational modeling tools were used to estimate the bioavailability, aqueous solubility, blood brain barrier potential, human intestinal absorption, the cytochrome P450 (*i.e.* CYP2D6) enzyme inhibition potential, mutagenicity, and hERG inhibition of the hits obtained from the database screening. The bioavailability, aqueous solubility, and human intestinal absorption were estimated using the Advanced Chemistry Development, Inc.

(ACD/Labs)/ADME Boxes software while mutagenicity, hERG and CYP2D6 inhibition were estimated with ACD/Tox screening (ACD Labs, Toronto, Canada) (15).

## **6.2 CELL CULTURE AND ASSAYS**

$3 \times 10^5$  (per 6 well) or  $4 \times 10^4$  (per 24 well) HepG2 hepatoblastoma cells and Huh7 adult HCC cells acquired from American Type Culture Collection (ATCC) were cultured in EMEM (ATCC) supplemented with 10% fetal bovine serum (FBS) (Atlanta Biologicals).  $3 \times 10^5$  (per 6 well)  $4 \times 10^4$  (per 24 well) Snu-449 and Snu-398 adult HCC cells (ATCC) were cultured in RPMI-1640 (ATCC) supplemented with 10% FBS. SK-Hep1 hepatic adenoma tumor associated endothelial cells (ATCC) were maintained in EMEM with 10% FBS.

### **6.2.1 Human HCC cell culture and establishing stable $\beta$ -catenin mutants**

Human HCC cell line Hep3B (ATCC) were plated in six-well plates and cultured in EMEM (ATCC) supplemented with 10% FBS (Atlanta Biologicals) at 37°C in a humidified 5% carbon dioxide atmosphere. Wild type  $\beta$ -catenin gene (WT) or  $\beta$ -catenin gene mutated at serine 33 to tyrosine (S33Y), which is constitutively active, were kindly provided by Dr. Jian Yu (Department of Pathology, Hillman Cancer Center, University of Pittsburgh, PA). The cells were grown to 90% confluence, 2  $\mu$ g of WT and S33Y  $\beta$ -catenin plasmid DNA was transfected with Lipofectamine™ 2000 (Invitrogen), as the manufacturer's instructions. 48 hours after transfection, the cells were selected by multiple passaging using Geneticin (G418; Sigma; 500  $\mu$ g/ml) to generate stable transfected cell lines.

For transient transfection, Huh7 human HCC cells (ATCC) were plated in 6 well plates and transfected using 5  $\mu$ l of FuGene HD (Roche) per well with either WT or S33Y  $\beta$ -catenin in normal EMEM (ATCC) containing 10% FBS (Atlanta Biologicals). Cells were incubated in transfection reaction overnight at 37°C, and after 24 hours, the media was changed to serum free EMEM and cells allowed to grow for additional 48 hours.

### 6.2.2 Preparation and Cell Culture Treatments

**PMED-1** and **PMED-2** (TimTec or Chembridge) were reconstituted in **DMSO** (Fisher-Scientific) to 50 mM stocks. Treatment concentrations ranging from 200  $\mu$ M to 25  $\mu$ M were serially diluted in respective culture media along with corrected **DMSO** percentage control. Single treatments were either for 24 or 48 hours. After synthesis, **MM**, **T1**, or **T2**  $\gamma$ GPNA were reconstituted in dH<sub>2</sub>O. HCC cells were treated with  $\gamma$ GPNA at concentrations ranging from 10  $\mu$ M to 250 nM from 24 to 72 hours. **EZN-3892** and **EZN-3046** LNA were provided by Enzon Pharmaceuticals. LNAs were reconstituted in HBSS (Lonza) followed by sterile filtration through a 10  $\mu$ m PES filter (Millipore). Concentrations of LNA were determined using a U/V spectrophotometer..

### 6.2.3 Kinase Assays

Kinase assays were performed assessing activity of **PMED-1** against AKT, protein kinase D (PKD), Polo like kinase 1 (Plk1) and Plk2, and cyclin-dependent kinase-activating kinase (CAK). Black (FP) and white (TR-FRET) opaque small volume plates were purchased from Greiner (Monroe, NC). IMAP binding reagent, binding buffer, terbium, peptide substrates

(AKT: 5FAM-GRPRTSSFAEG-COOH; PKD: 5FAM-KKLNRTLSVA-COOH; Plk1 and CAK: 5FAM-KKRNRRLSVA-OH; Plk2: 5FAM-LKKLTRRPSFSAQ-COOH), and kinase reaction buffers (10 mM Tris-HCl, pH 7.2, 10 mM MgCl<sub>2</sub>, 0.05% NaN<sub>3</sub>, 1 mM DTT and 'carrier' (PKD, AKT: 0.1% bovine serum albumin; Plk1, Plk2, CAK: 0.01% Tween-20) were purchased from Molecular Devices (Sunnyvale, CA). Active Plk1 and AKT were from Cell Signaling Technologies ; PKD and CAK from Upstate; and Plk2 from Invitrogen. ATP was purchased from GE Healthcare (Piscataway, NJ); and H89 from EMD Biosciences.

Compounds were solubilized in **DMSO** to stock 10 mM and then diluted to 3x starting concentration 300 μM (3% **DMSO**) and serially diluted in 3% **DMSO**-water. Briefly, 2 μL of 3x concentration substrate + ATP in 2x complete reaction buffer were added to each well of a microtiter plate. Following 2 μL additions of 3x concentration compound, 2 μL of 3x concentration enzyme in 1x complete reaction buffer was added to start the 6 μL total volume kinase reaction. At the designated time, the reaction was stopped by addition of binding solution containing the binding reagent (FP) or binding reagent + terbium (TR-FRET assays). Plates were read (FP Ex<sub>485</sub>/Em<sub>525</sub> or TR-FRET Ex<sub>330</sub> Em<sub>490, 520</sub>) on a Molecular Devices Spectramax M5. Specific reactions are summarized below:

#### **6.2.3.1 IMAP-based Plk2 TR-FRET Assay**

0.34 mUnits/μL Plk2; 550 nM substrate peptide; 35 μM ATP; 1% **DMSO**; 2.5 hour kinase reaction; 15 μl binding solution (70% A, 30% B + 1/600 binding reagent + 1/400 terbium); 2 hour binding incubation.

### **6.2.3.2 IMAP-based PKD FP Assay**

0.06 mUnits/ $\mu$ L PKD; 100 nM substrate peptide; 20  $\mu$ M ATP; 1% **DMSO**; 90 minute kinase reaction; 18  $\mu$ L binding solution (100% A + 1/400 binding reagent); 2 hour binding incubation.

### **6.2.3.3 IMAP-based Plk1 TR-FRET Assay**

0.034 mUnits/ $\mu$ L Plk1; 750nM substrate peptide; 25  $\mu$ M ATP; 1% **DMSO**; 3 hour kinase reaction; 18  $\mu$ L binding solution (70% A, 30% B + 1/600 binding reagent + 1/400 terbium); 5 hour binding incubation.

### **6.2.3.4 IMAP-based CAK TR-FRET Assay**

0.1 mUnits/ $\mu$ L CAK; 500 nM substrate peptide; 25  $\mu$ M ATP; 1% **DMSO**; 3 hour kinase reaction; 12  $\mu$ L binding solution (70% A, 30% B+ 1/600 binding reagent + 1/400 terbium).

### **6.2.3.5 IMAP-based AKT FP assay**

0.05 mUnits/ $\mu$ L AKT; 300 nM substrate peptide; 10  $\mu$ M ATP; 1% **DMSO**; 90 minute kinase reaction; 18  $\mu$ L binding solution (75% A, 25% B + 1/400 binding reagent); 45 minute binding incubation.

## **6.2.4 Transient Inhibition of $\beta$ -catenin via siRNA**

HepG2 cells cultured in 6 well plates were serum starved for 4 hours prior to addition of transfection reaction composed of Lipofectamine 2000 (3  $\mu$ l) (Invitrogen), OPTIMEM (100  $\mu$ l),

and 50 nanomoles of either *CTNNB1* or negative control siRNA per well. Reaction occurred for 4 hours at 37°C followed by addition of EMEM containing 4% FBS to cells which were incubated overnight. This was followed by complete replacement of media with EMEM containing 10% FBS. After 48 hours of transfection, cells were harvested.

### 6.2.5 $\beta$ -Catenin Luciferase Activity Assay

HCC cells were transfected using FuGene (Roche) with both Renilla luciferase and TOPFlash firefly luciferase plasmids together at the same time. Cells were treated with **T1**, **T2**, or **MM**  $\gamma$ GPNA 15 minutes after transfection for an additional 24 or 72 hours, whereas cells were treated with SMs **PMED-1**, **PMED-2**, **ICG-001** or **DMSO** control 24 hours after transfection for an additional 24 or 48 hours. Lysates were then harvested using the Dual-Luciferase Reporter Assay System (Promega). Luciferase signals were normalized to Renilla as transfection controls. Student's t-test was used to determine the significance of the differences between treatments and  $p < 0.05$  was considered significant and of  $p < 0.01$  was considered highly significant.

### 6.2.6 $\beta$ -Catenin Luciferase Activity Assay: Time Course

S33Y- $\beta$ -catenin stably-transfected Hep3B cells were cultured in serum free EMEM containing 500  $\mu$ g/ml G418 for 4 hours prior to Lipofectamine 2000 cotransfection using Renilla and TOPFlash luciferase plasmids for 4 hours. Cells were then exposed to EMEM containing 4% FBS and 500  $\mu$ g/ml G418 overnight. The following morning, cells were serum starved again for 4 hours in order to synchronize cell cycle followed by treatment with either 0.05% **DMSO** or 25

$\mu\text{M}$  **PMED-1** in EMEM containing 10% FBS and 500  $\mu\text{g/ml}$  G418 for 3, 6, 9, 12, 18, 24, 36, or 48 hours prior to harvest and analysis of samples for luciferase activity as described.

### **6.2.7 MTT Assay for Toxicity**

HCC cells were plated in 6 well plates while primary human hepatocytes were plated in 12 well plates for 24 hours. Cells were then treated with **MM**, **T1**, **DMSO**, **PMED-1** or **PMED-2**. After incubation, cultures were changed into 1% MTT (Sigma-Aldrich) wt/v in PBS for 0.5 hours at 37°C. Cells are then lysed using room temperature isopropanol. Samples were finally read at 570 nm for colorimetric assessment.

### **6.2.8 Thymidine Incorporation Proliferation Assay**

HepG2 or Snu-398 cells were plated in 6 well plates for 24 hours. Cells were then treated with  $\gamma\text{GPNA}$  for 72 hours while pulsed with 2.5  $\mu\text{Ci}$  of [5'- $^3\text{H}$ ]-Thymidine (PerkinElmer) for 48 hours. For **SMs**, cells were treated with **DMSO** or **PMED-1** for 24 or 72 hours in the presence of 2.5  $\mu\text{Ci}$  of [5'- $^3\text{H}$ ]-Thymidine. Media was aspirated and washed with 1x PBS and incubated with 5% Trichloroacetic acid (Sigma-Aldrich) for 15 minutes at 4°C. Plates were next washed in running water and placed to dry at 37°C. Cells were then lysed in 0.33 N NaOH for 20 minutes at room temperature. Samples were combined with scintillation fluid and measured in Beckman LS 6000 IC scintillation counter.

## **6.3 PROTEIN EXTRACTION AND WESTERN BLOTTING**

### **6.3.1 Whole Cell Lysate Preparation: Cell Culture**

Whole cell lysates (WCL) were prepared using Radio immunoprecipitation assay (RIPA) buffer containing 1% IgePAL CA-630, 0.5% Sodium Deoxycholate, 0.1% Sodium dodecyl sulfate in 1x Phosphate Buffered Saline (PBS) after  $\gamma$ GPNA, SM or LNA treatments. 200  $\mu$ l or 100  $\mu$ l of RIPA was used per 100 mm dish or 6 well plate, respectively, with phosphatase/protease cocktail inhibitor (Sigma Aldrich). Plates were incubated on ice for 30 minutes followed by removal of lysates to a fresh 1.5 ml tube. Lysates were centrifuged at 14,000 RPM for 10 minutes at 4°C in order to remove clear supernatant to a new 1.5 ml tube while disposing of the pellet. Samples were then stored at -80°C until utilization or determination of protein concentration via BCA protein assay (Pierce) to ensure equal protein concentrations for subsequent assays.

### **6.3.2 Whole Cell Lysate Preparation: Whole Liver Tissue**

At time of harvest, mice were anesthetized by isoflurane inhalation and subsequently killed by cervical dislocation. After sacrifice, the livers were extracted, washed in PBS, and then the tissue was flash frozen in liquid nitrogen and stored at -80°C until use. At time of use, tissue was homogenized in RIPA with protease/phosphatase inhibitor manually via glass mortar and pestle on ice. Lysates were removed to a fresh 1.5 ml tube and centrifuged at 14,000 RPM for 10 minutes at 4°C in order to remove clear supernatant to a new 1.5 ml tube while disposing of the pellet. Samples were then stored at -80°C until utilization or determination of protein

concentration via BCA protein assay (Pierce) to ensure equal protein concentrations for subsequent assays. All animal studies were approved by University of Pittsburgh IACUC office.

### **6.3.3 Western Blot Analysis**

9 to 60  $\mu\text{g}$  of lysate was run on precast 7.5% or 4-14% gradient polyacrylamide gel (Bio-Rad) at 60V for 30 minutes, then 100V for 1.5 hours. Gels were then transferred onto a polyvinylidene fluoride (PVDF) membrane (Millipore) for 1 hour at 4°C under 100V. Membranes were blocked in 5% milk (Labscientific) in Blotto [0.15M NaCl, 0.02M Tris pH 7.5, 0.1% Tween in dH<sub>2</sub>O] for 1 hour at room temperature. Primary antibodies were diluted in 5% milk/Blotto and incubated on membranes overnight at 4°C. Membranes were then washed in Blotto for 1 hour at room temperature prior to incubation of membranes with rabbit (1:10,000), mouse (1:25,000), or goat (1:10,000) secondary antibodies (Millipore) for one hour. Membranes were again washed in Blotto for 1 hour at room temperature prior to expose to either SuperSignal West Pico or Femto Chemiluminescent Substrate (ThermoScientific) for 1-2 minutes at room temperature. The bands reflective of target proteins were viewed by autoradiography.

### **6.3.4 Protein Complex Immunoprecipitation**

HepG2 cells treated with **DMSO**, 25  $\mu\text{M}$  **PMED-1**, or 25  $\mu\text{M}$  **ICG-001** for 24 hours in 10 cm dishes. WCLs were prepared as described and 0.25  $\mu\text{g}$  of control mouse IgG (Santa Cruz) was used to pre-clear lysates. 2  $\mu\text{g}$  of  $\beta$ -catenin monoclonal antibody (BD Transduction Laboratories) were added to 500  $\mu\text{g}$  of each sample for 1 hour at 4°C while rocking. 20 ml of Protein A/G+Agarose beads (Santa Cruz) were added to each sample over night at 4°C on a

rocker. Samples were then centrifuged at 13,000 rpm for 5 minutes prior to removing the supernatant. Bead pellet was then washed with RIPA buffer followed by 3 additional centrifugations and washes. After the final wash, bead pellets of each sample were resuspended in 40 ml of 2x SDS buffer (Bio-Rad) and boiled at 95°C for 5 minutes. Samples were centrifuged one last time for 1 minute and 20 µl of samples were run on a 5% polyacrylamide gel (Bio-Rad). Gel was run and transferred as previously described. The membrane was probed as described with primary antibody for CBP and secondary  $\alpha$ rabbit antibody (1:10,000 dilution in 1% milk/Blotto). West Pico chemiluminescence was used to develop the membrane as previously indicated.

#### **6.4 RNA EXTRACTION AND QRT-PCR**

RNA from HepG2 cells treated with 1 µM **MM** or **T1** for 72 hours or transfected with  $\beta$ -catenin or negative control siRNA for 48 hours was harvested using TRIzol (Invitrogen) and purified using a phenol-based method. RNA was DNase treated (Ambion), reverse-transcribed using SuperScript III (Invitrogen) cDNA synthesis kit, followed by RT-PCR for Fibroblast growth factor 2 (FGF2), VEGF-A and  $\beta$ -catenin. Primers used were: 5'-GGCTTCTAAATGTGTTACGGATG-3' and 5'-CCCAGGTCCTGTTTTGGAT-3' for FGF2, 5'-AGGAGGAGGGCAGAATCATCA-3' and 5'-CTCGATTGGATGGCAGTAGCT-3' for VEGF-A, 5'-CTGGCCATATCCACCAGAGT-3' and 5'-GAAACGGCTTTCAGTTGAGC-3' for  $\beta$ -catenin and 5'-TGCACCACCAACTGCTTAGC-3' and 5'-GGCATGGACTGTGGTCATGAG-3' for GAPDH. For identification of expression changes in genes involved in angiogenesis after GPNA treatment, RT<sup>2</sup> Profiler PCR Array System (SABiosciences) was used according to

manufacturer's instructions. Data was analyzed using web based QIAGEN RT<sup>2</sup> Profiler PCR Array Data Analysis version 3.5 for DDCT and significance.

## 6.5 IMAGING ANALYSIS

### 6.5.1 Live Cell Imaging

HepG2 cells plated in 6 well plates were maintained in media supplemented with either tetramethylrhodamine (TAMRA)-labeled **T1** at 1  $\mu$ M with Hoescht dye for a period of 19 hours or **DMSO** or 200  $\mu$ M **PMED-1** for 24 under live cell imaging. Imaging was conducted on Nikon Eclipse Ti live cell imager using Brightfield or DAPI and Cy3 filters.

### 6.5.2 TUNEL Staining

HepG2 cells were plated  $2 \times 10^3$  in 4 well chamber slides for 24 hours prior to 1  $\mu$ M treatment with either **T1** or **MM**. For Terminal deoxynucleotidyl transferase dUTP nick end labeling (TUNEL) immunohistochemistry, slides were fixed 72 hours after treatment in a 3:1 solution of methanol/glacial acetic acid for 5 min and allowed to air-dry and detection of apoptotic nuclei was determined by TUNEL staining using the ApopTag peroxidase kit (Intergen Co., Purchase, NY).

### **6.5.3 Immunohistochemistry**

Tissue samples were embedded in paraffin and cut into 4 $\mu$  sections. The slides were deparaffinized with xylene and graded alcohol washes from 100% to 95% finally to dH<sub>2</sub>O which were washed in 1xPBS. Sections were microwaved for 6 minutes twice in citrate buffer and allowed to cool for 30 minutes. Endogenous peroxidases were quenched with 3% hydrogen peroxide for 10 minutes. Slides were blocked with Super Block (UltraTek) for ten minutes before adding  $\beta$ -catenin (Santa Cruz) or GS (Santa Cruz) primary antibody diluted in PBS for 1 hour at room temperature. Sections were washed in PBS 3x followed by horseradish-peroxidase-conjugated secondary  $\alpha$ Goat (1:200) or  $\alpha$ Rabbit (1:200) antibodies (Millipore) added to the slides for 30 minutes at room temperature. Antigen retrieval was conducted using (Vector Labs). The secondary antibody signal was detected with DAB (Vector Labs) and the signal was quenched with dH<sub>2</sub>O before counterstaining with Shandon solution (Sigma Aldrich). The slides were re-graded through the alcohol from 75% to 100% leading to xylene washes before mounting the cover slips with DPX (Fluka Labs). Negative controls were generated as above, but without the primary antibody incubation. Images were taken on an Axioskop 40 (Zeiss) inverted brightfield microscope.

### **6.5.4 Hematoxylin and Eosin Staining**

Tissue sections were cut, prepared and deparaffinized as previously indicated in section 5.5.3. Slides were then incubated in Eosin stain for 30 seconds followed by 2 washes in 95% ethanol and 2 washes of 100% ethanol. Slides were then counterstained in Shandon solution for 1 minute followed by re-grading in alcohol from 75% to 100% leading to xylene washes before mounting the cover slips with DPX.

### **6.5.5 Immunofluorescence**

For detection of cells in S-phase of cell cycle, immunofluorescence for Ki-67 was performed. Briefly, after **DMSO**, **PMED-1**, **T1**, **MM** or no treatment control HepG2 cells were grown  $2 \times 10^3$  in 4 well chamber slides which were fixed in 4% paraformaldehyde. Wells were washed with 1x PBS and cells permeabilized with 0.1% Triton-X in PBS followed by washes in PBS alone and then and 0.5% bovine serum albumin (BSA) in PBS (PBB). Samples were blocked in 2% PBB for 1 hour, washed with 0.5% PBB and incubated in 0.5% PBB containing primary antibody for Ki-67 for 1 hour. After washing in 0.5% PBB, secondary antibodies- $\alpha$ Mouse-Alexa488 and  $\alpha$ Goat-Alexa555, made 1:1000 in 0.5% PBB was applied to each well except negative control for 1 hour. Wells were washed with 0.5% PBB, then with 1x PBS wash and subsequently stained with Hoescht dye for 30 seconds. Samples were cover-slipped and imaged using Nikon Eclipse Ti live cell imager.

## **6.6 ENDOTHELIAL ASSAYS**

### **6.6.1 *In vitro* Endothelial Spheroid Assay**

Serum free EMEM was used to create a 1.2% methocel stock solution using 4,000 centipoise methyl cellulose (Sigma). SK-Hep1 cells were trypsinized, counted and resuspended in a 20:80 ratio of 1.2% methocel stock:growth media. Cells were then seeded at approximately 3000 cells/well in non-adhesive, round bottom 96 well plates (Greiner bio-one) and grown for 6 days. Keeping everything on ice, rat-tail collagen and 10x MEM (Sigma-Aldrich) was mixed 9:1

respectively. Collagen mixture was then conditioned with Gentamycin (0.1% v/v), Insulin (1.0% v/v), and 3.5% NaOH (0.5% v/v). 250  $\mu$ l of collagen mixture was added per well to a 12 well plate and set at 37°C for 30 minutes for polymerization. After polymerization, residual media was removed via manual pipetting. SK-Hep1 spheroids were seeded on top of collagen gels and allowed to attach at 37°C for 30 minutes. Residual media was then removed again in order to lay a final 250  $\mu$ l of collagen on top of the attached spheroids and allowed to polymerize at 37°C for an additional 30 minutes. After polymerization, 100  $\mu$ l conditioned media from HepG2 cells treated with either 1  $\mu$ M **MM** or **T1**  $\gamma$ GPNA for 72 hours was mixed with 100  $\mu$ l serum free EMEM. Media was placed on top of the polymerized collagen sandwiches and incubated at 37°C under ambient oxygen, levels and 5.0% CO<sub>2</sub> for 24 hours. Images were taken using Nikon Eclipse Ti live cell imager. The number of tube sprouts and the length of the tubes from each spheroid were counted and averaged. Three spheroids from **MM** and four from **T1**-treated group were utilized for assessing tube sprout numbers and tube length. Using *Nikon Elements* software, a comparison of averages (+/-SD) was made and significance assessed by student *t* test and  $p < 0.05$  was considered significant and  $p < 0.01$  was considered highly significant.

### **6.6.2 *In vitro* Tubulogenesis Assay**

Tubulogenesis assay was conducted using *In Vitro* Angiogenesis Assay Kit (Millipore). 25  $\mu$ l of cold extracellular matrix was added to a 96 well plate (BD Falcon) and placed at 37°C for 1 hour. SK-Hep1 cells were seeded at  $8 \times 10^3$  cells per well after being resuspended in respective conditioned media (HepG2 conditioned media collected after 72 hour

treatment with either No Treatment, 1  $\mu$ M **MM**, or **T1**). Cells were incubated at 37°C for 3 hours prior to imaging under phase contrast using Nikon Eclipse *Ti* live cell imager.

To test if the conditioned media used for *in vitro* spheroid assay or tubulogenesis assay could have any remnant unused  $\gamma$ GPNA especially **T1**, the conditioned media used for these assays from **MM** or **T1**  $\gamma$ GPNA treated HepG2 cells for 72 hours was applied to fresh HepG2 transfected using FuGene with TOPFlash and Renilla plasmids as indicated previously for 24 hours and harvested for the luciferase assay as indicated earlier.

## **6.7 ANIMAL MODEL UTILIZATION**

### **6.7.1 Mouse Model Development**

All animal experiments were performed under the guidelines of the National Institutes of Health and the Institutional Animal Use and Care Committee at the University of Pittsburgh. The studies performed in the current report were approved by the Institutional Animal Use and Care Committee at the University of Pittsburgh. 6 week old C3H/He mice (Jackson Labs) were injected intraperitoneally with 90  $\mu$ g/g DEN (Sigma-Aldrich). Three weeks following the injection, mice were fed a diet containing 0.05% Phenobarbital-Sodium Salt (LabDiet) for the duration of the experiment, which ranged from 24-32 weeks.

### 6.7.2 LNA Administration *In Vivo*

**EZN-3046** (Scrambled Survivin Control) or **EZN-3892** ( $\beta$ -catenin) LNA antisense was injected intraperitoneally at either 0.03 or 15 mg/kg ten times every other day in either Wild-Type or DP mice. Mice were monitored for toxicity during course of injection period.

### 6.7.3 Zebrafish experiments

Embryos and adult fish were raised and maintained under standard laboratory conditions (332); we used the *Tg(OTM:d2EGFP)* line to assess Wnt/ $\beta$ -catenin signaling *in vivo* (258). A 5 mM stock of **PMED-1** and a 10 mM stock of XAV939 (Cayman Chemical) were prepared in 100% **DMSO** and diluted to 15 and 10  $\mu$ M, respectively, with egg water supplemented with 0.2 mM 1-phenyl-2-thiourea (Sigma-Aldrich). As a control, 0.5% **DMSO** solution in the egg water was used. For photography, embryos were anesthetized with 0.16 mg/ml tricaine (Sigma-Aldrich) and mounted in egg water containing 3% methyl cellulose (Sigma-Aldrich); a Leica M205 FA epifluorescence microscope was used to obtain bright field and GFP fluorescence images.

## APPENDIX A

### ANTIBODIES

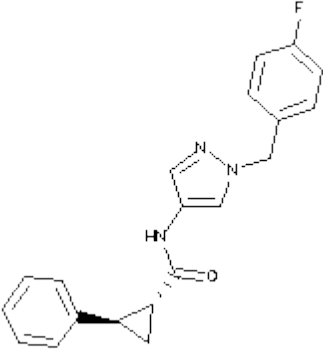
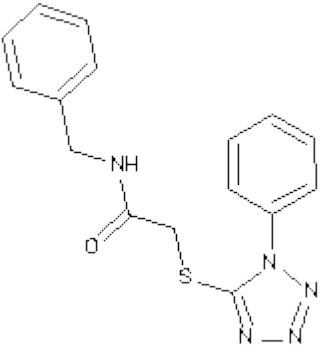
Table 1. Antibodies used for WB, IP, IF and IHC

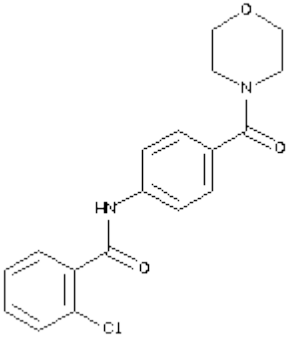
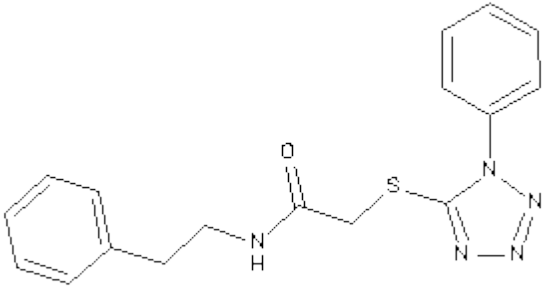
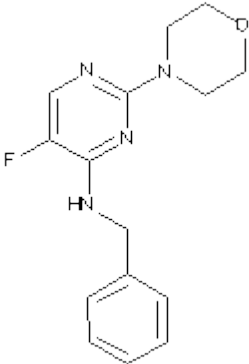
Protein	Antibody Species	Size (kDa)	WB Dilute	IP Dilute	IF/IHC Dilute	Company	Product Number
<b><math>\beta</math>-actin</b>	Mouse	42	1:2500	-	-	Millipore	MAB1501
<b><math>\beta</math>-catenin</b>	Mouse	92	1:1000	1:50	1:500	BD	610154
<b>c-myc</b>	Rabbit	67	1:200	-	-	Santa Cruz	sc-42
<b>CBP</b>	Rabbit	265	1:100	-	-	Santa Cruz	sc-369
<b>Conductin/Axin2</b>	Goat	97	1:200	-	-	Santa Cruz	sc-8570
<b>Cyclin-D1</b>	Rabbit	36	1:200	-	-	Neomarkers	RB-9041
<b>GAPDH</b>	Rabbit	37	1:800	-	-	Santa Cruz	sc-25778
<b>Glutamine Synthetase</b>	Rabbit	49	1:200	-	1:200	Santa Cruz	sc-9067
<b>Ki-67</b>	Mouse	-	-	-	1:100	Abcam	Ab833
<b>SMP30/Regucalcin</b>	Mouse	35	1:200	-	-	Santa Cruz	sc-130344
<b>VEGF-A</b>	Rabbit	42	1:200	-	-	Santa Cruz	sc-152

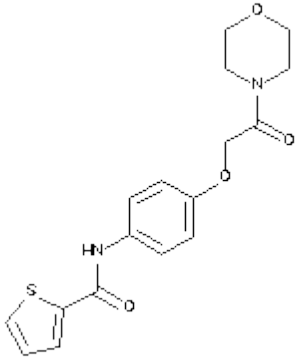
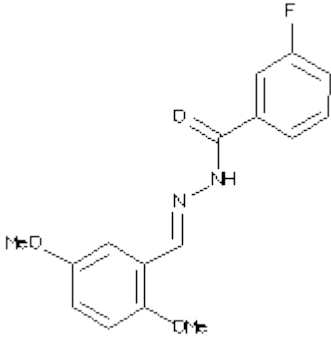
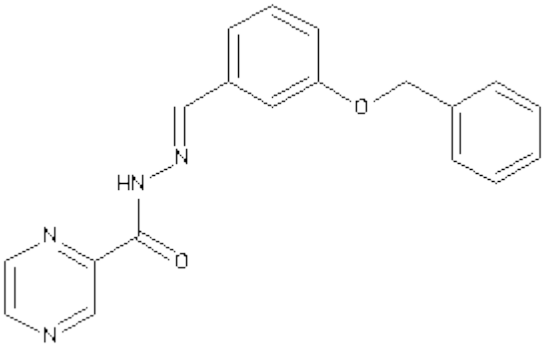
## APPENDIX B

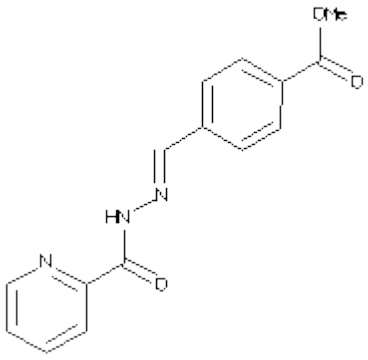
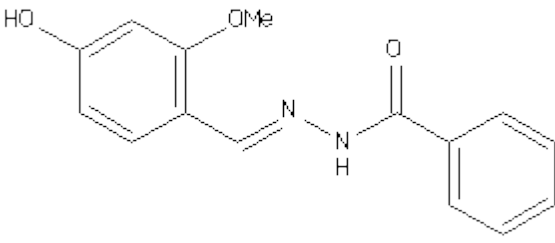
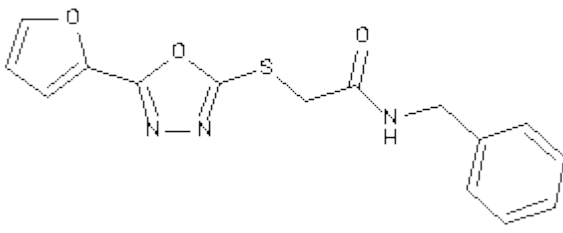
### LIST OF IDENTIFIED SMALL MOLECULES

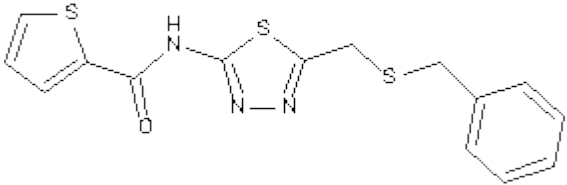
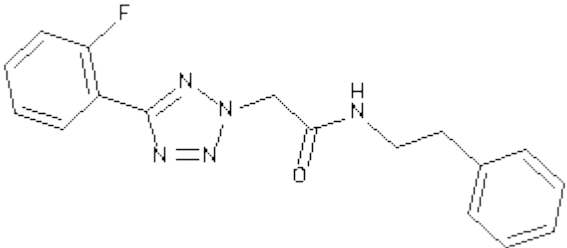
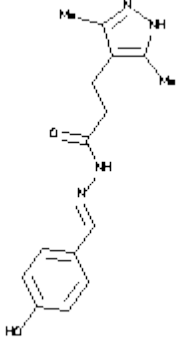
Table 2. SM structures and ZINC IDs

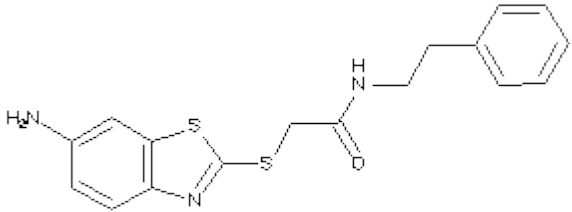
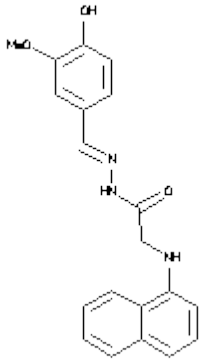
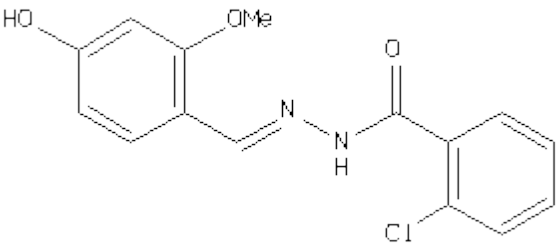
	ZINC00028435 (PMED-1)
	ZINC00036110 (PMED-2)

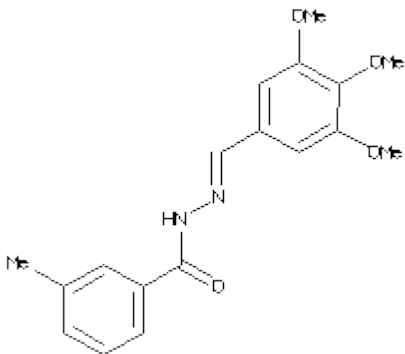
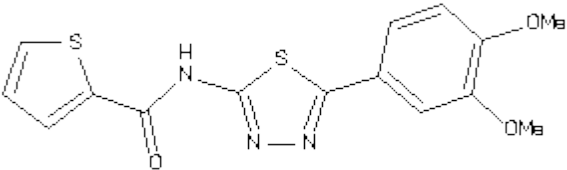
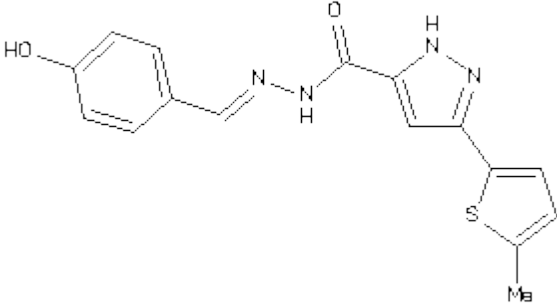
 <chem>O=C(NC1=CC=C(Cl)C=C1)C2=CC=C(C(=O)N3CCOCC3)C=C2</chem>	ZINC00036540
 <chem>O=C(NCCC1=CC=CC=C1)C2=CC=CN3C(=N2)N(C3)C4=CC=CC=C4</chem>	ZINC00036861
 <chem>NCC1=CC=CC=C1N2=CN(C3CCOCC3)C=C(F)N2</chem>	ZINC00038222

	<p>ZINC00038356</p>
	<p>ZINC00043304</p>
	<p>ZINC00045362</p>

	<p>ZINC00046955</p>
	<p>ZINC00050733</p>
	<p>ZINC00051170</p>

	<p>ZINC00052109</p>
	<p>ZINC00053871</p>
	<p>ZINC00055887</p>

	<p>ZINC00060369</p>
	<p>ZINC00060479</p>
	<p>ZINC00061679</p>

	<p>ZINC00062638</p>
	<p>ZINC00069134</p>
	<p>ZINC18175653</p>

## APPENDIX C

### TABLE OF *IN VIVO* LNA ADMINISTRATION GROUPS

Table 3. Categories of mice and LNA conditions

<b>Group</b>	<b>LNA Administration</b>	<b>DEN+PB Present</b>	<b>Dose (mg/kg)</b>	<b>n</b>
<b>WTC</b>	ENZ-3046	No	15	3
<b>WT<math>\beta</math></b>	ENZ-3892	No	15	3
<b>DP</b>	None	Yes	0	5
<b>DPC</b>	ENZ-3046	Yes	15	7
<b>DPCL</b>	ENZ-3046	Yes	0.03	5
<b>DP<math>\beta</math></b>	ENZ-3892	Yes	15	8
<b>DP<math>\beta</math>L</b>	ENZ-3892	Yes	0.03	4

## BIBLIOGRAPHY

1. J. Ferlay *et al.*, Estimates of worldwide burden of cancer in 2008: GLOBOCAN 2008. *Int J Cancer* **127**, 2893 (Dec 15, 2010).
2. A. Jemal *et al.*, Global cancer statistics. *CA Cancer J Clin* **61**, 69 (Mar-Apr, 2011).
3. A. Jemal, M. M. Center, C. DeSantis, E. M. Ward, Global patterns of cancer incidence and mortality rates and trends. *Cancer Epidemiol Biomarkers Prev* **19**, 1893 (Aug, 2010).
4. B. S. Hulka, P. G. Moorman, Breast cancer: hormones and other risk factors. *Maturitas* **38**, 103 (Feb 28, 2001).
5. M. D. Althuis, J. M. Dozier, W. F. Anderson, S. S. Devesa, L. A. Brinton, Global trends in breast cancer incidence and mortality 1973-1997. *Int J Epidemiol* **34**, 405 (Apr, 2005).
6. P. Autier *et al.*, Disparities in breast cancer mortality trends between 30 European countries: retrospective trend analysis of WHO mortality database. *BMJ* **341**, c3620 (2010).
7. M. M. Center, A. Jemal, E. Ward, International trends in colorectal cancer incidence rates. *Cancer Epidemiol Biomarkers Prev* **18**, 1688 (Jun, 2009).
8. M. M. Center, A. Jemal, R. A. Smith, E. Ward, Worldwide variations in colorectal cancer. *CA Cancer J Clin* **59**, 366 (Nov-Dec, 2009).
9. B. K. Edwards *et al.*, Annual report to the nation on the status of cancer, 1975-2006, featuring colorectal cancer trends and impact of interventions (risk factors, screening, and treatment) to reduce future rates. *Cancer* **116**, 544 (Feb 1, 2010).
10. W. K. Lam, N. W. White, M. M. Chan-Yeung, Lung cancer epidemiology and risk factors in Asia and Africa. *Int J Tuberc Lung Dis* **8**, 1045 (Sep, 2004).
11. P. Boffetta, F. Nyberg, Contribution of environmental factors to cancer risk. *Br Med Bull* **68**, 71 (2003).
12. M. J. Thun *et al.*, Lung cancer occurrence in never-smokers: an analysis of 13 cohorts and 22 cancer registry studies. *PLoS Med* **5**, e185 (Sep 30, 2008).
13. M. Ezzati, S. J. Henley, A. D. Lopez, M. J. Thun, Role of smoking in global and regional cancer epidemiology: current patterns and data needs. *Int J Cancer* **116**, 963 (Oct 10, 2005).
14. M. Ezzati, A. D. Lopez, Estimates of global mortality attributable to smoking in 2000. *Lancet* **362**, 847 (Sep 13, 2003).
15. F. I. Bray, E. Weiderpass, Lung cancer mortality trends in 36 European countries: secular trends and birth cohort patterns by sex and region 1970-2007. *Int J Cancer* **126**, 1454 (Mar 15, 2010).
16. A. Jemal *et al.*, Annual report to the nation on the status of cancer, 1975-2005, featuring trends in lung cancer, tobacco use, and tobacco control. *J Natl Cancer Inst* **100**, 1672 (Dec 3, 2008).
17. J. F. Perz, G. L. Armstrong, L. A. Farrington, Y. J. Hutin, B. P. Bell, The contributions of hepatitis B virus and hepatitis C virus infections to cirrhosis and primary liver cancer worldwide. *J Hepatol* **45**, 529 (Oct, 2006).

18. D. M. Parkin, The global health burden of infection-associated cancers in the year 2002. *Int J Cancer* **118**, 3030 (Jun 15, 2006).
19. J. D. Yang, L. R. Roberts, Hepatocellular carcinoma: A global view. *Nat Rev Gastroenterol Hepatol* **7**, 448 (Aug, 2010).
20. J. A. Davila, R. O. Morgan, Y. Shaib, K. A. McGlynn, H. B. El-Serag, Hepatitis C infection and the increasing incidence of hepatocellular carcinoma: a population-based study. *Gastroenterology* **127**, 1372 (Nov, 2004).
21. H. B. El-Serag, Epidemiology of hepatocellular carcinoma in USA. *Hepatol Res* **37 Suppl 2**, S88 (Sep, 2007).
22. H. Imamura *et al.*, Risk factors contributing to early and late phase intrahepatic recurrence of hepatocellular carcinoma after hepatectomy. *J Hepatol* **38**, 200 (Feb, 2003).
23. B. E. Fortune, V. Umman, T. Gilliland, S. Emre, Liver transplantation for hepatocellular carcinoma: a surgical perspective. *J Clin Gastroenterol* **47 Suppl**, S37 (Jul, 2013).
24. F. X. Bosch, J. Ribes, J. Borrás, Epidemiology of primary liver cancer. *Semin Liver Dis* **19**, 271 (1999).
25. F. X. Bosch, J. Ribes, M. Diaz, R. Cléries, Primary liver cancer: worldwide incidence and trends. *Gastroenterology* **127**, S5 (Nov, 2004).
26. R. P. Beasley, Hepatitis B virus. The major etiology of hepatocellular carcinoma. *Cancer* **61**, 1942 (May 15, 1988).
27. R. P. Beasley, L. Y. Hwang, C. C. Lin, C. S. Chien, Hepatocellular carcinoma and hepatitis B virus. A prospective study of 22 707 men in Taiwan. *Lancet* **2**, 1129 (Nov 21, 1981).
28. C. A. Sun *et al.*, Incidence and cofactors of hepatitis C virus-related hepatocellular carcinoma: a prospective study of 12,008 men in Taiwan. *Am J Epidemiol* **157**, 674 (Apr 15, 2003).
29. S. C. Larsson, A. Wolk, Overweight, obesity and risk of liver cancer: a meta-analysis of cohort studies. *Br J Cancer* **97**, 1005 (Oct 8, 2007).
30. G. A. Michelotti, M. V. Machado, A. M. Diehl, NAFLD, NASH and liver cancer. *Nat Rev Gastroenterol Hepatol* **10**, 656 (Nov, 2013).
31. Y. Arase *et al.*, Difference in malignancies of chronic liver disease due to non-alcoholic fatty liver disease or hepatitis C in Japanese elderly patients. *Hepatol Res* **42**, 264 (Mar, 2012).
32. N. Bhala *et al.*, The natural history of nonalcoholic fatty liver disease with advanced fibrosis or cirrhosis: an international collaborative study. *Hepatology* **54**, 1208 (Oct, 2011).
33. K. Yasui *et al.*, Clinical and pathological progression of non-alcoholic steatohepatitis to hepatocellular carcinoma. *Hepatol Res* **42**, 767 (Aug, 2012).
34. J. Ertle *et al.*, Non-alcoholic fatty liver disease progresses to hepatocellular carcinoma in the absence of apparent cirrhosis. *Int J Cancer* **128**, 2436 (May 15, 2011).
35. F. Hucke, W. Sieghart, M. Schoniger-Hekele, M. Peck-Radosavljevic, C. Muller, Clinical characteristics of patients with hepatocellular carcinoma in Austria - is there a need for a structured screening program? *Wien Klin Wochenschr* **123**, 542 (Sep, 2011).
36. S. M. Malik, P. A. Gupte, M. E. de Vera, J. Ahmad, Liver transplantation in patients with nonalcoholic steatohepatitis-related hepatocellular carcinoma. *Clin Gastroenterol Hepatol* **7**, 800 (Jul, 2009).

37. K. Ohata *et al.*, Hepatic steatosis is a risk factor for hepatocellular carcinoma in patients with chronic hepatitis C virus infection. *Cancer* **97**, 3036 (Jun 15, 2003).
38. J. R. Pekow, A. K. Bhan, H. Zheng, R. T. Chung, Hepatic steatosis is associated with increased frequency of hepatocellular carcinoma in patients with hepatitis C-related cirrhosis. *Cancer* **109**, 2490 (Jun 15, 2007).
39. A. Tanaka *et al.*, Hepatic steatosis as a possible risk factor for the development of hepatocellular carcinoma after eradication of hepatitis C virus with antiviral therapy in patients with chronic hepatitis C. *World J Gastroenterol* **13**, 5180 (Oct 21, 2007).
40. Y. Kawamura *et al.*, Large-scale long-term follow-up study of Japanese patients with non-alcoholic Fatty liver disease for the onset of hepatocellular carcinoma. *Am J Gastroenterol* **107**, 253 (Feb, 2012).
41. D. L. White, F. Kanwal, H. B. El-Serag, Association between nonalcoholic fatty liver disease and risk for hepatocellular cancer, based on systematic review. *Clin Gastroenterol Hepatol* **10**, 1342 (Dec, 2012).
42. M. W. Yu *et al.*, Body-mass index and progression of hepatitis B: a population-based cohort study in men. *J Clin Oncol* **26**, 5576 (Dec 1, 2008).
43. T. Akiyama *et al.*, Body mass index is associated with age-at-onset of HCV-infected hepatocellular carcinoma patients. *World J Gastroenterol* **17**, 914 (Feb 21, 2011).
44. G. N'Kontchou *et al.*, Risk factors for hepatocellular carcinoma in patients with alcoholic or viral C cirrhosis. *Clin Gastroenterol Hepatol* **4**, 1062 (Aug, 2006).
45. H. F. Chen, P. Chen, C. Y. Li, Risk of malignant neoplasms of liver and biliary tract in diabetic patients with different age and sex stratifications. *Hepatology* **52**, 155 (Jul, 2010).
46. W. P. Koh, R. Wang, A. Jin, M. C. Yu, J. M. Yuan, Diabetes mellitus and risk of hepatocellular carcinoma: findings from the Singapore Chinese Health Study. *Br J Cancer* **108**, 1182 (Mar 19, 2013).
47. V. Donadon, M. Balbi, M. D. Mas, P. Casarin, G. Zanette, Metformin and reduced risk of hepatocellular carcinoma in diabetic patients with chronic liver disease. *Liver Int* **30**, 750 (May, 2010).
48. C. L. Chen *et al.*, Metabolic factors and risk of hepatocellular carcinoma by chronic hepatitis B/C infection: a follow-up study in Taiwan. *Gastroenterology* **135**, 111 (Jul, 2008).
49. M. M. Hassan *et al.*, Association of diabetes duration and diabetes treatment with the risk of hepatocellular carcinoma. *Cancer* **116**, 1938 (Apr 15, 2010).
50. S. W. Lai *et al.*, Risk of hepatocellular carcinoma in diabetic patients and risk reduction associated with anti-diabetic therapy: a population-based cohort study. *Am J Gastroenterol* **107**, 46 (Jan, 2012).
51. G. Nkontchou *et al.*, Impact of metformin on the prognosis of cirrhosis induced by viral hepatitis C in diabetic patients. *J Clin Endocrinol Metab* **96**, 2601 (Aug, 2011).
52. J. M. Kane, 3rd *et al.*, Chronic hepatitis C virus infection in humans: induction of hepatic nitric oxide synthase and proposed mechanisms for carcinogenesis. *J Surg Res* **69**, 321 (May, 1997).
53. G. L. Armstrong, M. J. Alter, G. M. McQuillan, H. S. Margolis, The past incidence of hepatitis C virus infection: implications for the future burden of chronic liver disease in the United States. *Hepatology* **31**, 777 (Mar, 2000).

54. J. B. Wong, G. M. McQuillan, J. G. McHutchison, T. Poynard, Estimating future hepatitis C morbidity, mortality, and costs in the United States. *Am J Public Health* **90**, 1562 (Oct, 2000).
55. S. F. Altekruse, K. A. McGlynn, M. E. Reichman, Hepatocellular carcinoma incidence, mortality, and survival trends in the United States from 1975 to 2005. *J Clin Oncol* **27**, 1485 (Mar 20, 2009).
56. A. M. Di Bisceglie *et al.*, Hepatitis C-related hepatocellular carcinoma in the United States: influence of ethnic status. *Am J Gastroenterol* **98**, 2060 (Sep, 2003).
57. J. D. Yang *et al.*, Hepatocellular carcinoma in olmsted county, Minnesota, 1976-2008. *Mayo Clin Proc* **87**, 9 (Jan, 2012).
58. G. L. Armstrong *et al.*, The prevalence of hepatitis C virus infection in the United States, 1999 through 2002. *Ann Intern Med* **144**, 705 (May 16, 2006).
59. A. Wasley, S. Grytdal, K. Gallagher, Surveillance for acute viral hepatitis--United States, 2006. *MMWR Surveill Summ* **57**, 1 (Mar 21, 2008).
60. H. J. Alter, L. B. Seeff, Recovery, persistence, and sequelae in hepatitis C virus infection: a perspective on long-term outcome. *Semin Liver Dis* **20**, 17 (2000).
61. G. Fattovich *et al.*, Morbidity and mortality in compensated cirrhosis type C: a retrospective follow-up study of 384 patients. *Gastroenterology* **112**, 463 (Feb, 1997).
62. J. A. Marrero *et al.*, NAFLD may be a common underlying liver disease in patients with hepatocellular carcinoma in the United States. *Hepatology* **36**, 1349 (Dec, 2002).
63. S. D. Holmberg, P. R. Spradling, A. C. Moorman, M. M. Denniston, Hepatitis C in the United States. *N Engl J Med* **368**, 1859 (May 16, 2013).
64. E. E. Calle, C. Rodriguez, K. Walker-Thurmond, M. J. Thun, Overweight, obesity, and mortality from cancer in a prospectively studied cohort of U.S. adults. *N Engl J Med* **348**, 1625 (Apr 24, 2003).
65. S. Nair, A. Mason, J. Eason, G. Loss, R. P. Perrillo, Is obesity an independent risk factor for hepatocellular carcinoma in cirrhosis? *Hepatology* **36**, 150 (Jul, 2002).
66. M. Lazo *et al.*, Prevalence of nonalcoholic fatty liver disease in the United States: the Third National Health and Nutrition Examination Survey, 1988-1994. *Am J Epidemiol* **178**, 38 (Jul 1, 2013).
67. J. M. Clark, F. L. Brancati, A. M. Diehl, The prevalence and etiology of elevated aminotransferase levels in the United States. *Am J Gastroenterol* **98**, 960 (May, 2003).
68. L. A. Adams *et al.*, The natural history of nonalcoholic fatty liver disease: a population-based cohort study. *Gastroenterology* **129**, 113 (Jul, 2005).
69. A. J. McCullough, The clinical features, diagnosis and natural history of nonalcoholic fatty liver disease. *Clin Liver Dis* **8**, 521 (Aug, 2004).
70. F. X. Bosch, J. Ribes, R. Cleries, M. Diaz, Epidemiology of hepatocellular carcinoma. *Clin Liver Dis* **9**, 191 (May, 2005).
71. G. S. Qian *et al.*, A follow-up study of urinary markers of aflatoxin exposure and liver cancer risk in Shanghai, People's Republic of China. *Cancer Epidemiol Biomarkers Prev* **3**, 3 (Jan-Feb, 1994).
72. P. C. Turner *et al.*, The role of aflatoxins and hepatitis viruses in the etiopathogenesis of hepatocellular carcinoma: A basis for primary prevention in Guinea-Conakry, West Africa. *J Gastroenterol Hepatol* **17 Suppl**, S441 (Dec, 2002).
73. C. Brechot, Molecular mechanisms of hepatitis B and C viruses related to liver carcinogenesis. *Hepatology* **45 Suppl 3**, 1189 (Aug, 1998).

74. A. Dejean, P. Sonigo, S. Wain-Hobson, P. Tiollais, Specific hepatitis B virus integration in hepatocellular carcinoma DNA through a viral 11-base-pair direct repeat. *Proc Natl Acad Sci U S A* **81**, 5350 (Sep, 1984).
75. B. L. Slagle, Y. Z. Zhou, J. S. Butel, Hepatitis B virus integration event in human chromosome 17p near the p53 gene identifies the region of the chromosome commonly deleted in virus-positive hepatocellular carcinomas. *Cancer Res* **51**, 49 (Jan 1, 1991).
76. R. Truant, J. Antunovic, J. Greenblatt, C. Prives, J. A. Cromlish, Direct interaction of the hepatitis B virus HBx protein with p53 leads to inhibition by HBx of p53 response element-directed transactivation. *J Virol* **69**, 1851 (Mar, 1995).
77. X. W. Wang *et al.*, Hepatitis B virus X protein inhibits p53 sequence-specific DNA binding, transcriptional activity, and association with transcription factor ERCC3. *Proc Natl Acad Sci U S A* **91**, 2230 (Mar 15, 1994).
78. R. K. Ross *et al.*, Urinary aflatoxin biomarkers and risk of hepatocellular carcinoma. *Lancet* **339**, 943 (Apr 18, 1992).
79. S. P. Hussain *et al.*, Increased p53 mutation load in nontumorous human liver of wilson disease and hemochromatosis: oxyradical overload diseases. *Proc Natl Acad Sci U S A* **97**, 12770 (Nov 7, 2000).
80. D. A. Brenner *et al.*, New aspects of hepatic fibrosis. *J Hepatol* **32**, 32 (2000).
81. S. L. Friedman, Preface. Hepatic fibrosis: pathogenesis, diagnosis, and emerging therapies. *Clin Liver Dis* **12**, xiii (Nov, 2008).
82. M. Comporti *et al.*, F2-isoprostanes stimulate collagen synthesis in activated hepatic stellate cells: a link with liver fibrosis? *Lab Invest* **85**, 1381 (Nov, 2005).
83. M. Kojiro, T. Roskams, Early hepatocellular carcinoma and dysplastic nodules. *Semin Liver Dis* **25**, 133 (2005).
84. J. S. Campbell *et al.*, Platelet-derived growth factor C induces liver fibrosis, steatosis, and hepatocellular carcinoma. *Proc Natl Acad Sci U S A* **102**, 3389 (Mar 1, 2005).
85. A. J. Marrogi *et al.*, Oxidative stress and p53 mutations in the carcinogenesis of iron overload-associated hepatocellular carcinoma. *J Natl Cancer Inst* **93**, 1652 (Nov 7, 2001).
86. M. A. Nowak *et al.*, Viral dynamics in hepatitis B virus infection. *Proc Natl Acad Sci U S A* **93**, 4398 (Apr 30, 1996).
87. S. Wieland, R. Thimme, R. H. Purcell, F. V. Chisari, Genomic analysis of the host response to hepatitis B virus infection. *Proc Natl Acad Sci U S A* **101**, 6669 (Apr 27, 2004).
88. B. Rehermann, M. Nascimbeni, Immunology of hepatitis B virus and hepatitis C virus infection. *Nat Rev Immunol* **5**, 215 (Mar, 2005).
89. R. Shimoda *et al.*, Increased formation of oxidative DNA damage, 8-hydroxydeoxyguanosine, in human livers with chronic hepatitis. *Cancer Res* **54**, 3171 (Jun 15, 1994).
90. T. Kojima, Immune electron microscopic study of hepatitis B virus associated antigens in hepatocytes. *Gastroenterol Jpn* **17**, 559 (Dec, 1982).
91. A. Galli *et al.*, Oxidative stress stimulates proliferation and invasiveness of hepatic stellate cells via a MMP2-mediated mechanism. *Hepatology* **41**, 1074 (May, 2005).
92. A. S. Lok, E. J. Heathcote, J. H. Hoofnagle, Management of hepatitis B: 2000--summary of a workshop. *Gastroenterology* **120**, 1828 (Jun, 2001).

93. Y. Murakami *et al.*, Large scaled analysis of hepatitis B virus (HBV) DNA integration in HBV related hepatocellular carcinomas. *Gut* **54**, 1162 (Aug, 2005).
94. T. Tokino, H. Tamura, N. Hori, K. Matsubara, Chromosome deletions associated with hepatitis B virus integration. *Virology* **185**, 879 (Dec, 1991).
95. A. Weiner *et al.*, Persistent hepatitis C virus infection in a chimpanzee is associated with emergence of a cytotoxic T lymphocyte escape variant. *Proc Natl Acad Sci U S A* **92**, 2755 (Mar 28, 1995).
96. J. B. Hoek, J. G. Pastorino, Ethanol, oxidative stress, and cytokine-induced liver cell injury. *Alcohol* **27**, 63 (May, 2002).
97. C. J. McClain, D. B. Hill, Z. Song, I. Deaciuc, S. Barve, Monocyte activation in alcoholic liver disease. *Alcohol* **27**, 53 (May, 2002).
98. M. A. Feitelson *et al.*, Genetic mechanisms of hepatocarcinogenesis. *Oncogene* **21**, 2593 (Apr 11, 2002).
99. F. Aguilar, C. C. Harris, T. Sun, M. Hollstein, P. Cerutti, Geographic variation of p53 mutational profile in nonmalignant human liver. *Science* **264**, 1317 (May 27, 1994).
100. B. Bressac, M. Kew, J. Wands, M. Ozturk, Selective G to T mutations of p53 gene in hepatocellular carcinoma from southern Africa. *Nature* **350**, 429 (Apr 4, 1991).
101. I. C. Hsu *et al.*, Mutational hotspot in the p53 gene in human hepatocellular carcinomas. *Nature* **350**, 427 (Apr 4, 1991).
102. M. Ozturk, p53 mutation in hepatocellular carcinoma after aflatoxin exposure. *Lancet* **338**, 1356 (Nov 30, 1991).
103. J. Riley, H. G. Mandel, S. Sinha, D. J. Judah, G. E. Neal, In vitro activation of the human Harvey-ras proto-oncogene by aflatoxin B1. *Carcinogenesis* **18**, 905 (May, 1997).
104. M. C. Kew, Synergistic interaction between aflatoxin B1 and hepatitis B virus in hepatocarcinogenesis. *Liver Int* **23**, 405 (Dec, 2003).
105. J. C. Bourdon, p53 and its isoforms in cancer. *Br J Cancer* **97**, 277 (Aug 6, 2007).
106. K. H. Vousden, D. P. Lane, p53 in health and disease. *Nat Rev Mol Cell Biol* **8**, 275 (Apr, 2007).
107. C. M. Kim, K. Koike, I. Saito, T. Miyamura, G. Jay, HBx gene of hepatitis B virus induces liver cancer in transgenic mice. *Nature* **351**, 317 (May 23, 1991).
108. K. Minouchi, S. Kaneko, K. Kobayashi, Mutation of p53 gene in regenerative nodules in cirrhotic liver. *J Hepatol* **37**, 231 (Aug, 2002).
109. H. Nose, F. Imazeki, M. Ohto, M. Omata, p53 gene mutations and 17p allelic deletions in hepatocellular carcinoma from Japan. *Cancer* **72**, 355 (Jul 15, 1993).
110. N. Nishida *et al.*, Role and mutational heterogeneity of the p53 gene in hepatocellular carcinoma. *Cancer Res* **53**, 368 (Jan 15, 1993).
111. T. Teramoto *et al.*, p53 gene abnormalities are closely related to hepatoviral infections and occur at a late stage of hepatocarcinogenesis. *Cancer Res* **54**, 231 (Jan 1, 1994).
112. H. Ueda *et al.*, Functional inactivation but not structural mutation of p53 causes liver cancer. *Nat Genet* **9**, 41 (Jan, 1995).
113. C. Tarn, S. Lee, Y. Hu, C. Ashendel, O. M. Andrisani, Hepatitis B virus X protein differentially activates RAS-RAF-MAPK and JNK pathways in X-transforming versus non-transforming AML12 hepatocytes. *J Biol Chem* **276**, 34671 (Sep 14, 2001).
114. R. Nijhara *et al.*, Sustained activation of mitogen-activated protein kinases and activator protein 1 by the hepatitis B virus X protein in mouse hepatocytes in vivo. *J Virol* **75**, 10348 (Nov, 2001).

115. R. Nijhara, S. S. Jana, S. K. Goswami, V. Kumar, D. P. Sarkar, An internal segment (residues 58-119) of the hepatitis B virus X protein is sufficient to activate MAP kinase pathways in mouse liver. *FEBS Lett* **504**, 59 (Aug 24, 2001).
116. J. Benn, R. J. Schneider, Hepatitis B virus HBx protein activates Ras-GTP complex formation and establishes a Ras, Raf, MAP kinase signaling cascade. *Proc Natl Acad Sci U S A* **91**, 10350 (Oct 25, 1994).
117. Y. H. Lee, Y. Yun, HBx protein of hepatitis B virus activates Jak1-STAT signaling. *J Biol Chem* **273**, 25510 (Sep 25, 1998).
118. U. S. Park, S. K. Park, Y. I. Lee, J. G. Park, Hepatitis B virus-X protein upregulates the expression of p21waf1/cip1 and prolongs G1-->S transition via a p53-independent pathway in human hepatoma cells. *Oncogene* **19**, 3384 (Jul 13, 2000).
119. M. Y. Cha, C. M. Kim, Y. M. Park, W. S. Ryu, Hepatitis B virus X protein is essential for the activation of Wnt/beta-catenin signaling in hepatoma cells. *Hepatology* **39**, 1683 (Jun, 2004).
120. Z. Lian *et al.*, Enhanced cell survival of Hep3B cells by the hepatitis B x antigen effector, URG11, is associated with upregulation of beta-catenin. *Hepatology* **43**, 415 (Mar, 2006).
121. R. W. Pang *et al.*, PIN1 expression contributes to hepatic carcinogenesis. *J Pathol* **210**, 19 (Sep, 2006).
122. R. Pang *et al.*, Pin1 interacts with a specific serine-proline motif of hepatitis B virus X-protein to enhance hepatocarcinogenesis. *Gastroenterology* **132**, 1088 (Mar, 2007).
123. N. A. Osna, D. L. Clemens, T. M. Donohue, Jr., Ethanol metabolism alters interferon gamma signaling in recombinant HepG2 cells. *Hepatology* **42**, 1109 (Nov, 2005).
124. O. Hino, K. Kajino, T. Umeda, Y. Arakawa, Understanding the hypercarcinogenic state in chronic hepatitis: a clue to the prevention of human hepatocellular carcinoma. *J Gastroenterol* **37**, 883 (2002).
125. A. Macdonald *et al.*, The hepatitis C virus non-structural NS5A protein inhibits activating protein-1 function by perturbing ras-ERK pathway signaling. *J Biol Chem* **278**, 17775 (May 16, 2003).
126. Y. Kanai, S. Ushijima, H. Tsuda, M. Sakamoto, S. Hirohashi, Aberrant DNA methylation precedes loss of heterozygosity on chromosome 16 in chronic hepatitis and liver cirrhosis. *Cancer Lett* **148**, 73 (Jan 1, 2000).
127. Y. Kanai *et al.*, DNA hypermethylation at the D17S5 locus and reduced HIC-1 mRNA expression are associated with hepatocarcinogenesis. *Hepatology* **29**, 703 (Mar, 1999).
128. Y. Kanai *et al.*, Aberrant DNA methylation on chromosome 16 is an early event in hepatocarcinogenesis. *Jpn J Cancer Res* **87**, 1210 (Dec, 1996).
129. J. Yu *et al.*, Methylation profiling of twenty four genes and the concordant methylation behaviours of nineteen genes that may contribute to hepatocellular carcinogenesis. *Cell Res* **13**, 319 (Oct, 2003).
130. I. H. Wong *et al.*, Detection of aberrant p16 methylation in the plasma and serum of liver cancer patients. *Cancer Res* **59**, 71 (Jan 1, 1999).
131. Y. Matsuda, T. Ichida, J. Matsuzawa, K. Sugimura, H. Asakura, p16(INK4) is inactivated by extensive CpG methylation in human hepatocellular carcinoma. *Gastroenterology* **116**, 394 (Feb, 1999).
132. H. Murata *et al.*, Promoter hypermethylation silences cyclooxygenase-2 (Cox-2) and regulates growth of human hepatocellular carcinoma cells. *Lab Invest* **84**, 1050 (Aug, 2004).

133. P. M. Sharma *et al.*, Inhibition of phosphatidylinositol 3-kinase activity by adenovirus-mediated gene transfer and its effect on insulin action. *J Biol Chem* **273**, 18528 (Jul 17, 1998).
134. B. Cheatham *et al.*, Phosphatidylinositol 3-kinase activation is required for insulin stimulation of pp70 S6 kinase, DNA synthesis, and glucose transporter translocation. *Mol Cell Biol* **14**, 4902 (Jul, 1994).
135. J. W. Lee *et al.*, PIK3CA gene is frequently mutated in breast carcinomas and hepatocellular carcinomas. *Oncogene* **24**, 1477 (Feb 17, 2005).
136. K. Tokushige, E. Hashimoto, Y. Horie, M. Taniai, S. Higuchi, Hepatocellular carcinoma in Japanese patients with nonalcoholic fatty liver disease, alcoholic liver disease, and chronic liver disease of unknown etiology: report of the nationwide survey. *J Gastroenterol* **46**, 1230 (Oct, 2011).
137. M. Torbenson *et al.*, Concurrent evaluation of p53, beta-catenin, and alpha-fetoprotein expression in human hepatocellular carcinoma. *Am J Clin Pathol* **122**, 377 (Sep, 2004).
138. J. S. Lee, S. S. Thorgeirsson, Functional and genomic implications of global gene expression profiles in cell lines from human hepatocellular cancer. *Hepatology* **35**, 1134 (May, 2002).
139. M. M. Hassan *et al.*, Genetic variation in the PNPLA3 gene and hepatocellular carcinoma in USA: Risk and prognosis prediction. *Mol Carcinog* **52 Suppl 1**, 139 (Nov, 2013).
140. J. Napetschnig, H. Wu, Molecular basis of NF-kappaB signaling. *Annu Rev Biophys* **42**, 443 (2013).
141. R. G. Baker, M. S. Hayden, S. Ghosh, NF-kappaB, inflammation, and metabolic disease. *Cell Metab* **13**, 11 (Jan 5, 2011).
142. A. Dela Pena *et al.*, NF-kappaB activation, rather than TNF, mediates hepatic inflammation in a murine dietary model of steatohepatitis. *Gastroenterology* **129**, 1663 (Nov, 2005).
143. L. Romics, Jr. *et al.*, Diverse regulation of NF-kappaB and peroxisome proliferator-activated receptors in murine nonalcoholic fatty liver. *Hepatology* **40**, 376 (Aug, 2004).
144. K. Nejak-Bowen, A. Kikuchi, S. P. Monga, Beta-catenin-NF-kappaB interactions in murine hepatocytes: a complex to die for. *Hepatology* **57**, 763 (Feb, 2013).
145. I. Locatelli, S. Sutti, M. Vacchiano, C. Bozzola, E. Albano, NF-kappaB1 deficiency stimulates the progression of non-alcoholic steatohepatitis (NASH) in mice by promoting NKT-cell-mediated responses. *Clin Sci (Lond)* **124**, 279 (Feb, 2013).
146. S. Maeda, H. Kamata, J. L. Luo, H. Leffert, M. Karin, IKKbeta couples hepatocyte death to cytokine-driven compensatory proliferation that promotes chemical hepatocarcinogenesis. *Cell* **121**, 977 (Jul 1, 2005).
147. J. T. Fox, P. J. Stover, Folate-mediated one-carbon metabolism. *Vitam Horm* **79**, 1 (2008).
148. S. C. Lu, J. M. Mato, S-Adenosylmethionine in cell growth, apoptosis and liver cancer. *J Gastroenterol Hepatol* **23 Suppl 1**, S73 (Mar, 2008).
149. K. L. Oden, K. Carson, J. O. Mecham, R. M. Hoffman, S. Clarke, S-adenosylmethionine synthetase in cultured normal and oncogenically-transformed human and rat cells. *Biochim Biophys Acta* **760**, 270 (Oct 18, 1983).
150. C. W. Tabor, H. Tabor, Methionine adenosyltransferase (S-adenosylmethionine synthetase) and S-adenosylmethionine decarboxylase. *Adv Enzymol Relat Areas Mol Biol* **56**, 251 (1984).

151. J. E. Heady, S. J. Kerr, Purification and characterization of glycine N-methyltransferase. *J Biol Chem* **248**, 69 (Jan 10, 1973).
152. T. O. Eloranta, Tissue distribution of S-adenosylmethionine and S-adenosylhomocysteine in the rat. Effect of age, sex and methionine administration on the metabolism of S-adenosylmethionine, S-adenosylhomocysteine and polyamines. *Biochem J* **166**, 521 (Sep 15, 1977).
153. S. C. Lu *et al.*, Methionine adenosyltransferase 1A knockout mice are predisposed to liver injury and exhibit increased expression of genes involved in proliferation. *Proc Natl Acad Sci U S A* **98**, 5560 (May 8, 2001).
154. M. L. Martinez-Chantar *et al.*, Spontaneous oxidative stress and liver tumors in mice lacking methionine adenosyltransferase 1A. *FASEB J* **16**, 1292 (Aug, 2002).
155. Y. W. Teng, M. G. Mehedint, T. A. Garrow, S. H. Zeisel, Deletion of betaine-homocysteine S-methyltransferase in mice perturbs choline and 1-carbon metabolism, resulting in fatty liver and hepatocellular carcinomas. *J Biol Chem* **286**, 36258 (Oct 21, 2011).
156. M. A. Avila *et al.*, Reduced mRNA abundance of the main enzymes involved in methionine metabolism in human liver cirrhosis and hepatocellular carcinoma. *J Hepatol* **33**, 907 (Dec, 2000).
157. J. Cai, W. M. Sun, J. J. Hwang, S. C. Stain, S. C. Lu, Changes in S-adenosylmethionine synthetase in human liver cancer: molecular characterization and significance. *Hepatology* **24**, 1090 (Nov, 1996).
158. K. Tamai *et al.*, LDL-receptor-related proteins in Wnt signal transduction. *Nature* **407**, 530 (Sep 28, 2000).
159. J. Noordermeer, J. Klingensmith, N. Perrimon, R. Nusse, dishevelled and armadillo act in the wingless signalling pathway in *Drosophila*. *Nature* **367**, 80 (Jan 6, 1994).
160. N. Funayama, F. Fagotto, P. McCrea, B. M. Gumbiner, Embryonic axis induction by the armadillo repeat domain of beta-catenin: evidence for intracellular signaling. *J Cell Biol* **128**, 959 (Mar, 1995).
161. B. Rubinfeld *et al.*, Binding of GSK3beta to the APC-beta-catenin complex and regulation of complex assembly. *Science* **272**, 1023 (May 17, 1996).
162. C. Yost *et al.*, The axis-inducing activity, stability, and subcellular distribution of beta-catenin is regulated in *Xenopus* embryos by glycogen synthase kinase 3. *Genes Dev* **10**, 1443 (Jun 15, 1996).
163. A. de La Coste *et al.*, Somatic mutations of the beta-catenin gene are frequent in mouse and human hepatocellular carcinomas. *Proc Natl Acad Sci U S A* **95**, 8847 (Jul 21, 1998).
164. S. Munemitsu, I. Albert, B. Souza, B. Rubinfeld, P. Polakis, Regulation of intracellular beta-catenin levels by the adenomatous polyposis coli (APC) tumor-suppressor protein. *Proc Natl Acad Sci U S A* **92**, 3046 (Mar 28, 1995).
165. D. J. Sussman *et al.*, Isolation and characterization of a mouse homolog of the *Drosophila* segment polarity gene dishevelled. *Dev Biol* **166**, 73 (Nov, 1994).
166. M. Tsang *et al.*, Isolation and characterization of mouse dishevelled-3. *Dev Dyn* **207**, 253 (Nov, 1996).
167. A. Hecht, K. Vleminckx, M. P. Stemmler, F. van Roy, R. Kemler, The p300/CBP acetyltransferases function as transcriptional coactivators of beta-catenin in vertebrates. *Embo J* **19**, 1839 (Apr 17, 2000).

168. K. I. Takemaru, R. T. Moon, The transcriptional coactivator CBP interacts with beta-catenin to activate gene expression. *J Cell Biol* **149**, 249 (Apr 17, 2000).
169. J. Behrens *et al.*, Functional interaction of beta-catenin with the transcription factor LEF-1. *Nature* **382**, 638 (Aug 15, 1996).
170. J. Sampietro *et al.*, Crystal structure of a beta-catenin/BCL9/Tcf4 complex. *Mol Cell* **24**, 293 (Oct 20, 2006).
171. O. Tetsu, F. McCormick, Beta-catenin regulates expression of cyclin D1 in colon carcinoma cells. *Nature* **398**, 422 (Apr 1, 1999).
172. T. C. He *et al.*, Identification of c-MYC as a target of the APC pathway. *Science* **281**, 1509 (Sep 4, 1998).
173. S. Loeppen *et al.*, Overexpression of glutamine synthetase is associated with beta-catenin-mutations in mouse liver tumors during promotion of hepatocarcinogenesis by phenobarbital. *Cancer Res* **62**, 5685 (Oct 15, 2002).
174. V. Korinek *et al.*, Constitutive transcriptional activation by a beta-catenin-Tcf complex in APC<sup>-/-</sup> colon carcinoma. *Science* **275**, 1784 (Mar 21, 1997).
175. Y. Miyoshi *et al.*, Activation of the beta-catenin gene in primary hepatocellular carcinomas by somatic alterations involving exon 3. *Cancer Res* **58**, 2524 (Jun 15, 1998).
176. S. Y. Peng *et al.*, High alpha-fetoprotein level correlates with high stage, early recurrence and poor prognosis of hepatocellular carcinoma: significance of hepatitis virus infection, age, p53 and beta-catenin mutations. *Int J Cancer* **112**, 44 (Oct 20, 2004).
177. F. Q. An *et al.*, Tumor heterogeneity in small hepatocellular carcinoma: analysis of tumor cell proliferation, expression and mutation of p53 AND beta-catenin. *Int J Cancer* **93**, 468 (Aug 15, 2001).
178. S. S. Thorgeirsson, J. W. Grisham, Molecular pathogenesis of human hepatocellular carcinoma. *Nat Genet* **31**, 339 (Aug, 2002).
179. H. C. Hsu *et al.*, Beta-catenin mutations are associated with a subset of low-stage hepatocellular carcinoma negative for hepatitis B virus and with favorable prognosis. *Am J Pathol* **157**, 763 (Sep, 2000).
180. H. Huang *et al.*, Beta-catenin mutations are frequent in human hepatocellular carcinomas associated with hepatitis C virus infection. *Am J Pathol* **155**, 1795 (Dec, 1999).
181. M. Gross-Goupil *et al.*, Analysis of chromosomal instability in pulmonary or liver metastases and matched primary hepatocellular carcinoma after orthotopic liver transplantation. *Int J Cancer* **104**, 745 (May 10, 2003).
182. D. F. Calvisi, V. M. Factor, S. Ladu, E. A. Conner, S. S. Thorgeirsson, Disruption of beta-catenin pathway or genomic instability define two distinct categories of liver cancer in transgenic mice. *Gastroenterology* **126**, 1374 (May, 2004).
183. K. N. Nejak-Bowen, S. P. Monga, Beta-catenin signaling, liver regeneration and hepatocellular cancer: sorting the good from the bad. *Semin Cancer Biol* **21**, 44 (Feb, 2011).
184. J. Zucman-Rossi *et al.*, Differential effects of inactivated Axin1 and activated beta-catenin mutations in human hepatocellular carcinomas. *Oncogene* **26**, 774 (Feb 1, 2007).
185. H. Fujie *et al.*, Frequent beta-catenin aberration in human hepatocellular carcinoma. *Hepatol Res* **20**, 39 (May 1, 2001).
186. Y. D. Kim *et al.*, Genetic alterations of Wnt signaling pathway-associated genes in hepatocellular carcinoma. *J Gastroenterol Hepatol* **23**, 110 (Jan, 2008).

187. Y. Kondo *et al.*, Beta-catenin accumulation and mutation of exon 3 of the beta-catenin gene in hepatocellular carcinoma. *Jpn J Cancer Res* **90**, 1301 (Dec, 1999).
188. K. Breuhahn, P. Schirmacher, Signaling networks in human hepatocarcinogenesis--novel aspects and therapeutic options. *Prog Mol Biol Transl Sci* **97**, 251 (2010).
189. B. Ciepły, G. Zeng, T. Proverbs-Singh, D. A. Geller, S. P. Monga, Unique phenotype of hepatocellular cancers with exon-3 mutations in beta-catenin gene. *Hepatology* **49**, 821 (Mar, 2009).
190. C. M. Wong, S. T. Fan, I. O. Ng, beta-Catenin mutation and overexpression in hepatocellular carcinoma: clinicopathologic and prognostic significance. *Cancer* **92**, 136 (Jul 1, 2001).
191. J. S. Lee *et al.*, Application of comparative functional genomics to identify best-fit mouse models to study human cancer. *Nat Genet* **36**, 1306 (Dec, 2004).
192. J. M. Lee *et al.*, beta-Catenin signaling in hepatocellular cancer: Implications in inflammation, fibrosis, and proliferation. *Cancer Lett*, (Sep 23, 2013).
193. K. Suzuki *et al.*, Transcatheter arterial chemo-embolization for humoral hypercalcemia of hepatocellular carcinoma. *Gastroenterol Jpn* **23**, 29 (Feb, 1988).
194. X. Li, G. S. Feng, C. S. Zheng, C. K. Zhuo, X. Liu, Expression of plasma vascular endothelial growth factor in patients with hepatocellular carcinoma and effect of transcatheter arterial chemoembolization therapy on plasma vascular endothelial growth factor level. *World J Gastroenterol* **10**, 2878 (Oct 1, 2004).
195. B. Wang *et al.*, Increased expression of vascular endothelial growth factor in hepatocellular carcinoma after transcatheter arterial chemoembolization. *Acta Radiol* **49**, 523 (Jun, 2008).
196. A. Sergio *et al.*, Transcatheter arterial chemoembolization (TACE) in hepatocellular carcinoma (HCC): the role of angiogenesis and invasiveness. *Am J Gastroenterol* **103**, 914 (Apr, 2008).
197. H. Jiang *et al.*, Antiangiogenic therapy enhances the efficacy of transcatheter arterial embolization for hepatocellular carcinomas. *Int J Cancer* **121**, 416 (Jul 15, 2007).
198. P. Stock *et al.*, Platelet-derived growth factor receptor-alpha: a novel therapeutic target in human hepatocellular cancer. *Mol Cancer Ther* **6**, 1932 (Jul, 2007).
199. I. O. Ng *et al.*, Microvessel density, vascular endothelial growth factor and its receptors Flt-1 and Flk-1/KDR in hepatocellular carcinoma. *Am J Clin Pathol* **116**, 838 (Dec, 2001).
200. D. K. Dhar *et al.*, Requisite role of VEGF receptors in angiogenesis of hepatocellular carcinoma: a comparison with angiopoietin/Tie pathway. *Anticancer Res* **22**, 379 (Jan-Feb, 2002).
201. J. M. Llovet *et al.*, Sorafenib in advanced hepatocellular carcinoma. *N Engl J Med* **359**, 378 (Jul 24, 2008).
202. S. M. Wilhelm *et al.*, BAY 43-9006 exhibits broad spectrum oral antitumor activity and targets the RAF/MEK/ERK pathway and receptor tyrosine kinases involved in tumor progression and angiogenesis. *Cancer Res* **64**, 7099 (Oct 1, 2004).
203. M. Kudo *et al.*, Phase III study of sorafenib after transarterial chemoembolisation in Japanese and Korean patients with unresectable hepatocellular carcinoma. *Eur J Cancer* **47**, 2117 (Sep, 2011).

204. T. M. Pawlik *et al.*, Phase II trial of sorafenib combined with concurrent transarterial chemoembolization with drug-eluting beads for hepatocellular carcinoma. *J Clin Oncol* **29**, 3960 (Oct 20, 2011).
205. G. K. Abou-Alfa *et al.*, Doxorubicin plus sorafenib vs doxorubicin alone in patients with advanced hepatocellular carcinoma: a randomized trial. *JAMA* **304**, 2154 (Nov 17, 2010).
206. K. E. O'Reilly *et al.*, mTOR inhibition induces upstream receptor tyrosine kinase signaling and activates Akt. *Cancer Res* **66**, 1500 (Feb 1, 2006).
207. S. L. Chan, T. Mok, B. B. Ma, Management of hepatocellular carcinoma: beyond sorafenib. *Curr Oncol Rep* **14**, 257 (Jun, 2012).
208. S. R. Alberts *et al.*, Gemcitabine and docetaxel for hepatocellular carcinoma: a phase II North Central Cancer Treatment Group clinical trial. *Am J Clin Oncol* **35**, 418 (Oct, 2012).
209. R. Coriat *et al.*, Feasibility of oxaliplatin, 5-fluorouracil and leucovorin (FOLFOX-4) in cirrhotic or liver transplant patients: experience in a cohort of advanced hepatocellular carcinoma patients. *Invest New Drugs* **30**, 376 (Feb, 2012).
210. C. H. Hsu *et al.*, Phase II study of combining sorafenib with metronomic tegafur/uracil for advanced hepatocellular carcinoma. *J Hepatol* **53**, 126 (Jul, 2010).
211. S. L. Chan *et al.*, New utility of an old marker: serial alpha-fetoprotein measurement in predicting radiologic response and survival of patients with hepatocellular carcinoma undergoing systemic chemotherapy. *J Clin Oncol* **27**, 446 (Jan 20, 2009).
212. A. L. Cheng *et al.*, Sunitinib Versus Sorafenib in Advanced Hepatocellular Cancer: Results of a Randomized Phase III Trial. *J Clin Oncol* **31**, 4067 (Nov 10, 2013).
213. J. W. Park *et al.*, Phase II, open-label study of brivanib as first-line therapy in patients with advanced hepatocellular carcinoma. *Clin Cancer Res* **17**, 1973 (Apr 1, 2011).
214. Z. W. Cai *et al.*, Discovery of brivanib alaninate ((S)-((R)-1-(4-(4-fluoro-2-methyl-1H-indol-5-yloxy)-5-methylpyrrolo[2,1-f][1,2,4] triazin-6-yloxy)propan-2-yl)2-aminopropanoate), a novel prodrug of dual vascular endothelial growth factor receptor-2 and fibroblast growth factor receptor-1 kinase inhibitor (BMS-540215). *J Med Chem* **51**, 1976 (Mar 27, 2008).
215. A. B. Siegel *et al.*, Phase II trial evaluating the clinical and biologic effects of bevacizumab in unresectable hepatocellular carcinoma. *J Clin Oncol* **26**, 2992 (Jun 20, 2008).
216. R. S. F. A. X. Zhu, M. F. Mulcahy, J. S. Gurtler, W. Sun, J. D. Schwartz, P. Rojas, A. Dontabhaktuni, H. Youssoufian and K. E. Stuart, A phase II study of ramucirumab as first-line monotherapy in patients (pts) with advanced hepatocellular carcinoma (HCC). *J Clin Oncol* **28**, (May 20, 2010, 2010).
217. P. A. Philip *et al.*, Phase II study of Erlotinib (OSI-774) in patients with advanced hepatocellular cancer. *J Clin Oncol* **23**, 6657 (Sep 20, 2005).
218. M. B. Thomas *et al.*, Phase 2 study of erlotinib in patients with unresectable hepatocellular carcinoma. *Cancer* **110**, 1059 (Sep 1, 2007).
219. R. K. Ramanathan *et al.*, A phase II study of lapatinib in patients with advanced biliary tree and hepatocellular cancer. *Cancer Chemother Pharmacol* **64**, 777 (Sep, 2009).
220. T. Bekaii-Saab *et al.*, A multi-institutional phase II study of the efficacy and tolerability of lapatinib in patients with advanced hepatocellular carcinomas. *Clin Cancer Res* **15**, 5895 (Sep 15, 2009).

221. A. X. Zhu *et al.*, Phase 2 study of cetuximab in patients with advanced hepatocellular carcinoma. *Cancer* **110**, 581 (Aug 1, 2007).
222. M. B. Thomas *et al.*, Phase II trial of the combination of bevacizumab and erlotinib in patients who have advanced hepatocellular carcinoma. *J Clin Oncol* **27**, 843 (Feb 20, 2009).
223. C. H. Hsu *et al.*, Efficacy and tolerability of bevacizumab plus capecitabine as first-line therapy in patients with advanced hepatocellular carcinoma. *Br J Cancer* **102**, 981 (Mar 16, 2010).
224. A. Kiss, N. J. Wang, J. P. Xie, S. S. Thorgeirsson, Analysis of transforming growth factor (TGF)-alpha/epidermal growth factor receptor, hepatocyte growth Factor/c-met, TGF-beta receptor type II, and p53 expression in human hepatocellular carcinomas. *Clin Cancer Res* **3**, 1059 (Jul, 1997).
225. J. Y. Ljubimova, L. M. Petrovic, S. E. Wilson, S. A. Geller, A. A. Demetriou, Expression of HGF, its receptor c-met, c-myc, and albumin in cirrhotic and neoplastic human liver tissue. *J Histochem Cytochem* **45**, 79 (Jan, 1997).
226. A. S. P. Zucali, C. Rodriguez-Lope, M. Simonelli, L. H. Camacho, N. N. Senzer, L. Bolondi, M. Lamar, G. Abbadessa and B. E. Schwartz, Final results from ARQ 197-114: A phase Ib safety trial evaluating ARQ 197 in cirrhotic patients (pts) with hepatocellular carcinoma (HCC). *J Clin Oncol* **28**, (May 20 2010, 2010).
227. A. Villanueva *et al.*, Pivotal role of mTOR signaling in hepatocellular carcinoma. *Gastroenterology* **135**, 1972 (Dec, 2008).
228. F. Sahin *et al.*, mTOR and P70 S6 kinase expression in primary liver neoplasms. *Clin Cancer Res* **10**, 8421 (Dec 15, 2004).
229. A. X. Zhu *et al.*, Phase 1/2 study of everolimus in advanced hepatocellular carcinoma. *Cancer* **117**, 5094 (Nov 15, 2011).
230. H. Huynh *et al.*, Over-expression of the mitogen-activated protein kinase (MAPK) kinase (MEK)-MAPK in hepatocellular carcinoma: its role in tumor progression and apoptosis. *BMC Gastroenterol* **3**, 19 (Aug 8, 2003).
231. B. H. O'Neil *et al.*, Phase II study of the mitogen-activated protein kinase 1/2 inhibitor selumetinib in patients with advanced hepatocellular carcinoma. *J Clin Oncol* **29**, 2350 (Jun 10, 2011).
232. M. Rodriguez-Paredes, M. Esteller, Cancer epigenetics reaches mainstream oncology. *Nat Med* **17**, 330 (Mar, 2011).
233. T. H. Um *et al.*, Aberrant CpG island hypermethylation in dysplastic nodules and early HCC of hepatitis B virus-related human multistep hepatocarcinogenesis. *J Hepatol* **54**, 939 (May, 2011).
234. B. B. Ma *et al.*, The preclinical activity of the histone deacetylase inhibitor PXD101 (belinostat) in hepatocellular carcinoma cell lines. *Invest New Drugs* **28**, 107 (Apr, 2010).
235. D. Carlisi *et al.*, The histone deacetylase inhibitor suberoylanilide hydroxamic acid sensitises human hepatocellular carcinoma cells to TRAIL-induced apoptosis by TRAIL-DISC activation. *Eur J Cancer* **45**, 2425 (Sep, 2009).
236. D. Carlisi *et al.*, Histone deacetylase inhibitors induce in human hepatoma HepG2 cells acetylation of p53 and histones in correlation with apoptotic effects. *Int J Oncol* **32**, 177 (Jan, 2008).
237. W. Yeo *et al.*, Epigenetic therapy using belinostat for patients with unresectable hepatocellular carcinoma: a multicenter phase I/II study with biomarker and

- pharmacokinetic analysis of tumors from patients in the Mayo Phase II Consortium and the Cancer Therapeutics Research Group. *J Clin Oncol* **30**, 3361 (Sep 20, 2012).
238. T. Nakamura *et al.*, Antiangiogenic agent SU6668 suppresses the tumor growth of xenografted A-431 cells. *Oncol Rep* **15**, 79 (Jan, 2006).
  239. A. D. Laird *et al.*, SU6668 is a potent antiangiogenic and antitumor agent that induces regression of established tumors. *Cancer Res* **60**, 4152 (Aug 1, 2000).
  240. S. H. Lee *et al.*, In vivo target modulation and biological activity of CHIR-258, a multitargeted growth factor receptor kinase inhibitor, in colon cancer models. *Clin Cancer Res* **11**, 3633 (May 15, 2005).
  241. H. Huynh *et al.*, Dovitinib demonstrates antitumor and antimetastatic activities in xenograft models of hepatocellular carcinoma. *J Hepatol* **56**, 595 (Mar, 2012).
  242. H. van Malenstein, J. van Pelt, C. Verslype, Molecular classification of hepatocellular carcinoma anno 2011. *Eur J Cancer* **47**, 1789 (Aug, 2011).
  243. H. Wada *et al.*, Combination therapy of interferon-alpha and 5-fluorouracil inhibits tumor angiogenesis in human hepatocellular carcinoma cells by regulating vascular endothelial growth factor and angiopoietins. *Oncol Rep* **18**, 801 (Oct, 2007).
  244. J. Behari *et al.*, R-Etodolac decreases beta-catenin levels along with survival and proliferation of hepatoma cells. *J Hepatol* **46**, 849 (May, 2007).
  245. K. H. Emami *et al.*, A small molecule inhibitor of beta-catenin/CREB-binding protein transcription [corrected]. *Proc Natl Acad Sci U S A* **101**, 12682 (Aug 24, 2004).
  246. M. D. Thompson, M. J. Dar, S. P. Monga, Pegylated interferon alpha targets Wnt signaling by inducing nuclear export of beta-catenin. *J Hepatol* **54**, 506 (Mar, 2011).
  247. X. H. Wang *et al.*, beta-catenin siRNA regulation of apoptosis- and angiogenesis-related gene expression in hepatocellular carcinoma cells: potential uses for gene therapy. *Oncol Rep* **24**, 1093 (Oct, 2010).
  248. E. Delgado *et al.*, beta-Catenin Knockdown in Liver Tumor Cells by a Cell Permeable Gamma Guanidine-based Peptide Nucleic Acid. *Curr Cancer Drug Targets*, (Jul 1, 2013).
  249. F. Takahashi-Yanaga, M. Kahn, Targeting Wnt signaling: can we safely eradicate cancer stem cells? *Clin Cancer Res* **16**, 3153 (Jun 15, 2010).
  250. Y. C. Martin, J. L. Kofron, L. M. Traphagen, Do structurally similar molecules have similar biological activity? *J Med Chem* **45**, 4350 (Sep 12, 2002).
  251. A. Wallqvist, R. Huang, N. Thanki, D. G. Covell, Evaluating chemical structure similarity as an indicator of cellular growth inhibition. *J Chem Inf Model* **46**, 430 (Jan-Feb, 2006).
  252. J. J. Irwin, B. K. Shoichet, ZINC--a free database of commercially available compounds for virtual screening. *J Chem Inf Model* **45**, 177 (Jan-Feb, 2005).
  253. X. Zhang, J. P. Gaspard, D. C. Chung, Regulation of vascular endothelial growth factor by the Wnt and K-ras pathways in colonic neoplasia. *Cancer Res* **61**, 6050 (Aug 15, 2001).
  254. G. Zeng, U. Apte, B. Cieply, S. Singh, S. P. Monga, siRNA-mediated beta-catenin knockdown in human hepatoma cells results in decreased growth and survival. *Neoplasia* **9**, 951 (Nov, 2007).
  255. G. Carruba *et al.*, Truncated form of beta-catenin and reduced expression of wild-type catenins feature HepG2 human liver cancer cells. *Ann N Y Acad Sci.* **886**, 212 (1999).

256. T. Cagatay, M. Ozturk, P53 mutation as a source of aberrant beta-catenin accumulation in cancer cells. *Oncogene* **21**, 7971 (Nov 14, 2002).
257. S. Satoh *et al.*, AXIN1 mutations in hepatocellular carcinomas, and growth suppression in cancer cells by virus-mediated transfer of AXIN1. *Nat Genet* **24**, 245 (Mar, 2000).
258. N. Shimizu, K. Kawakami, T. Ishitani, Visualization and exploration of Tcf/Lef function using a highly responsive Wnt/beta-catenin signaling-reporter transgenic zebrafish. *Dev Biol* **370**, 71 (Oct 1, 2012).
259. S. M. A. Huang *et al.*, Tankyrase inhibition stabilizes axin and antagonizes Wnt signalling. *Nature* **461**, 614 (Oct 1, 2009).
260. P. Teriete, A. B. Pinkerton, N. D. Cosford, Inhibitors of tissue-nonspecific alkaline phosphatase (TNAP): from hits to leads. *Methods Mol Biol* **1053**, 85 (2013).
261. H. Yao *et al.*, AV-65, a novel Wnt/beta-catenin signal inhibitor, successfully suppresses progression of multiple myeloma in a mouse model. *Blood Cancer J* **1**, e43 (Nov, 2011).
262. Y. Dong *et al.*, Lipopeptide nanoparticles for potent and selective siRNA delivery in rodents and nonhuman primates. *Proc Natl Acad Sci U S A*, (Feb 10, 2014).
263. R. S. Yu *et al.*, Preliminary Study on Hepatocyte-Targeted Phosphorus-31 MRS Using ATP-Loaded Galactosylated Chitosan Oligosaccharide Nanoparticles. *Gastroenterol Res Pract* **2013**, 512483 (2013).
264. A. Gougelet *et al.*, T-cell factor 4 and beta-catenin chromatin occupancies pattern zonal liver metabolism. *Hepatology*, (Nov 9, 2013).
265. T. Miyabayashi *et al.*, Wnt/beta-catenin/CBP signaling maintains long-term murine embryonic stem cell pluripotency. *Proc Natl Acad Sci U S A* **104**, 5668 (Mar 27, 2007).
266. P. E. Nielsen, M. Egholm, R. H. Berg, O. Buchardt, Sequence-selective recognition of DNA by strand displacement with a thymine-substituted polyamide. *Science* **254**, 1497 (Dec 6, 1991).
267. P. E. Nielsen, Peptide Nucleic Acid. A Molecule with Two Identities. *Accounts of Chemical Research* **32**, 624 (1999/07/01, 1999).
268. R. L. Juliano, H. Yoo, Aspects of the transport and delivery of antisense oligonucleotides. *Curr Opin Mol Ther* **2**, 297 (Jun, 2000).
269. P. Zhou *et al.*, Novel binding and efficient cellular uptake of guanidine-based peptide nucleic acids (GPNA). *J Am Chem Soc* **125**, 6878 (Jun 11, 2003).
270. P. Zhou *et al.*, Synthesis of cell-permeable peptide nucleic acids and characterization of their hybridization and uptake properties. *Bioorg Med Chem Lett* **16**, 4931 (Sep 15, 2006).
271. A. Dragulescu-Andrasi, P. Zhou, G. He, D. H. Ly, Cell-permeable GPNA with appropriate backbone stereochemistry and spacing binds sequence-specifically to RNA. *Chem Commun (Camb)*, 244 (Jan 14, 2005).
272. V. Easwaran *et al.*, beta-Catenin regulates vascular endothelial growth factor expression in colon cancer. *Cancer Res* **63**, 3145 (Jun 15, 2003).
273. M. Mise *et al.*, Clinical significance of vascular endothelial growth factor and basic fibroblast growth factor gene expression in liver tumor. *Hepatology* **23**, 455 (Mar, 1996).
274. S. C. Heffelfinger, H. H. Hawkins, J. Barrish, L. Taylor, G. J. Darlington, SK HEP-1: a human cell line of endothelial origin. *In Vitro Cell Dev Biol* **28A**, 136 (Feb, 1992).
275. A. De Mesmaeker, R. Haener, P. Martin, H. E. Moser, Antisense Oligonucleotides. *Accounts of Chemical Research* **28**, 366 (1995/09/01, 1995).

276. J. Wengel, Synthesis of 3'-C- and 4'-C- Branched Oligodeoxynucleotides and the Development of Locked Nucleic Acid (LNA). *Accounts of Chemical Research* **32**, 301 (1999).
277. B. Sahu *et al.*, Synthesis of conformationally preorganized and cell-permeable guanidine-based gamma-peptide nucleic acids (gammaGPNAs). *J Org Chem* **74**, 1509 (Feb 20, 2009).
278. A. Dragulescu-Andrasi *et al.*, Cell-permeable peptide nucleic acid designed to bind to the 5'-untranslated region of E-cadherin transcript induces potent and sequence-specific antisense effects. *J Am Chem Soc* **128**, 16104 (Dec 20, 2006).
279. A. X. Zhu, D. G. Duda, D. V. Sahani, R. K. Jain, HCC and angiogenesis: possible targets and future directions. *Nat Rev Clin Oncol* **8**, 292 (May, 2011).
280. S. K. Jimenez *et al.*, Transcriptional regulation of FGF-2 gene expression in cardiac myocytes. *Cardiovasc Res* **62**, 548 (Jun 1, 2004).
281. J. Hu *et al.*, Blockade of Wnt signaling inhibits angiogenesis and tumor growth in hepatocellular carcinoma. *Cancer Res* **69**, 6951 (Sep 1, 2009).
282. A. A. Koshkin *et al.*, LNA (Locked Nucleic Acids): Synthesis of the adenine, cytosine, guanine, 5-methylcytosine, thymine and uracil bicyclonucleoside monomers, oligomerisation, and unprecedented nucleic acid recognition. *Tetrahedron* **54**, 3607 (1998).
283. S. Obika *et al.*, Stability and structural features of the duplexes containing nucleoside analogues with a fixed N-type conformation, 2'-O,4'-C-methyleneribonucleosides. *Tetrahedron Letters* **39**, 5401 (1998).
284. C. B. Nielsen, S. K. Singh, J. Wengel, J. P. Jacobsen, The solution structure of a locked nucleic acid (LNA) hybridized to DNA. *J Biomol Struct Dyn* **17**, 175 (Oct, 1999).
285. C. Wahlestedt *et al.*, Potent and nontoxic antisense oligonucleotides containing locked nucleic acids. *Proc Natl Acad Sci U S A* **97**, 5633 (May 9, 2000).
286. K. Bondensgaard *et al.*, Structural studies of LNA:RNA duplexes by NMR: conformations and implications for RNase H activity. *Chemistry* **6**, 2687 (Aug 4, 2000).
287. O. Moennikes *et al.*, Lack of phenobarbital-mediated promotion of hepatocarcinogenesis in connexin32-null mice. *Cancer Res* **60**, 5087 (Sep 15, 2000).
288. X. F. Zhang *et al.*, Conditional beta-catenin loss in mice promotes chemical hepatocarcinogenesis: role of oxidative stress and platelet-derived growth factor receptor alpha/phosphoinositide 3-kinase signaling. *Hepatology* **52**, 954 (Sep, 2010).
289. K. N. Nejak-Bowen *et al.*, Accelerated liver regeneration and hepatocarcinogenesis in mice overexpressing serine-45 mutant beta-catenin. *Hepatology* **51**, 1603 (May, 2010).
290. A. D. Tward *et al.*, Distinct pathways of genomic progression to benign and malignant tumors of the liver. *Proc Natl Acad Sci U S A* **104**, 14771 (Sep 11, 2007).
291. L. Amicone *et al.*, Synergy between truncated c-Met (cyto-Met) and c-Myc in liver oncogenesis: importance of TGF-beta signalling in the control of liver homeostasis and transformation. *Oncogene* **21**, 1335 (Feb 21, 2002).
292. H. Aydinlik, T. D. Nguyen, O. Moennikes, A. Buchmann, M. Schwarz, Selective pressure during tumor promotion by phenobarbital leads to clonal outgrowth of beta-catenin-mutated mouse liver tumors. *Oncogene* **20**, 7812 (Nov 22, 2001).
293. L. Verna, J. Whysner, G. M. Williams, N-nitrosodiethylamine mechanistic data and risk assessment: bioactivation, DNA-adduct formation, mutagenicity, and tumor initiation. *Pharmacol Ther* **71**, 57 (1996).

294. B. U. Bradford *et al.*, Cytochrome P450 CYP2E1, but not nicotinamide adenine dinucleotide phosphate oxidase, is required for ethanol-induced oxidative DNA damage in rodent liver. *Hepatology* **41**, 336 (Feb, 2005).
295. J. S. Kang, H. Wanibuchi, K. Morimura, F. J. Gonzalez, S. Fukushima, Role of CYP2E1 in diethylnitrosamine-induced hepatocarcinogenesis in vivo. *Cancer Res* **67**, 11141 (Dec 1, 2007).
296. H. Yamazaki, Y. Inui, C. H. Yun, F. P. Guengerich, T. Shimada, Cytochrome P450 2E1 and 2A6 enzymes as major catalysts for metabolic activation of N-nitrosodialkylamines and tobacco-related nitrosamines in human liver microsomes. *Carcinogenesis* **13**, 1789 (Oct, 1992).
297. A. M. Camus *et al.*, High variability of nitrosamine metabolism among individuals: role of cytochromes P450 2A6 and 2E1 in the dealkylation of N-nitrosodimethylamine and N-nitrosodiethylamine in mice and humans. *Mol Carcinog* **7**, 268 (1993).
298. S. Mutoh *et al.*, Dephosphorylation of threonine 38 is required for nuclear translocation and activation of human xenobiotic receptor CAR (NR1I3). *J Biol Chem* **284**, 34785 (Dec 11, 2009).
299. P. Honkakoski, I. Zelko, T. Sueyoshi, M. Negishi, The nuclear orphan receptor CAR-retinoid X receptor heterodimer activates the phenobarbital-responsive enhancer module of the CYP2B gene. *Mol Cell Biol* **18**, 5652 (Oct, 1998).
300. T. Sueyoshi, T. Kawamoto, I. Zelko, P. Honkakoski, M. Negishi, The repressed nuclear receptor CAR responds to phenobarbital in activating the human CYP2B6 gene. *J Biol Chem* **274**, 6043 (Mar 5, 1999).
301. T. Kawamoto *et al.*, Phenobarbital-responsive nuclear translocation of the receptor CAR in induction of the CYP2B gene. *Mol Cell Biol* **19**, 6318 (Sep, 1999).
302. S. P. Monga *et al.*, Beta-catenin antisense studies in embryonic liver cultures: role in proliferation, apoptosis, and lineage specification. *Gastroenterology* **124**, 202 (Jan, 2003).
303. N. Jacobsen *et al.*, Genotyping of the apolipoprotein B R3500Q mutation using immobilized locked nucleic acid capture probes. *Clin Chem* **48**, 657 (2002).
304. M. Petersen, K. Bondensgaard, J. Wengel, J. P. Jacobsen, Locked nucleic acid (LNA) recognition of RNA: NMR solution structures of LNA:RNA hybrids. *J Am Chem Soc* **124**, 5974 (May 29, 2002).
305. A. Simeonov, T. T. Nikiforov, Single nucleotide polymorphism genotyping using short, fluorescently labeled locked nucleic acid (LNA) probes and fluorescence polarization detection. *Nucleic Acids Res* **30**, e91 (Sep 1, 2002).
306. A. N. Elayadi, D. A. Braasch, D. R. Corey, Implications of high-affinity hybridization by locked nucleic acid oligomers for inhibition of human telomerase. *Biochemistry* **41**, 9973 (Aug 6, 2002).
307. K. Fluiter *et al.*, In vivo tumor growth inhibition and biodistribution studies of locked nucleic acid (LNA) antisense oligonucleotides. *Nucleic Acids Res* **31**, 953 (Feb 1, 2003).
308. A. N. Elayadi, D. R. Corey, Application of PNA and LNA oligomers to chemotherapy. *Curr Opin Investig Drugs* **2**, 558 (Apr, 2001).
309. D. Bianchini *et al.*, First-in-human Phase I study of EZN-4176, a locked nucleic acid antisense oligonucleotide to exon 4 of the androgen receptor mRNA in patients with castration-resistant prostate cancer. *Br J Cancer* **109**, 2579 (Nov 12, 2013).

310. I. Sancho-Martinez, J. C. Izpisua Belmonte, Will SCNT-ESCs be better than iPSCs for personalized regenerative medicine? *Cell Stem Cell* **13**, 141 (Aug 1, 2013).
311. M. Prague, D. Commenges, R. Thiebaut, Dynamical models of biomarkers and clinical progression for personalized medicine: the HIV context. *Adv Drug Deliv Rev* **65**, 954 (Jun 30, 2013).
312. M. N. Nikiforova, A. I. Wald, S. Roy, M. B. Durso, Y. E. Nikiforov, Targeted Next-Generation Sequencing Panel (ThyroSeq) for Detection of Mutations in Thyroid Cancer. *J Clin Endocrinol Metab* **98**, E1852 (Nov, 2013).
313. W. Wei, M. S. Chua, S. Grepper, S. K. So, Blockade of Wnt-1 signaling leads to anti-tumor effects in hepatocellular carcinoma cells. *Mol Cancer* **8**, 76 (2009).
314. R. Gebhardt, D. Mecke, Heterogeneous distribution of glutamine synthetase among rat liver parenchymal cells in situ and in primary culture. *EMBO J* **2**, 567 (1983).
315. H. Clevers, R. Nusse, Wnt/beta-catenin signaling and disease. *Cell* **149**, 1192 (Jun 8, 2012).
316. E. D. Wickline *et al.*, Hepatocyte gamma-catenin compensates for conditionally deleted beta-catenin at adherens junctions. *J Hepatol* **55**, 1256 (Dec, 2011).
317. X. Tan, J. Behari, B. Ciepły, G. K. Michalopoulos, S. P. Monga, Conditional deletion of beta-catenin reveals its role in liver growth and regeneration. *Gastroenterology* **131**, 1561 (Nov, 2006).
318. E. D. Wickline, Y. Du, D. B. Stolz, M. Kahn, S. P. Monga, gamma-Catenin at adherens junctions: mechanism and biologic implications in hepatocellular cancer after beta-catenin knockdown. *Neoplasia* **15**, 421 (Apr, 2013).
319. M. R. Diaz, P. E. Vivas-Mejia, Nanoparticles as Drug Delivery Systems in Cancer Medicine: Emphasis on RNAi-Containing Nanoliposomes. *Pharmaceuticals (Basel)* **6**, 1361 (2013).
320. P. K. Awuah, B. H. Rhieu, S. Singh, A. Misse, S. P. Monga, beta-Catenin loss in hepatocytes promotes hepatocellular cancer after diethylnitrosamine and phenobarbital administration to mice. *PLoS One* **7**, e39771 (2012).
321. F. Bronte *et al.*, Targeted Therapies in Hepatocellular Carcinoma. *Curr Med Chem*, (Aug 23, 2013).
322. N. Ibrahim, Y. Yu, W. R. Walsh, J. L. Yang, Molecular targeted therapies for cancer: sorafenib mono-therapy and its combination with other therapies (review). *Oncol Rep* **27**, 1303 (May, 2012).
323. U. Apte *et al.*, Wnt/beta-catenin signaling mediates oval cell response in rodents. *Hepatology* **47**, 288 (Jan, 2008).
324. J. Ji, X. W. Wang, Clinical implications of cancer stem cell biology in hepatocellular carcinoma. *Semin Oncol* **39**, 461 (Aug, 2012).
325. T. Yamashita, A. Budhu, M. Forgues, X. W. Wang, Activation of hepatic stem cell marker EpCAM by Wnt-beta-catenin signaling in hepatocellular carcinoma. *Cancer Res* **67**, 10831 (Nov 15, 2007).
326. S. Tardito *et al.*, L-Asparaginase and inhibitors of glutamine synthetase disclose glutamine addiction of beta-catenin-mutated human hepatocellular carcinoma cells. *Curr Cancer Drug Targets* **11**, 929 (Oct, 2011).
327. Y. Hoshida *et al.*, Molecular classification and novel targets in hepatocellular carcinoma: recent advancements. *Semin Liver Dis* **30**, 35 (Feb, 2010).

328. J. C. Nault, J. Zucman-Rossi, Genetics of hepatobiliary carcinogenesis. *Semin Liver Dis* **31**, 173 (May, 2011).
329. L. Liu *et al.*, Sorafenib blocks the RAF/MEK/ERK pathway, inhibits tumor angiogenesis, and induces tumor cell apoptosis in hepatocellular carcinoma model PLC/PRF/5. *Cancer Res* **66**, 11851 (Dec 15, 2006).
330. L. Christensen *et al.*, Solid-phase synthesis of peptide nucleic acids. *J Pept Sci* **1**, 175 (May-Jun, 1995).
331. A. N. Jain, Morphological similarity: a 3D molecular similarity method correlated with protein-ligand recognition. *J Comput Aided Mol Des* **14**, 199 (Feb, 2000).
332. M. Westerfield, *The Zebrafish Book: A Guide for the Laboratory Use of Zebrafish (Danio rerio)*. (University of Oregon Press, 2000).